

TRIUMF	UNIVERSITY OF ALBERTA EDMONTON, ALBERTA	
	Date 2005/08/19	File No. TRI-DNA-05-1
Author GM Stinson	Page 1 of 83	

Subject Present status of the beam transport to the ISAC-II experimental area

1. Introduction

Various studies of possible beam-transport configurations to the experimental hall of ISAC-II have been reported earlier¹⁻⁵). In most of these investigations the intrinsic emittance of the beams extracted from the medium- β accelerator complex has been taken to be $\epsilon_0 = 0.2\pi$ mm-mr. It is expected that this intrinsic emittance could be increased to $\epsilon_0 = 0.3\pi$ mm-mr when the charge-state booster (CSB) is installed. Further, an estimate of the emittance variation as a function of the acceleration of the ions is now available. Consequently, it becomes necessary to investigate the effect of the emittance variation on beam profiles along the various beamlines.

The beamline configuration presented here is a slight modification of those presented earlier. In particular, the configuration has been modified to allow a future expansion that would permit one experiment to move back and forth between two target locations. Further, it is proposed to change the first dipole in the experimental area from one which bends $+30^\circ/-9a.5^\circ$ to one bending $+30^\circ/-30^\circ$, with the (unconventional) definition of a positive bend as a bend to the left looking downstream. This change facilitates beam delivery to the TGT4 location.

It is expedient to discuss the beam transport to the experimental area in terms of an initial installation and of future expansions. Consequently, this report presents an overview of the proposed complete beam delivery system and deals in detail with the proposed initial and expansion installations.

2. Emittance as a function of accelerated energy

As noted above an estimate of the variation of the emittance as a function of the accelerated energy of an ion over a range of energies from $0.5 \text{ MeV}/\mu$ to $15 \text{ MeV}/\mu$. This is shown in figure 1(a). Figure 1(b) is a similar plot over a range of energies from $0.5 \text{ MeV}/\mu$ to $7 \text{ MeV}/\mu$. The curves in cyan and marked $\epsilon_0 = 0.2\pi$ mm-mr correspond to the intrinsic emittances of the present ISAC ion sources. These may be taken as 2σ emittances for operation *without* the CSB⁶). Those in magenta and marked $\epsilon_0 = 0.3\pi$ mm-mr are estimated to be the intrinsic emittances for operation *with* the CSB. For this case the emittances also may be considered as emittances at the 2σ level⁶).

Values for these curves were obtained by first computing the value of $\beta_i = v_i/c$ of an ion at an accelerated energy of $T_i \text{ MeV}/\mu$ using the relationship

$$\beta_i = \sqrt{\frac{T_i}{T_0}} \cdot \beta_0 ,$$

where β_0 is the (known) value of β for the ion at an accelerated energy of $T_0 \text{ MeV}/\mu$. Then if the intrinsic emittance of the beam at the energy T_0 is ϵ_0 , the emittance ϵ_i at the energy T_i is obtained from

$$\epsilon_i = \frac{\epsilon_0}{\beta_i} .$$

In the present case we use⁶) $T_0 = 1.5 \text{ MeV}/\mu$, $\beta_0 = 0.056$, and $\epsilon_0 = 0.2\pi$ (or 0.3π) mm-mr.

3. Proposed phasing of beamline installations

The proposed layout of the experimental area of ISAC-II is shown in figure 2. The large rectangle indicates the extent of the experimental area and the colored sections indicate the installation phases of beamlines

to the experimental area.

When this report was written it is proposed that beamline installation proceed in four phases. The first phase, shown black in figure 2, is the completion of the beamline from the exit of the medium- β accelerator (labeled ' $m\beta$ exit') to the object point (labeled 'M5') for the beamlines that feed the various target locations in the experimental hall. The points labeled M1 through M5 are the end points of the five sections that make up this beamline and are described below. This installation is expected to be accomplished by the end of 2005.

The second phase, colored green, is the transport line to the target location TGT4 with an anticipated installation in the spring of 2006. This target location is nominally assigned to the HERACLES experiment. It is the dipole on this line that is proposed to be changed.

The third phase, colored cyan, is the beamline to the target locations TGT5 and TGT6. The TIGRESS experiment will be installed at the TGT5 location and the TUDA experiment will be sited at the TGT6 position. Completion of this phase is expected by the end of 2007.

Finally, the fourth phase, colored red, is to the location marked TGT1. The EMMA experiment will be mounted here. As well, a rail system will be installed between the TGT5 location and the TGT1 position such that the apparatus of the TIGRESS experiment can be moved from one location to the other. Completion of this phase is expected in 2008.

[Note: The unusual numbering of the target locations is historical. As initially envisaged the beamline to the TGT1 position was to be installed first. A mirror image of the the section of line from the last dipole on this line to TGT1 was also to be installed and was labeled TGT2. A 'straight-through' beamline to a TGT3 location was considered but rejected by experimenters. Next the beamline to the TGT4 location was to have been installed. Later came the proposal for the installation of the components for the beamlines to the TGT5 and TGT6 positions.]

In the following sections we discuss beam transport to the experimental area in the order that they would be installed given the phasing order given above. First, however, we present an overview of the optics of the beamlines.

4. An overview of the optics of the beamlines

For beam delivery to the experimental target locations it is assumed that the vault transport has been tuned to produce a double waist at the M5 position. The designs of the systems transporting beams to the experimental targets are such as to produce a doubly-achromatic double waist at all target locations *except* at the TGT4 position. At other than at the TGT4 location the 'nominal' diameter of the beam spot may be either 1 mm or 2 mm. We put nominal in single quotes here because the design parameters in TRANSPORT fits were 0.9 mm for the 1 mm beam spot and 0.17 mm for the 2 mm beam spot.

In general, production of a 2 mm diameter beam spot is possible at all target locations for most of the emittances that one would expect from the accelerator system. On the other hand, production of a beam spot 1 mm in diameter is possible only over a limited range of emittances. This is due to the apertures and strengths of the quadrupoles that are available *and* of the limited vertical (in particular) and horizontal apertures of the the dipole magnets and their existing vacuum boxes.

This system of beamlines naturally breaks into two sections: that within the accelerator vault and those leading to the experimental targets. In terms of the labels in figure 2, the section of beamline within the accelerator vault is that between the location labeled ' $m\beta$ exit', the exit of the medium- β accelerator complex, and the location labeled 'M5'. Because they are common to all beamlines we consider the two quadrupoles downstream of M5 as part of the beamlines to the experimental targets although they too are physically within the accelerator vault.

For beam delivery to TGT1 the 10-quadrupole, 2-dipole configuration is operated such that the transfer matrix from M5 to the target is $+\mathbf{I}$ in the horizontal plane and $-\mathbf{I}$ in the vertical plane. Thus the beam spot at TGT1 is identical to that at M5 except for an inversion in the vertical plane. Because of these unit transformations it is *not* necessary to retune this section for differing emittances provided that the vault section is tuned to present the required beam size at the M5 location.

A similar situation holds for beam delivery to the TGT5 location. Again, this is a 10-quadrupole, 2-dipole configuration. The beam spot at M5 is reproduced at the object point of the system; that point is indicated in figure 2 as M6.

At the TGT6 location unit transformations in x - θ and y - ϕ can be produced. However, although the sub-matrices $\mathbf{R}_{x,\theta}$ and $\mathbf{R}_{y,\phi}$ are each equal to $-\mathbf{I}$, the matrix element $R_{16} \neq 0$ downstream of the first dipole and $R_{16} = 0$ only at the target position. Further, the the matrix element $R_{16} \neq 0$ downstream of the first dipole and $R_{26} \sim -6$ at the target position. This results in increased beam sizes in both x and y downstream of the second dipole. Consequently, this section of beamline is tuned to produce a doubly achromatic, double waist of size equal to that at the M6 location. As a result some retuning of the beamline is required as the extracted emittance changes.

At the TGT4 location we have considered *only* production of a beam spot nominally 2 mm in diameter. With the revised beam-transport configuration a double waist can be produced with a small (≤ 0.02 cm/% $\delta p/p$) spatial dispersion and a somewhat larger (~ 4.2 mr/% $\delta p/p$) angular dispersion.

We return to a more detailed discussion of each of these beamlines. This will be done in the order of the phasing given above.

5. Phase 1 – Transport within the accelerator vault

Initially beam will be extracted from the medium- β accelerator section. Later a high- β accelerator section will be added. Beam transport within the accelerator vault has been designed to accommodate both accelerator sections as easily as possible.

The length of the medium- β accelerator is 10.44 m and that of the high- β accelerator is 8.84 m. For the transport of a multi-charged beam it is necessary that beam transport sections must be shorter than ~ 5 m⁴). Based on these lengths, a distance of 16.73 m from the exit of the high- β accelerator to the vault wall, and a distance of 3.24 m from the M5 location to the vault wall, R. Laxdal⁷) has designed a transport line that is suitable for transporting a multi-charged beam from the medium- β exit to the M5 location.

His system consists of three four-quadrupole systems each of length 4.42 m and two four-quadrupole systems each of length 4.54 m. When operating with the medium- β accelerator the first system is used to match the accelerator output to the beamline and the last system is used to tune to the required beam characteristics at the M5 location. When the high- β accelerator is ready for installation the first two systems are removed (thus freeing up eight quadrupoles) and are replaced by the accelerator. Then the (former) third and fifth systems act as matching sections.

This beam-transport system can be used both for transport of a multi-charge beam and for transport of a single-charge beam. Each has its advantages and its disadvantages. We discuss each mode of operation below.

5.1 Transport of a multi-charge beam

Laxdal used the program LANA for the design of the vault beamline; we used the program TRANSPORT. Input of beam parameters to LANA requires the use of the so-called Twiss parameters α , β , and γ in each of the horizontal and vertical planes. These are independent of the emittance of the beam. Although TRANSPORT can be run using those parameters, the standard input to TRANSPORT uses units of cm for beam positions

(x and y) and mr for beam divergences (θ and ϕ), which are emittance dependent. Regardless of which program is used it is necessary to specify the beam emittance in order to obtain the size of the beam throughout the transport line. Consequently, it is necessary to convert between the two. This is done as follows.

Laxdal gives an example of a beam with $A/q = 3$ accelerated with the medium- β section to an energy of $E = 7.162 \text{ MeV}/\mu$. For $A = 30$ and $q = 10$ the Twiss parameters at the accelerator exit are given as $\alpha_x = -0.107$, $\beta_x = 0.799 \text{ mm/mr}$, $\alpha_y = 0.249$, and $\beta_y = 1.036 \text{ mm/mr}$. Taking the rest mass of the ion to be $E_{i0} = (30 \mu)(0.9315 \text{ GeV}/\mu) = 27.945 \text{ GeV}$ we have the following.

$$\begin{aligned} T_i &= \text{energy of ion} = (30 \mu)(0.007162 \text{ GeV}/\mu) = 0.21486 \text{ GeV} , \\ p_i &= \text{momentum of ion} = T_i \sqrt{1 + (2E_{i0}/T_i)} = 3.47199 \text{ GeV}/c , \\ p_p &= \text{momentum of equivalent proton} = p_i/q = 0.347199 \text{ GeV}/c , \\ (B\rho)_i &= \text{magnetic rigidity of ion and proton} = 3.3356 p_p = 1.15812 \text{ T-m} . \end{aligned}$$

From the given Twiss parameters we calculate the geometric phase-space values at the exit of the medium- β accelerator for $\epsilon_x = \epsilon_y = 3\pi \text{ mm-mr}$.

$$\begin{aligned} \pm x &= \sqrt{\beta_x \epsilon_x} = \sqrt{(0.799 \text{ mm/mr})(3 \text{ mm-mr})} = 1.548 \text{ mm} \\ \gamma_x &= (1 + \alpha_x^2)/\beta_x = (1 + (-0.107)^2)/0.799 = 1.266 \text{ mm/mr} \\ \pm \theta &= \sqrt{\gamma_x \epsilon_x} = \sqrt{(1.266 \text{ mr/mm})(3 \text{ mm-mr})} = 1.949 \text{ mr} \\ r_{21} &= -\alpha_x/\sqrt{1 + \alpha_x^2} = 0.107/\sqrt{1 + (-0.107)^2} = 0.1064 \\ \pm y &= \sqrt{\beta_y \epsilon_y} = \sqrt{(1.036 \text{ mm/mr})(3 \text{ mm-mr})} = 1.763 \text{ mm} \\ \gamma_y &= (1 + \alpha_y^2)/\beta_y = (1 + (0.249)^2)/1.036 = 1.025 \text{ mm/mr} \\ \pm \phi &= \sqrt{\gamma_y \epsilon_y} = \sqrt{(1.025 \text{ mr/mm})(3 \text{ mm-mr})} = 1.754 \text{ mr} \\ r_{43} &= -\alpha_y/\sqrt{1 + \alpha_y^2} = -0.249/\sqrt{1 + (0.249)^2} = -0.2416 \end{aligned}$$

We note that for a given set of $\alpha_{x,y}$ and $\beta_{x,y}$ and emittances $\epsilon_{x,y}$ the phase-space parameters x , θ , y , and ϕ scale from the above values by a factor of $\sqrt{\epsilon_{x,y}/3}$.

5.1.1 Production of a 2 mm beam spot at M5—medium- β accelerator

Table 1 lists TRANSPORT input for transport within the accelerator vault for this case ($A = 30$, $q = 10$, and $E = 7.162 \text{ MeV}/\mu$) and emittances of $\epsilon_x = \epsilon_y = 3\pi \text{ mm-mr}$. The ends of each transport section are labeled M1, M2, . . . M5. In this listing all of the quadrupoles have been taken as being of the L2, or long, type. Any section of four quadrupoles could be replaced with the shorter L1 type provided that the overall length of the section is maintained.

Note: We note that the quadrupole fields and half-apertures given in table 1 are in kG and cm respectively. The latter have been taken as 100 cm. Consequently, the strengths of the quadrupoles in units of T/m are simply the quadrupole field in kG divided by 10. This convention will be used throughout this report in any tabulation of TRANSPORT input.

The first section is 4.42 m long and matches the output of the medium- β accelerator to the parameters required for the transmission of a multi-charge beam. These are $x = y = 0.426 \text{ cm}$, $r_{21} = 0.600$, and $r_{43} = -0.600$.

The second and third sections, each also 4.42 m long, are repeating sections. In Laxdal's design the quadrupoles of each section alternate in a strength of absolute value of 3 T/m. The strengths given in table 1— ± 3.00242 T/m—are those found by TRANSPORT to be necessary to reproduce the matching parameters at the end of each of these two sections.

Sections four and five in table 1 each have a length of 4.6745 m rather than of 4.54 m as used by Laxdal. This is because of a difference in the calculation of the position of the M5 location. The fourth section is tuned to reproduce the matching parameters and the fifth section is tuned to produce a double waist at M5 with a beam spot nominally 2 mm in diameter.

For emittances larger than 3π mm-mr the settings of the first sixteen quadrupoles (VQ1, VQ2, . . . , VQ16) are *unchanged*. Only the settings of the last four (matching) quadrupoles are changed to produce the required beam size at the M5 location. These settings are given in table 2.

Figure 3 shows the beam profiles for beams with emittances of 3π , 4π , 5π , and 6π mm-mr. This figure shows the advantage of using such a transport system. Once matched to the transport system the beam envelope is smooth and its size is small. The only irregularity occurs when it is necessary to match to the required beam conditions at M5. Here approximately 60% of the quadrupole apertures are required in the final matching section—assuming that quadrupoles with bores of 2 inches are used. This value is somewhat larger than the (more desirable) use of a maximum of 50% of quadrupole aperture, but it is acceptable.

A possible problem with this transfer line is as follows. At the ends of each section of the transport line the beam spot is just that—a beam spot. As an example, for an emittance of 3π mm-mr its dimensions are approximately $\pm x = \pm y = 0.3$ cm. There is neither a waist nor a focus. Because beam diagnostics would normally be put at these end points, it may be difficult to properly assess beam quality along the beamline, particularly in the transport of a singly-charged beam.

However, a 2 mm beam spot can readily be produced at the M5 location for beams of emittances equal to or less than 6π mm-mr.

5.1.2 Production of a 1 mm beam spot at M5—medium- β accelerator

When the EMMA experiment is mounted at the TGT4 position a beam spot 1 mm or less in diameter is required at its target. To produce this beam size at the M5 location the settings of the first sixteen quadrupoles remain the same as given in table 1 and, again, only those of the four quadrupoles of the last matching section are altered to produce the appropriate beam size at the M5 location. The required settings are listed in table 3 for emittances of 3π , 4π , 5π , and 6π mm-mr.

Figure 4 shows the beam envelopes for those emittances. Again we see smooth beam envelopes along the beamline upstream of the final matching section. Beam sizes become quite large in that matching section, exceeding ± 3 cm in the horizontal plane in last two quadrupoles. Consequently, quadrupoles with larger bores would be required were it necessary to transport higher emittance beams. In fact, it would be best to use two quadrupoles, each with a bore of four inches, as the last two quadrupoles of this matching section. However, as will be shown later, large emittance beams cannot be transmitted by the transport systems to the experimental targets. We shall return to this point in a later section.

5.1.3 Production of a 2 mm beam spot at M5—high- β accelerator

As noted above, when the high- β accelerator is ready for installation the first two sections of the vault transport line will be removed and this accelerator installed in their place.

In a previous note⁸⁾ Laxdal considers transport from the exit of the high- β accelerator for the case of an acceleration energy of $E = 7.88$ MeV/ μ , $A = 30$, and $q = 5$. The Twiss parameters for this case are given as $\alpha_x = 0.023$, $\beta_x = 0.938$ mm/mr, $\alpha_y = 0.0$, and $\beta_y = 1.969$ mm/mr. In a similar manner to above we

find for emittances of $\epsilon_x = \epsilon_y = 3\pi$ that the phase-space parameters for TRANSPORT are $x = \pm 1.678$ mm, $\theta = \pm 1.789$ mr, $r_{21} = -0.0230$, $y = \pm 2.430$ mm, $\phi = \pm 1.234$ mr, and $r_{34} = 0.0$.

Quadrupoles VQ9/10/11/12 are allowed to vary independently to set the matching conditions for r_{12} and r_{43} at M3 while, at the same time, allowing quadrupoles VQ13/14/15/16 to set the complete matchings of x , y , r_{12} , and r_{43} at M4. The last four quadrupoles then fix the beam size and double-waist conditions at M5.

Table 4 lists the TRANSPORT input for transport from the high- β accelerator to produce a 2 mm spot at M5 for a beam with the above emittances. For beams of larger emittances we again change only the settings of the quadrupoles of the last matching section in order to produce the required beam size at the M5 position. The settings of these quadrupoles for emittances of 3π , 4π , 5π , and 6π mm-mr are given in table 5.

The beam envelopes for this case are shown in figure 5. It is seen that only for emittances above 5π mm-mr does the horizontal beam size exceed 1.5 cm or 60% of the quadrupole aperture if it is assumed that all quadrupoles have a bore of 2 inches.

5.1.4 Production of a 1 mm beam spot at M5—high- β accelerator

To produce a 1 mm beam spot at M5 only the fields of the last four quadrupoles are varied. Table 6 lists the settings of quadrupoles VQ17/18/19,20 that are required for this mode of operation.

Figure 6 shows the beam envelopes for a 1 mm beam spot at M5. It is seen that the bores of the last two quadrupoles of the final matching section must be large if a 1 mm beam spot is to be produced at the M5 location. That being the case it is suggested that each of these two quadrupoles has a bore of 4 inches.

5.2 Transport of a single-charge beam

As was noted previously operation of the vault section of the beamline in a multi-charge mode may not be appropriate when transporting a single-charge beam. This is because in that mode there is no specific waist or focus at the end of each of the sub-sections of the beamline and it is at these points that one may wish to have definitive beam diagnostics. This (potential) problem can be alleviated if the beamline is operated in a single-charge mode.

By a single-charge mode of operation we mean that the sections between M1 and M4 for beam from the medium- β accelerator and between M3 and M4 for beam from the high- β accelerator are each operated as a *unit* section. The section between the accelerator exit and M1 (medium- β) and M3 (high- β) is treated as a matching section that brings the beam to a double waist at the entrance of the first unit section. The unit sections then transport this beam to final matching section where the required beam size at the M5 location is produced.

There are (at least) two ways in which to operate such a system. In one, which we shall call Case 1, the first matching section brings the beam to the beam size required at M5. The remaining sections *and* the last matching section all operate as unit sections. Thus the required beam spot is transported from the accelerator exit to the M5 location with one matching requirement only. In the other, which we call Case 2, the first matching section operates to produce an intermediate beam size at its exit and this intermediate beam is transported to the last matching section in which the beam required at M5 is produced.

The difference between the two modes of operation lies in the beam sizes in the beamline. Case 1 tends to produce a larger beam size than does Case 2. Each of these modes of operation is discussed below.

5.2.1 Production of a 2 mm beam spot at M5—medium- β accelerator, Case 1

Because all distances given in table 1 are unchanged we list in table 7 *only* the settings of the (vault) quadrupoles for Case 1. Here the first matching section (between the exit of the medium- β accelerator and

M1) is tuned to produce a 2 mm beam spot at M1. Each of the remaining sections is tuned as a unitsection, thus delivering a 2 mm beam spot at the M5 location. Figure 7 shows the beam envelopes for this case.

Although the profiles shown in this figure are not as smooth as those for a multi-charge tune, they are reasonably small and are acceptable for producing a 2 mm beam spot at the M5 location.

For the beam profiles shown in figure 7 the first four quadrupoles were tuned to produce a double waist 1.7 mm in diameter at the M1 location. This double waist is translated to the M1, M2, M3, M4, and M5 locations downstream. There is ‘almost’ a double focus at each location. The term almost is used because for a double focus the R_{12} and R_{34} elements of the transfer matrix are each equal to zero. In this case given the absolute value of each of these matrix elements is less than 0.02 cm/mr, which for practical purposes is zero. These ‘foci’ are also translated downstream along with the double waists.

5.2.2 Production of a 1 mm beam spot at M5—medium- β accelerator, Case 1

To produce a 1 mm beam spot at M5 the four quadrupoles between the exit of the medium- β accelerator are set to produce a double waist at M1 of 0.9 mm diameter. The settings of quadrupoles VQ1, VQ2, VQ3, and VQ4 required to produce this size beam spot at M1 are listed in table 8 for the various emittances. All of the remaining quadrupoles have the settings listed in table 7.

Figure 8 shows the beam profiles along the beamline for this tune. This figure illustrates the problem of beam size that was alluded to above with respect to Case 1 operation. Clearly, if we wish to operate in this mode *and* to transport beams of emittance 6π mm-mr then at least one-half of the quadrupoles must have large bores. In this case bores of four inches would be appropriate. Consequently, although Case 1 operation would be suitable for a beam size of 2 mm at M5, we consider now operation in a Case 2 mode.

5.2.2 Production of a 2 mm beam spot at M5—medium- β accelerator, Case 2

For Case 2 operation with the production of a 2 mm beam spot at M5 we adjust the first four quadrupoles to produce a double waist 3 mm in diameter at the M1 location. This double waist is transmitted to the M4 location by the three unit sections downstream of M1. The final matching section of quadrupoles VQ17/18/19/20 is then adjusted to produce a double waist 2 mm in diameter at the M5 location. Quadrupole settings for VQ1/2/3/4 and VQ17/18/19/20 for this case are listed in table 9. The remaining quadrupoles are set to the settings given in table 7.

Figure 9 shows the beam envelopes for this operating mode. Again they are not as smooth as those for multi-charge operation but they are smaller upstream of M4 than are those shown in figure 7.

5.2.3 Production of a 1 mm beam spot at M5—medium- β accelerator, Case 2

Although a 1 mm beam spot could be produced at M5 by only varying quadrupoles VQ17/18/19/20, it was found that a better beam envelope could be produced throughout the beamline by setting quadrupoles VQ1/2/3/4 to produce a double waist at M1 with a horizontal size of $\pm x = 0.075$ cm and a vertical size $\pm y = 0.125$ cm. This asymmetric beam is then translated by the unit sections to the M4 location. The matching section between M4 and M5 is then adjusted to produce the required beam at the M5 location.

Table 10 lists the settings of quadrupoles VQ1/2/3/4 and VQ17/18/19/20 to produce the 1 mm beam spot at M5. The remaining quadrupoles are set to the values given in table 7.

Beam profiles along the beamline are shown in figure 10. Those between the exit of the medium- β accelerator are seen to be reasonable. Once again, however, it is seen that the last two quadrupoles of the last matching section are required to have large bores if a beam of emittance 6π mm-mr is to be transported.

5.2.4 Production of a 2 mm beam spot at M5—high- β accelerator

To produce a 2 mm beam spot at the M5 location with beam extracted from the high- β accelerator we

revert to Case 1 above. The four quadrupoles in the matching section between the exit of the high- β accelerator and M3 are adjusted to produce a double waist 1.7 mm in diameter at the M3 location. The two sections between M3 and M4 and between M4 and M5 are tuned as unit sections, thus transporting the double waist to the M5 location. The quadrupole settings for this mode of operation are given in table 11.

Figure 11 shows the beam envelopes along the beamline. The beam profiles are seen to be reasonable for this tune.

5.2.5 Production of a 1 mm beam spot at M5—high- β accelerator

To produce a 1 mm beam spot at M5 the quadrupole settings for quadrupoles VQ9 through VQ16 are retained and quadrupoles VQ17/18/19/20 are set to produce the required beam size at M5. The settings of these four quadrupoles are listed in table 12.

Figure 12 shows the beam envelopes along the beamline. As has been seen previously for the production of a 1 mm beam spot at M5, it is necessary that the last two quadrupoles of this matching section require large bores if beam of large emittance are required to be transported.

5.3 Discussion of the results of this section

In this section we have presented two modes of operation of beam transport in the vault section of ISAC-II—operation in a multi-charge mode and operation in a single-charge mode. Overall, it was shown that the former operating mode resulted in smaller beam envelopes in the vault, although there was little difference when a 2 mm beam spot was to be produced at the M5 location. However, it was noted that the single-charge mode of operation might be appropriate for the transport of singly-charged beams because of the specific beam characteristics at each of the M1 through M5 locations at which beam diagnostics could be placed.

The use of larger-bore quadrupoles in the accelerator vault has been mentioned. This will definitely be necessary when the EMMA apparatus is installed some years in the future because such quadrupoles are necessary to produce the 1 mm beam spot required at the M5 location. For this purpose it will suffice to install two quadrupoles, each with a bore of four inches, as the last two quadrupoles upstream of M5. However, these large-bore quadrupoles are *not* absolutely necessary unless a 1 mm diameter beam spot is required at any of the experimental locations that will be in operation before the EMMA experimental apparatus is installed.

As will be shown later, regardless of whether the beam size at the M5 location is 2 mm or 1 mm it is necessary that the two vault quadrupoles downstream of M5 *must* have large bores if the beams of large emittance are to be transported to the various target locations. Given that this is the case it and eventually two more such quadrupoles will be needed in the accelerator vault, a decision must be made as to whether it would be best to install all four large-bore quadrupoles initially rather than have to replace two quadrupoles at a later date. Were this not done initially it would be necessary to install new power supplies and cabling at the time the larger quadrupoles were installed.

Finally, for completeness we list in table 13(a) the input parameters to the program TRANSPORT for beam transport from the exit of the medium- β accelerator. Similar parameters are given in table 13(b) for transport of beam extracted from the high- β accelerator.

6. Beam transport to the experimental targets

In this section we describe the transport of beam to the various experimental locations. However, as this report was being written another suggestion for the initial configuration of beam transport was put forward⁹⁾. This layout is shown in figure 13.

In this configuration the TIGRESS experiment would be located at the TGT1 location and the TUDA at the TGT4 position. When the EMMA apparatus is ready for installation the transport configuration of the experimental hall shown in figure 2 would be completed. The TUDA experiment could move to the TGT6 location or could remain at the TGT4 position. The TIGRESS experimental apparatus would then shuttle between the TGT1 and TGT5 positions.

Consequently, rather than as stated previously, we first discuss beam transport to the TGT1 and TGT4 locations. Transport to the TGT4 position is dealt with first because it would probably be the first commissioned beam delivery system in the ISAC-II experimental hall.

There is one major design constraint that is common to all of the beamlines discussed below. Each dipole that is to be used has a vertical aperture of ± 11 mm and a horizontal one of ± 22 mm. The vertical aperture in particular is the most restrictive and, in some cases, definitely limits the emittance that can be transported by the beamline. In general, however, if the desired beam spot on target is 2 mm or larger in diameter there is no problem. Problems arise, however, for smaller beam diameters.

In the following sections unless otherwise stated, the beam envelopes shown are for beams with a momentum spread of $\pm 1\% \delta p/p$. This affects beam sizes downstream of the first dipole of the beamline and then only in those that are *not* doubly achromatic. Given that the beamlines to the TGT1, TGT5, and TGT6 targets have been designed to be doubly achromatic, the momentum spread of the delivered beams will only affect beam sizes between dipoles that are labeled B1 and B2 on the beamline to the TGT1 location and between dipoles labeled B3 and B4 on the beamline to the TGT5 and TGT6 positions.

Further, for consistency in what follows, all TRANSPORT listings and beam profiles have been obtained assuming that the vault section of beam transport has been tuned to the single-charge tune, case 1, of §5.2 and shown in figures 7 and 8.

A note on quadrupole nomenclature

1. Because the last two quadrupoles in the accelerator vault and the first quadrupole in the experimental area, which are colored green in figure 2, are common to all beamlines, these quadrupoles will be denoted CQ1, CQ2, and CQ3. Similarly, the six quadrupoles between the first dipole, colored green, and first cyan-colored dipole in the experimental area are common (among others) to the beamlines to TGT5 and TGT6, these quadrupoles will be denoted CQ4 through CQ9.
2. Quadrupoles downstream of these dipoles will be labeled sequentially beginning with Q1 and prefixed with 'T(target number)'. Thus the quadrupoles shown in figure 13 leading to the TGT4 and TGT4A locations are labeled T4Q1 through T4Q6 and those leading to the TGT1 position are labeled T1Q1 through T4Q7.
3. Because the quadrupoles between the two cyan-colored dipoles in figure 2 are common to beamlines to the TGT5 and TGT6 locations these are labeled T56Q1 through T56Q4 in the text and tables. However, because the TRANSPORT program allows only four characters in a label, TRANSPORT listings will show these quadrupoles as 56Q1 through 56Q4.
4. The three quadrupoles downstream of the second cyan-colored dipole in figure 2 are designated T5Q1 through T5Q3 on the leg leading to TGT5 and T6Q1 through T6Q3 on the leg leading to TGT6.

6.1 Beam transport to the TGT4 and TGT4A locations

As shown in figure 13, the beamlines to the TGT1 and TGT4 locations have their first three quadrupoles in common. The beamline to the TGT4 location is completed by installing three more quadrupoles T4Q1, T4Q2, and T4Q3 that are placed in positions symmetric with quadrupoles CQ3, CQ2, and CQ1 with

respect to the dipole labeled B1, which deflects beam 30° to the right looking downstream, in the figure. These quadrupoles are also powered symmetrically; the outer pair CQ1 and T4Q3, the middle pair CQ2 and T4Q2, and the inner pair CQ3 and T4Q1 are each powered identically but each pair is powered at a different excitation. These pairs are powered so as to reproduce at the TGT4 location the double waist at the M5 position.

Figure 14(a) shows the beam profiles along the beamline from the exit of the medium- β accelerator to the TGT and TGT4A positions. Figure 14(b) shows the beam profile between the M5 and the TGT4 positions in more detail. The (symmetric) triplet between the two target locations translates the double waist at the TGT4 location to the TGT4A location. The solid lines are profiles of beams of different emittances that have been extracted from the medium- β accelerator with a momentum spread of $\pm 1.0\% \delta p/p$. The nominal beam sizes at the TGT4 and TGT4A locations are $x = y = \pm 1$ mm; TRANSPORT was required to fit to the values of $x = y = \pm 0.85$ mm.

To show the effect of momentum spread in the extracted beams, the red dashed lines in figures 14(a) and (b) are the horizontal beam profiles of a beam with an emittance of 3π mm-mr and a momentum spread of $\pm 0.1\% \delta p/p$. The effect on the beam size for that momentum is quite obvious. On the other hand, the effect on a beam with an emittance of 6π mm-mr is not so dramatic; downstream of the B1 dipole the beam profile of a 6π mm-mr, $\pm 0.1\% \delta p/p$ beam would be virtually identical to that of the 5π mm-mr, $\pm 1.0\% \delta p/p$ beam shown in the figures. This is to be expected because for a given beam size low-emittance beams have a smaller divergence than do high-emittance beams. Therefore dispersion effects will have a larger effect on divergence of low-emittance beams than on that of high-emittance beams.

The wild excursions in the horizontal motion on either side of the B1 dipole are caused not so much by dispersion as by optics. Downstream of the dipole they are exacerbated by dispersion effects. Beam profiles in the horizontal plane would be symmetric for a mono-energetic beam—as is evident in figures 14(a) and 14(b) for a beam with an emittance of 3π mm-mr, and a momentum spread of $\pm 0.1\% \delta p/p$.

As has been noted previously the nominal target location is that designated TGT4. The distance between the TGT4 and the quadrupole immediately upstream is 1.5 m. Should this distance be too small a symmetric quadrupole triplet can be installed to increase the distance between the last upstream quadrupole and a new target location that is designated TGT4A. As shown in figures 2 and 4, the additional triplet lies 2.25 m downstream of TGT4 and 2.25 m upstream of TGT4A.

Because the first two quadrupoles downstream of the M5 location are common to all beamlines feeding the experimental hall, maintaining symmetry and beam sizes require that they (CQ1 and CQ2) and the two quadrupoles upstream of TGT4 (T4Q3 and T4Q2) have large apertures. Thus it is intended to install quadrupoles with bores of four inches at these (and other) locations. A beam of emittance 6π mm-mr and a momentum spread of $\pm 1.0\% \delta p/p$ would occupy 70% of the the apertures of such quadrupoles; one of the same emittance and a momentum spread of $\pm 0.1\% \delta p/p$ would occupy 60% of their apertures. A preferred value would be 50% but, unfortunately, no other quadrupoles are available.

Table 14 lists the TRANSPORT input for the production of a beam spot 2 mm in diameter for the case of a beam with $A = 30$ and $q = 10$ that has been accelerated to an energy of $E = 7.162$ MeV/ μ in the medium- β accelerator. This listing *begins* at the M5 location; the initial short (0.00001 m) drift labeled M5 signals that this input is to be appended to any of the beam tunes of §5 that produce a 2 mm beam spot at the M5 location. A beam of emittance 3π mr-mr was assumed in this listing. Table 15(a) lists the settings of the quadrupoles as a function of emittance. Tables 15(b) and 15(c) give the beam parameters and overall transfer matrix elements at the TGT4 and TGT4A locations, respectively, for each emittance.

It is useful to have a close look at the parameters given in tables 15(b) and 15(c). The optics design of this beamline is to reproduce at the TGT4 location the double waist at the M5 location. For practical purposes

there is also a double focus at M5; this too is reproduced (for practical purposes) at the TGT4 location. That this is so can be seen by the values of the R_{12} and R_{34} elements of the overall transfer matrix that are given in tables 15(b) and 15(c). For a double focus these elements should be zero and it is seen that they both are small.

To be doubly achromatic both the R_{16} and R_{26} matrix elements should be zero. For practical purposes the R_{16} matrix elements listed in tables 15(b) and 15(c) are zero. This means that the horizontal position of the beam at the targets are independent of the momentum spread of the beam. However, the absolute values of the R_{26} matrix elements are of the order of $4 \text{ mr}/\% \delta p/p$ and are clearly non-zero. Because of this the horizontal divergence of the beam at the TGT4 and TGT4A locations are momentum dependent. Thus the horizontal divergence at the target is a combination of that generated by the geometrical optics and that generated from chromatic effects.

This becomes quite clear when the spatial parameters of the beam are examined. Consider, for example, the case of a beam with an emittance of $3\pi \text{ mm-mr}$. At the target in the vertical plane—in which there is no dispersion—and because there is a waist one has $y = \pm 0.85 \text{ mm}$ and $\phi = \pm 3.53 \text{ mr}$; this corresponds to a vertical emittance of $\pi y \phi = \pi 0.85(3.53) = 3\pi \text{ mm-mr}$ (as advertised). However, in the horizontal plane where there also is a waist one has $x = \pm 0.85 \text{ mm}$ and $\theta = 5.49 \text{ mr}$; this corresponds to an emittance of $\pi x \theta = \pi 0.85(5.49) = 4.67\pi \text{ mm-mr}$ rather than the $3\pi \text{ mm-mr}$ emittance of the initial beam. Thus the dispersion induced in the horizontal divergence of the beam has effectively *increased* the horizontal emittance by approximately 50%.

This effect becomes smaller as the emittance is increased. At an emittance of $6\pi \text{ mm-mr}$ one sees from table 15(b) that the effective horizontal emittance is $\pi x \theta = \pi 0.85(7.916) = 6.73\pi \text{ mm-mr}$ rather than that in the vertical plane of $\pi y \phi = \pi 0.85(7.060) = 6.00\pi \text{ mm-mr}$. Thus the effective horizontal emittance is increased by approximately 12% at an initial emittance of $6\pi \text{ mm-mr}$.

Assuming that the extracted beam from the accelerator is not dispersed, it is not possible to produce a doubly achromatic beam in a beamline with only one dipole. The only way to reduce this effect is to increase the beam size at the target and/or decrease the momentum spread of the initial beam. The latter is of course a machine problem. The former can be dealt with to some extent in the beamline optics. Thus, for an emittance of $6\pi \text{ mm-mr}$, if the beam size at TGT4 is doubled to $x = y = \pm 1.7 \text{ mm}$ it is found that the horizontal divergence $\theta = 3.56 \text{ mr}$ and $\phi = 3.53 \text{ mr}$, which implies an effective increase of the horizontal emittance of approximately 1%.

This aspect of the proposed design is mentioned because the apparent increase of the horizontal emittance may need to be taken into consideration for some experiments.

Figure 15(a) shows the beam envelopes for the various emittances with beam extracted from the high- β accelerator. Those between the M5 location and the TGT4 and TGT4A locations are shown in figure 15(b). Again, the solid curves are for beams with a momentum spread of $\pm 1\% \delta p/p$ and the dotted curve is for a beam with an emittance of $3\pi \text{ mm-mr}$ and a momentum spread of $\pm 0.1\% \delta p/p$. The envelope of a beam of emittance $6\pi \text{ mm-mr}$ and a momentum spread of $\pm 0.1\% \delta p/p$ virtually overlays that of a $5\pi \text{ mm-mr}$, $\pm 1\% \delta p/p$ beam downstream of the dipole B1.

Table 16(a) lists the settings of the transport elements as a function of emittance for this case of extraction from the high- β accelerator. Listed in table 16(b) are the predictions of TRANSPORT for the beam and elements of the overall transfer matrix at the TGT4 location.

6.2 Beam transport to the TGT1 location

As noted in §4, the 10-quadrupole, 2-dipole configuration between the M5 and TGT1 locations is tuned such that the transfer matrix between the two points is $+I$ in the horizontal plane and $-I$ in the vertical

plane, thus imaging at the TGT1 location the beam spot at the M5 location. This is accomplished with a $+30^\circ$ bend in each of the B1 and B2 dipoles shown figure 13 and by powering quadrupoles equally in pairs working from the ends of the M5–TGT1 section toward its center. Thus this beamline section is symmetric about its midpoint.

Because this section is tuned as a unit section quadrupole settings are *independent* of the beam emittance provided, of course, that the beam conditions at the M5 location are those desired at the TGT1 position. These quadrupole settings also scale with momentum; consequently, they need to be changed only when the beam momentum is changed.

6.2.1 Version 1 of the transport system

Table 17(a) lists the TRANSPORT input from the M5 to the TGT1 positions for acceleration from the medium- β accelerator with either a 1 mm or a 2 mm beam spot at each of M5 and TGT1. Settings of the vault quadrupoles are given in tables 9 and 7.

Notes on data listed in table 17(a):

1. The fitting parameters listed following the TGT1 entry are for fitting between the M5 and TGT1 positions *only*. These conditions produce the unit-section behavior of this transport section.
2. The polarities of quadrupoles CQ1, CQ2, and CQ3 are *reversed* with respect to those given in table 16(a). Consequently, the power supplies of these quadrupoles must be equipped with reversing switches.

Listed in table 17(b) are the settings of the quadrupoles and dipoles for beams extracted from the medium- β and high- β accelerators for beam delivered to the TGT1 location. These settings are valid for either a 1 mm or a 2 mm beam spot at each of M5 and TGT1. We also include in this table the element settings for a beam with an equivalent proton momentum of 0.93 GeV/c. Such a beam would correspond to ions with $A = 150$ and $A/q = 7$ that have been accelerated to an energy of $E = 6.5 \text{ MeV}/\mu^{10}$. This (equivalent proton) momentum is the design limit of dipoles B1 and B2.

Table 18(a) lists the beam parameters at the M5, MID (the symmetry point of the system), and TGT1 locations; a beam with a momentum spread of $\pm 1\% \delta p/p$ has been assumed. It is seen that the beam conditions at M5 are reproduced at TGT1. Table 18(b) gives the elements of the overall transfer matrix from the medium- β exit to the TGT1 location. Here it is seen that the beam is doubly achromatic; that the R_{16} and R_{26} matrix elements are zero implies that there is neither spatial nor angular dispersion dispersion at the target.

There is also a double waist at the target location. Table 18(b) also shows that there is *almost* a double focus there too because the R_{12} and R_{34} matrix elements, which should be zero for a double focus, are small.

Figure 16(a) shows the beam profiles for beam extraction from the exit of the medium- β accelerator to the TGT1 position. Figure 16(b) shows the profiles in more detail between the M5 location and the target position. In each case the vault quadrupoles have been tuned to produce a 2 mm beam spot at the M5 position. Therefore the M5–TGT1 transfer line produces the same beam spot at the TGT1 location. It is seen that the M5–TGT1 transfer line easily accommodates beams with emittances of $6\pi \text{ mm-mr}$ and below when required to produce a 2 mm beam spot at the TGT1 target location.

Although not listed in the tables, the R_{16} and R_{26} matrix elements of the overall transfer matrix at the MID location are $R_{16} = -0.5505 \text{ cm}/\% \delta p/p$ and $R_{26} = 0 \text{ mr}/\% \delta p/p$, conditions necessary at the symmetry point of an overall non-dispersive system. Thus there is spatial dispersion there but there is no angular

dispersion at that point. The effects of this spatial dispersion between dipoles B1 and B2 are seen in figures 16(a) and 16(b). In these figures the solid curves are for a beam with a momentum spread of $\pm 1\% \delta p/p$. The dotted curve is for a beam with a momentum spread of $\pm 0.1\% \delta p/p$ and an emittance of 3π mm-mr.

Table 19(a) lists as a function of emittance the beam parameters at the M5, MID, and TGT1 locations for the production of a 1 mm beam spot at the TGT1 target with extraction from the medium- β accelerator. Elements of the overall transfer matrix at the TGT1 position are given in table 19(b) for this tune.

The profiles of a beam extracted from the medium- β accelerator with the system adjusted to produce a 1 mm beam spot at the M5 and TGT1 locations are shown in figure 17(a). Figure 17(b) shows the profiles between M5 and TGT1 in more detail. From the latter it becomes obvious that beams of emittance greater than 4π mm-mr cannot be transported in the proposed system without filling the apertures of quadrupoles CQ1, CQ2, T1Q6, and T1Q7, the first two and last two quadrupoles shown in figure 17(b). Further, this figure indicates that even for an emittance of 4π mm-mr the apertures of the first quadrupole downstream of B1 and that upstream of B2 should be at least 60 mm in order to avoid filling too much of their apertures. Ideally, all four quadrupoles between the dipoles should have larger apertures.

TRIUMF has on hand five quadrupoles of type L5 that would be suitable for use in this area. These quadrupoles have 70 mm apertures and would be ideal these locations. Unfortunately, these quadrupoles require different power supplies than are needed for the other quadrupoles, the 4-inch bore quadrupoles excluded. However, for operation until the EMMA experiment is ready to be installed, only a 2 mm diameter beam spot is required and the conventional L2 variety quadrupoles would be satisfactory. Later they could be replaced by the type L5 when required. In anticipation of the discussion of the beamlines to the TGT5 and TGT6 locations we mention that more type L5 quadrupoles will be required for that beamline.

Settings of the vault quadrupoles for beam delivery from the high- β accelerator to the M5 location were given in tables 11 and 12 and those of the elements of the M5 to TGT1 section in table 17(b). Table 20(a) lists as a function of emittance the beam parameters at the M5, MID, and TGT1 locations for a tune that produces a 2 mm beam spot at the TGT1 target. Elements of the overall transfer matrix to the TGT1 target are given in table 20(b) for this tune.

Figures 18(a) and 18(b) show beam profiles along the beamline for extraction from the high- β accelerator with the production of a 2 mm diameter beam spot at the TGT1 location.

Table 21(a) gives the beam parameters at the M5, MID, and TGT1 locations for a tune that produces a 2 mm beam spot at the TGT1 target. Elements of the overall transfer matrix to the TGT1 target are given in table 21(b) for this tune. Beam profiles along the beamline are shown in figures 19(a) and in 19(b) in more detail. Comments made above concerning the data shown in figures 16(a) and 16(b) and in figures 17(a) and 17(b) apply as well to figures 18(a) and 18(b) and to figures 19(a) and 19(b) respectively.

It should also be pointed out that the beam profiles between the M5 and TGT1 locations are identical for a given spot size and are independent of the accelerator being used. Thus figures 16(b) and 18(b) that show profiles for a 2 mm beam spot are the same. Similarly, this is also true for figures 17(b) and 19(b) that show profiles for a 2 mm beam spot. This is a property of the unit (except for sign) transformation between these two locations.

It has been stated that the M5 to TGT1 transport section has been designed, apart from sign, as a unit section. That being the case one would expect that beam profiles throughout this section would be the same for extraction from both the medium- β and high- β accelerators for a given beam size at M5. That this is indeed the case may be seen by examination of figures 16(b) and 18(b) for the production of 2 mm beam spot and figures 17(b) and 19(b) for the production of 1 mm beam spot.

6.2.2 Version 2 of the transport system

As noted above, the polarities of quadrupoles CQ1, CQ2, and CQ3 were reversed from those settings for the TGT4 target. The cost of reversing switches is estimated at \$1K per pole or \$2K per magnet¹¹). Because a total of six quadrupoles (CQ1, CQ2, CQ3, T1Q5, T1Q6, and T1Q7) would require polarity switches, the cost for them would be in the order of \$12K. Consequently, it is useful to see if it is possible to find a beam-transport system to the TGT1 target that does not require the use of reversing switches.

In table 21(c) the settings of the elements between the M5 and TGT1 locations for a configuration in which the polarities of the first and last three quadrupoles are reversed relative to those of §6.2.1. These apply to extraction from both the medium- β and the high- β accelerators. Settings for the highest momentum (0.93 GeV/c) that can be accepted by the existing dipoles are also given.

In order to make this truly a unit (except for sign) section it was necessary to slightly shift the positions of the two doublets between dipoles B1 and B2. Thus the distance from the exit of dipole B1 to the entrance of quadrupole T1Q1 and that from the exit of quadrupole T1Q4 to the entrance of dipole B2 were increased from 1.52211 m given in table 17(a) to 1.59479 m. To keep a constant overall length of the system the distance from the exit of quadrupole T1Q2 to the midpoint of the section and that from the midpoint to the entrance of quadrupole T1Q3 were reduced from the value of 1.63400 m given in that table to 1.56132 m. Contrary to what might be expected because of the reversal of the quadrupole polarities, the transfer matrix between the M5 to the TGT1 locations remains $-I$ in the horizontal plane and $+I$ in the vertical plane.

Table 21(d) lists the beam sizes at the M5, MID, and TGT1 locations for a tune that produces a beam spot 2 mm in diameter at the TGT1 target for a beam extracted from the medium- β accelerator. At the midpoint of this section the spatial dispersion is $R_{16} = -0.75 \text{ cm}/\% \delta p/p$ and the angular dispersion R_{26} is zero. Table 21(e) gives the elements of the overall transfer matrix there for this tune. Figure 19(c) shows the beam profiles along this beamline between the M5 and TGT1 locations as a function of emittance. The beam profile for the production of a beam spot of the same size from beam extracted from the high- β accelerator will be identical to that shown in figure 19(c).

Beam sizes at the above locations for a tune that produces a beam spot 1 mm in diameter at the TGT1 target are given in table 21(f). Elements of the overall transfer matrix at the target are given in table 21(g). The beam profiles between M5 and TGT1 are shown in figure 19(d).

6.2.3 Comparison of the two tunes

From the settings of the transport elements given in table 17(b) for version 1 and in table 21(c) for version 2 it is seen that the latter tune requires that the first and last three quadrupoles run slightly harder than does the former tune. However, the tune of version 1 requires that the four quadrupoles between the two dipoles be powered significantly higher than does the tune of version 1. On the other hand, neither tune demands that the quadrupoles be powered beyond their design specifications.

More important however are the beam envelopes in the two versions of the transport section. A comparison of figures 16(b) and 19(c) showing beam envelopes for a 2 mm beam spot shows more-or-less what one would expect—roughly speaking the horizontal and vertical beam profiles are reversed in the two tunes. In the first and last two quadrupoles of the beamline the vertical profile is slightly larger in version 2 than the horizontal profile in version 1. On the other hand the vertical profile of version 2 is smaller than the horizontal profile in version 1 in the four quadrupoles between the two dipoles but the reverse is true at the symmetry point of the section. In the dipoles the vertical profile is slightly smaller in the version 2 tune than in that of version 1.

A comparison of figures 17(b) and 19(d), which show beam envelopes for the production of a 1 mm beam

spot, show similar results. Restricting discussion to emittances of 4π mm-mr and lower it is again seen that the horizontal beam size in the first and last two quadrupoles is slightly larger in the version 1 tune than the vertical beam size there in the version 1 tune. Again, the vertical and horizontal beam sizes are larger at the midplane for the version 2 tune than for the version 1 tune. The beam is smaller in the horizontal plane in the quadrupoles between the the dipoles for the version 2 tune than for the version 1 tune.

Overall there is little difference in the two tunes except at the midplane of the systems. There the version 1 tune for a 2 mm beam spot produces a beam size of $(\pm x, \pm y) \approx (0.6 \text{ cm}, 0.2 \text{ cm})$ whereas with the tune of version 2 that size is $(\pm x, \pm y) \approx (0.9 \text{ cm}, 1 \text{ cm})$. The increase in the horizontal beam size is caused by the increased dispersion at the midplane of the version 2 tune— $0.75 \text{ cm}\% \delta p/p$ —as opposed to $0.55 \text{ cm}\% \delta p/p$ for the version 1 tune. That in the vertical plane arises from the optics of the beamline. For the 1 mm tune, beam sizes at the midplane are approximately twice that in the version 2 tune than in the version 1 tune— $(\pm x, \pm y) \approx (1 \text{ cm}, 0.5 \text{ cm})$ and $(\pm x, \pm y) \approx (0.5 \text{ cm}, 0.3 \text{ cm})$ respectively. If such a beam size is suitable for any instrumentation that is inserted at the midplane it is recommended that the version 2 tune of the beamline be the used in practice. This would save the expense of purchasing six reversing switches.

6.3 Beam transport to the TGT5 and TGT6 locations

Historically the beamlines to the TGT1 and TGT2 target positions were the first to be designed. Subsequently it was suggested that the transport system be expanded to provide beams to the two additional target locations TGT5 and TGT6. The result was the configuration shown in figure 2.

This was achieved by adding a quadrupole triplet downstream of the first dipole in the experimental hall. These quadrupoles, which have been designated CQ4/5/6, together with the last two quadrupoles in the accelerator vault and the first quadrupole in the experimental area, which have been designated CQ1/2/3, form a transport system that has two purposes. First, this section was designed to reproduce at the M6 location the 2 mm diameter double waist that had been formed at the M5 position. This section is also used to produce the a 1 mm diameter spot at the M6 location should such a beam spot be required at the TGT5 target. Second and equally important, this section was designed to maintain a small vertical beam size through the B1 dipole; thus a vertical waist was required at the center of that dipole. In principle, five quadrupoles are required to meet the five conditions of horizontal and vertical beam sizes, a double waist, and a waist in the B1 dipole. However, the use of six quadrupoles worked well (primarily because the transport section is not symmetric) and no attempt was made to refine the transport section further.

A prime consideration in the design of the section between the M5 and TGT5 locations was that they be positioned such that an experimental setup could be moved along a straight line from the TGT5 location to the TGT1 location. This condition defined the length of the beamline between M6 and the TGT5 target location.

6.3.1 Beam transport to the TGT5 location

The section between the M6 and TGT5 locations operates in the same manner as that described above for beam transport between the M5 and TGT1 positions. Thus the transfer matrix between M6 and TGT5 is $+\mathbf{I}$ in the horizontal plane and $-\mathbf{I}$ in the vertical plane. This transfer line produces a double waist at the TGT5 location. The line is also doubly achromatic.

Table 22 lists the TRANSPORT input for the production of a beam spot 2 mm in diameter at the TGT5 target location with a beam extracted from the medium- β accelerator with an emittance 3π mm-mr. The vault quadrupoles are powered according to the values listed in table 7. Table 23(a) lists the settings of the elements as a function of emittance. Table 23(b) gives the beam sizes at the M6, MID, and TGT5 locations for this tune. Notice that this table indicates that the design value for the beam spot at TGT5 was $x = y = \pm 0.80 \text{ mm}$ rather than the value of $x = y = \pm 0.85 \text{ mm}$ that has been used previously. In table

23(c) are listed the elements of the overall transfer matrix at the TGT5 target.

Figures 20(a) and 20(b) show profiles along the beamline for this tune. This data shows that there should be no problem with the production of a 2 mm beam spot at the TGT5 location. Aperture limits of dipoles B1, B3, and B4 are not exceeded. Because operation of this beamline between M6 and TGT5 is similar to that of the beamline between M5 and TGT1, there is spatial dispersion in the region between dipoles B3 and B4. At the MID location this dispersion has a magnitude of $1.7 \text{ cm}/\% \delta p/p$. There is no angular dispersion at this point. However, the effect of momentum spread in the primary beam on the horizontal beam size between the dipoles is quite evident in figures 20(a) and 20(b).

To produce a beam spot (nominally) 1 mm in diameter at TGT5 the settings of the vault quadrupoles are maintained to produce a 2 mm beam spot at M5 and those of quadrupoles CQ1 through CQ6 are set to produce a 1 mm diameter double waist at M6. The settings for this situation are given in table 24(a). Beam sizes at the M6, MID, and the TGT5 locations are given in table 24(b). Elements of the overall transfer matrix at TGT5 are given in table 24(c).

Figures 21(a) and 21(b) show beam profiles along the beamline when a 1 mm beam spot is produced at the TGT5 location. From these figures it is again seen that a 1 mm beam spot can be produced there only for emittances of $4\pi \text{ mm-mr}$ or less. Even at an emittance of $4\pi \text{ mm-mr}$ it is seen that quadrupole CQ5 must have a large bore; a quadrupole of the type L5 that was mentioned in §6.2 would be adequate. Further, approximately 85% of the vertical apertures of dipoles B3 and B4 are occupied by the beam at that emittance.

It will be noted that table 19 shows that quadrupoles CQ7, CQ9, T5Q1, and T5Q3 have been taken to be of the type L5, which have an effective length 0.2 m and a bore diameter of 70 mm. This was based on the assumption that a larger emittance would be transported through the system. They are no necessary for the production of a 2 mm beam spot from a beam of emittance $6\pi \text{ mm-mr}$ or lower. However, if a 1 mm beam spot will be required, approximately 80% of the apertures of these quadrupoles would be filled.

Similarly, if the four quadrupoles between B3 and B4 are of type L2 as indicated in table 19, approximately 70% of their apertures would be filled *if* the momentum spread of the primary beam is $\pm 1\% \delta p/p$. The difference in the beam envelope between a beam with that momentum spread and one with a momentum spread of $\pm 0.1\% \delta p/p$ is readily apparent in figures 21(a) and 21(b).

Quadrupole settings are given in table 25(a) for the production of a 2 mm beam spot at the TGT5 location with beam extracted from the high- β accelerator. Again, because the transport section between M6 and the TGT5 target operates as a unit section (aside from sign) the settings of elements downstream of M6 are independent of emittance and scale with momentum. Table 25(b) lists the beam sizes at the M6, MID, and the TGT5 positions for this case. The elements of the overall transfer matrix at the TGT5 target are given in table 25(c).

Figures 22(a) and 22(b) show the beam profiles along the beamline for this case. The effect of dispersion between the two dipoles is again seen. Dispersion at the MID position is the same as that for extraction from the medium- β accelerator— $1.7 \text{ cm}/\% \delta p/p$.

Table 26(a) lists the quadrupole settings for the production of a 1 mm beam spot at the TGT5 target when beam is extracted from the high- β accelerator. Because of the (aside from sign) unit transformation between the M6 and TGT5 positions settings of the elements downstream of M6 are a function of momentum only and not a function of emittance. Beam sizes at the M6, MID, and TGT5 locations for this tune as a function of emittance are given in table 26(b). Elements of the overall transfer matrix at the TGT5 target are listed in table 26(c). Again, because the R_{16} and R_{26} elements are zero a doubly-achromatic condition exists at the TGT5 target location.

Figures 23(a) and 23(b) show the beam profiles along the beamline for this case. The effect of dispersion between the two dipoles is again seen. The absolute value of the dispersion at the MID position is the same as that for extraction from the medium- β accelerator— $1.7 \text{ cm}/\% \delta p/p$.

One aspect of these tunes to the TGT5 location needs to be noted. Because of the (relatively) large dispersion at the midpoint of this transport section the beam size there can be dominated by the dispersion component. This is seen in the data presented in tables 23(b), 24(b), 25(b), and 26(b) for which a momentum spread of $\pm 1\%/\delta p/p$ was assumed in the primary beam. The effect on the beam sizes between the B3 and B4 dipoles as a function of momentum spread of the primary beam is clearly shown in figures 20 through 23. Consequently, care to have appropriate beam clearance in this region may have to be taken should the accelerated beam have a large momentum spread.

6.3.2 Beam transport to the TGT6 location

Because it has been indicated that a 2 mm beam spot at the TGT6 target is suitable we report here only the beam-transport settings for the production of such a beam size at the target location.

To deliver beam to TGT6, the direction of the field of dipole B4 is reversed. As a result it is not possible to produce a system that has a transfer matrix between M6 and TGT6 that is $+\mathbf{I}$ in the horizontal plane and $-\mathbf{I}$ in the vertical plane *and* is simultaneously doubly achromatic at the target. Consequently, this section of beamline is designed to produce at the target location a double waist of the size of that at M6 *and* a doubly achromatic condition.

The settings of the vault quadrupoles and quadrupoles CQ1 through CQ6 remain the same as those for the production of a 2 mm beam spot at the TGT5 target. In table 27 are listed the settings of the elements downstream of M5 that are required for extraction from the medium- β accelerator. It is noted that these settings are a function of emittance because the transport section is not a unit section between M6 and the TGT6 locations.

Table 28(a) lists the beam sizes at the M6, MID, and TGT6 locations as a function of emittance. We note here that at the symmetry point the design of this section is such that there is *no* spatial dispersion—that is, the R_{16} matrix element is zero. There is, however, angular dispersion of the order of $22 \text{ mr}/\% \delta p/p$ there. Notice that the fitting requirements in this run were for a beam 1.6 mm in diameter. Table 28(b) gives the elements of the overall transfer matrix at the TGT6 target position. Figure 24(a) shows the beam envelopes along the beamline for this particular tune. These are shown in more detail between M5 and the TGT6 position in figure 24(b).

Table 29 lists the element settings between M5 and the TGT6 locations for the production of a 2 mm beam spot from beam extracted from the high- β accelerator. Beam sizes at the M6, MID, and TGT6 locations are given in table 30(a) as a function of emittance. In this case the fitting requirements were a beam 1.7 mm in diameter. Elements of the overall transfer matrix at the TGT6 location are given in table 30(b). Figure 25(a) shows the beam envelopes along the beamline for this particular tune. These are shown in more detail between M5 and the TGT6 position in figure 25(b).

The penalty paid in not being able to operate the M6 to TGT6 section of beamline as either $+\mathbf{I}$ or $-\mathbf{I}$ section together with the conditions of double achromaticity is that quadrupole settings are a function of both the momentum and of the emittance of the extracted beam. There is, however, an alternate mode of operation that eliminates retuning of the M6 to TGT6 section as a function of emittance. Unfortunately, it too has its drawbacks.

6.3.3 Alternate beam transport to the TGT6 location

The section of beamline between the M6 and TGT6 locations can be tuned such that the transfer matrix

between these locations is $-I$ in geometric space—each of the $x-\theta$ and $y-\phi$ phase spaces—and such that the beam is spatially achromatic at the TGT6 target but has angular dispersion there. However, it is important to stress that the spatially achromatic condition occurs *only* at the target location; at any other point downstream of the B3 dipole both R_{16} and R_{26} are non-zero.

Table 31(a) lists the settings of the elements between the M6 and TGT6 locations to produce a 2 mm beam spot at the TGT6 target location for extraction from the medium- β and from the high- β accelerators. Upstream elements are set according to values listed in tables 27 and 29. Beam sizes at the M6, MID, and TGT6 locations are given in table 31(b). Note that the beam is strongly convergent at the midpoint of the section. At the midpoint there is a small amount of spatial dispersion ($R_{16} = -0.72 \text{ cm}/\% \delta p/p$) and a large amount of angular dispersion ($R_{26} = 19.7 \text{ mr}/\% \delta p/p$). At the TGT6 target there is a double waist.

However, because of the angular dispersion there the horizontal divergence is (relatively) large. As was discussed in §6.1, the angular dispersion causes an effective increase in the horizontal emittance that could be detrimental to experiments performed at this location.

Table 31(c) lists the elements of the overall transfer matrix at the TGT6 target location. It is seen from this table that there is no spatial dispersion ($R_{16} = 0$) but there is a moderate angular dispersion ($R_{26} = -6.1 \text{ mr}/\% \delta p/p$).

Table 31(a) lists the settings of the elements between the M6 and TGT6 locations to produce a 2 mm beam spot at the TGT6 target location for extraction from the medium- β and from the high- β accelerators. Upstream elements are set according to values listed in tables 27 and 29. Beam sizes at the M6, MID, and TGT6 locations are given in table 31(b). Note that the beam is strongly convergent at the midpoint of the section. At the midpoint there is a small amount of spatial dispersion ($R_{16} = -0.72 \text{ cm}/\% \delta p/p$) and a large amount of angular dispersion ($R_{26} = 19.7 \text{ mr}/\% \delta p/p$). At the TGT6 target there is a double waist. However, because of the angular dispersion there the horizontal divergence is (relatively) large. As was discussed in §6.1, the angular dispersion causes an effective increase in the horizontal emittance that could be detrimental to experiments performed at this location.

Table 31(c) lists the elements of the overall transfer matrix at the TGT6 target location. It is seen from this table that there is no spatial dispersion ($R_{16} = 0$) but there is a moderate angular dispersion ($R_{26} = -6.1 \text{ mr}/\% \delta p/p$).

Figure 26 shows the beam profiles between the M5 and TGT6 locations when the beamline is tuned to produce a 2 mm diameter beam spot with beam extracted from the medium- β accelerator. Beam profiles would be the same for beam extracted from the high- β accelerator with the production of a 2 mm beam spot. The (unlabeled) M6 position lies at the hatch mark between between dipoles B1 and B3. The effect of the spatial dispersion on the horizontal beam size between dipoles B3 and B4 is evident in this figure. However, the vertical beam size in this region requires that the four quadrupoles there have large apertures. They would have to be quadrupoles of the type L5 if emittances larger than 5π mm-mr were to be transported to the target.

Unfortunately, as is clearly visible in figure 26, the vertical beam size in dipoles B3 and B4 is large. The vertical aperture of each of these dipoles is 22 mm or ± 11 mm about their symmetry plane. The vertical beam size is maximum at the exit of dipole B3 and at the entrance of dipole B4. At those points the vertical beam size is ± 7.8 mm for an emittance of 3π mm-mr and ± 10.3 mm for an emittance of 4π mm-mr. At higher emittances the beam sizes exceed the vertical apertures of the dipoles. To allow for the possibility of beam halo one would prefer that the vertical beam height be kept to one-half of the vertical aperture (≈ 6 mm) or less. Consequently, unless one wishes to be restricted to beams of low emittance this alternate solution is not viable.

7. Revision of the transport line in the accelerator vault

While this report was being written a decision was made to alter the quadrupole configuration in the accelerator vault. Also a discrepancy concerning the location of the east wall of the accelerator vault was clarified. We deal with the latter first.

In laying out the beamlines reported here an Cartesian coordinate frame is used. The origin of the coordinate system is located at the intersection of a north-south through the ISAC-I rfq and an east-west line through the ISAC-I DTLs. The positive y axis points north and the positive x axis is directed east. The intersection of a line drawn through the accelerators and beamlines in the accelerator vault is located at the point $(x, y) = (0 \text{ m}, 19 \text{ m})$ in this coordinate system. There are (at least) two other fixed points: the exit of the medium- β accelerator and the location designated M5 in this report. The former is defined by the accelerator itself and has the coordinate $(x, y) = (26.101 \text{ m}, 19 \text{ m})$ ⁸⁾. The latter is defined by the transport system to the experimental area as the distance between the M5 location and the wall that separates the accelerator vault and the experimental area. It is defined in this report to be 3.240 m. The length of the transport line from the exit of the medium- β accelerator to the M5 point thus depends on the distance from the x -axis to the vault wall.

Recently that distance was measured and found to be $(51,682 \pm 2) \text{ mm}$ ¹¹⁾. A result of this measurement is that the value used in this report for this distance was 10 mm too long. Albeit this is a small error and is easily corrected, but recalculations are required.

Modification of the transport line itself involves using two types of quadrupoles. In this report all of the quadrupoles between the exit of the medium- β accelerator and the M5 location have been assumed to be of the L2 variety. These have nominal effective lengths of 0.325 m, a nominal gradient of 27.0 T/m, and a maximum gradient of 30 T/m. Three of the five quadruplets in the vault—the first, third, and fifth—will use these quadrupoles. The change is that the remaining two quadruplets—the second and fourth—will use quadrupoles of the L1 type. Their nominal effective lengths are 0.180 m and their nominal and maximum gradients are the same as the type L2 quadrupoles.

In table 32, which was constructed by A. Hurst¹³⁾, are listed the quadrupoles that will be used between the exit of the medium- β accelerator and the M5 location. Given that all of these quadrupoles have been mapped both the nominal and the measured effective lengths of the quadrupoles are included. However, the drift lengths that are listed are relative to the *nominal* effective length. Therefore it is recommended that the appropriate distances be added/subtracted from the upstream and downstream distances for each quadrupole doublet.

In the column headed ‘Label’ are the nomenclatures that are to be used for these quadrupoles; these correspond to the labels VQ1, VQ2, etc that have been used in this report. The labels M1 through M5 are the locations similarly designated in this report.

Thus the distance from the point $(x, y) = (0 \text{ m}, 19 \text{ m})$ to the M5 location is $(26.101 \text{ m} + 22.340 \text{ m}) = 48.441 \text{ m}$. Then the distance from M5 to the wall is $(51.682 \text{ m} - 48.441 \text{ m}) = 3.241 \text{ m}$, 1 mm longer than requested.

8. Discussion

This note has presented a comprehensive overview of the present status of the beam transport to the experimental area of ISAC-II. Because of the information given above in §7 the results given for beam transport in the accelerator vault will require recalculation. However, because of the small changes in distances, there will be no significant changes to the results presented. Calculations from the M5 location to the various targets in the experimental area will be unaffected.

Throughout these calculations the effect of various emittances has been noted on the sizes of the beam in the transport sections. It must be remembered that the emittances used are based on *estimates* of the emittances to be expected from the accelerators. Until those emittances have been measured beam sizes should *not* be taken as engraved in stone. Only when actual emittances are used will it be possible to calculate beam envelopes with more certainty.

It also has been noted several times that the use of quadrupoles with large apertures is required in some cases. In general, large-bore quadrupoles are *not* required for any tunes that produce a beam spot of 2 mm diameter at any target *except* as listed below.

a) During initial operation it is assumed that a beam spot 2 mm in diameter will be standard at target locations TGT1 and TGT4/4A.

1. The last two quadrupoles in the accelerator vault—those labeled CQ1 and CQ2 in this report—are required to have large bores. For reasons of symmetry the two quadrupoles immediately upstream of the TGT1, labeled T1Q6 and T1Q7, and TGT4, labeled T4Q2 and T4Q3, are required to be of the same type.

It is recommended that these be TRIUMF standard 4Q14/8 quadrupoles. It is further recommended that they be installed in the initial beamline configuration shown in figure 13.

2. If it is intended to install the extension between TGT4 and TGT4A as shown in figure 14(b), it is recommended that the middle quadrupole of the triplet also be a standard 4Q14/8 quadrupole.

b) When beam transport to the is installed to the TGT5 and TGT6 targets, the latter will presumably be working with beams of large emittance—that is, low energy.

1. At an emittance of 6π mm-mr the vertical beam size in the middle quadrupole, labeled CQ5 in this report, of the triplet that lies between dipole B1 and the M6 location is ± 20 mm and fills 80% of the beam pipe.

It is recommended that quadrupole CQ5 be one of the L5 variety.

c) The design of the beamlines to the TGT5 and TGT6 targets purposely uses type L5 and type 4Q14/8 quadrupoles. This was done to shorten these beamlines such that the TIGRESS experimental apparatus could be moved between the TGT5 and TGT1 locations. In the terminology used in this report, quadrupoles CQ7, CQ9, T5Q1, T5Q3, T6Q1, and T6Q3 are type L5 quadrupoles. Quadrupoles CQ8, T5Q2, and T6Q2 are type 4Q14/8 quadrupoles.

d) When the apparatus for the EMMA experiment has been installed a beam spot of 1 mm in diameter (or smaller) is required.

1. To produce the required 1 mm spot at the M5 location it is necessary to replace vault quadrupoles VQ19 and VQ20 with quadrupoles of the 4Q14/8 family.
2. The four quadrupoles between dipoles B1 and B2 must be replaced with quadrupoles of the L5 type if version 1 of the beamline to the TGT1 target is installed.
3. If version 2 of the beamline is installed replacement of those quadrupoles should be considered. Although not absolutely necessary, this would make accommodation of the larger beam size at the midplane less difficult. Perhaps these quadrupoles should be installed in the initial configuration. If so, four new power supplies are required.

In this report only the transport of singly-charged beams has been considered. Transport of multi-charged beams within the accelerator vault was given only to report what had been done to date. In fact, multi-charged beams cannot be transported to targets on any of the beamlines considered in this report because only one charge would be transported; the others would be lost after passing through the first dipole.

A multi-charged beam could be transported only on a ‘straight-through’ beamline—that is, a beamline with dipole B1 turned off. However, as that beamline is presently configured it too cannot successfully transport a multi-charged beam. This is because beamline sections for transporting such a beam must be (relatively) short (≈ 5 m) and with the B1 dipole installed this cannot be done.

It has been stated that with the existing B1 and B2 dipoles it is possible to produce a beam spot 1 mm in diameter at the TGT1 target *provided* that it is required to transport beams with emittances of 4π mm-mr or less. It has also been noted that the production of such a beam spot at the TGT5 (or TGT6, for that matter) is practical only for beams of emittances of 3π mm-mr or less. The reason for this is that the apertures of B3 and B4 are too small. Although a beam spot of 1 mm diameter has not been requested, it is possible that such may be required in the future. Should this turn out to be the case it is recommended that these dipoles be redesigned with larger apertures. To accept beams of emittance 6π mm-mr and less their *clear* apertures should be at least 6 cm. This implies an air gap of at least 3 inches. Further, should this be contemplated, consideration should also be given to the replacement of dipoles B1 and B2.

As has been mentioned previously, the quadrupole configuration in the accelerator vault that has been used in this report is incorrect. A future note will clarify this layout.

Note added in proof

Early this year R. Laxdal asked the following question concerning the production of 1 mm diameter beams at the TGT1 location.

Given the difficulty in producing a 1 mm diameter beam spot at the EMMA target because of aperture constraints, is it possible to operate this beamline in the 2 mm beam spot mode and add a matching section to produce the required beam size further down the beamline? Even if special quadrupoles were required this might prove less costly than procuring larger aperture quadrupoles for the main beamline.

A first attempt to find such a solution was not successful. However, when this question was raised recently again it was found that indeed there was a feasible solution. In this section we give two possible scenarios that could prove suitable.

Scaling from drawing ISK0116U the distance from the TGT1 target location to the north wall of the experimental area is 20.1 m (along the beamline). The length of the EMMA experimental apparatus scales to approximately 9.3 m. Thus there are approximately 10.8 m along the beamline from the end of the EMMA apparatus to the north wall. Assuming a distance of (at least) 2 m between the end of the EMMA equipment and the wall would allow an insertion with a maximum length of 8.8 m. We take this maximum insertion length to be 8.5 m. It is also assumed that the minimum distance downstream of TGT1 for the location of any transport elements is 1.5—m. A like distance is assumed between the last transport element and the EMMA target, which we call TGT1A.

Table 33 lists the settings for a VHHV configuration of quadrupoles that will produce a 1 mm beam spot at the TGT1A target. The settings are given as a function of emittance; it is seen that some tuning is required as a function of emittance.

Quadrupole types have been optimized for the predicted beam sizes along the beamline. The first quadrupole downstream of TGT1 is one of the type L2, the second and fourth are of the type 4Q14/8,

and the third is of the type 8Q16/8—a standard 8-inch quadrupole. The short drift lengths upstream and downstream of the 4Q14/8 and 8Q16/8 quadrupoles account for the differences between the physical and effective lengths of these two quadrupole types. Effective lengths of the types L1, L2, and L5 have been found to be approximately the same as their physical lengths. The length of this insertion is 7.795 m and is less than the maximum length quoted above.

The reason for this choice of quadrupoles is seen in figure 27(a), which shows the beam profiles as a function of emittance. In this and the following figure quadrupoles have been labeled IQ n for the n th I(nsertion) Q(uadrupole). With this configuration all emittances of 6π mm-mr and less are transmitted to the TGT1A target.

As a second and shorter example, we give the transport settings for a VHVHV configuration in table 34. Again, these are given as a function of the emittance of the beam. The first, second and fifth quadrupoles are of the type L5, the third is of type 4Q14/8, and the fourth is of type 8Q16/8. In this configuration the setting of quadrupole IQ2 is critical; it has been fixed at a low value in order to maintain the VHVHV tuning. The length of this insertion is 6.623 m and is approximately 1.2 m shorter than that of example 1, albeit there is one additional quadrupole involved.

Figure 27(b) shows the beam envelopes along this particular beamline layout. It is seen again that all emittances of 6π mm-mr and less are transmitted to the TGT1A target.

References

1. G. M. Stinson, *An additional beamline in the ISAC-II experimental area*, TRIUMF report TRI-DNA-04-3, March, 2004.
2. G. M. Stinson, *Beam transport from the medium β exit to beam transport to the ISAC-II experimental area*, TRIUMF report TRI-DNA-04-2, February, 2004.
3. G. M. Stinson, *A revision of beam transport to the ISAC-II experimental area*, TRIUMF report TRI-DNA-04-1, January, 2004.
4. Z. H. Peng and R. E. Laxdal, *A Design Layout for ISAC-II Post-SCLinac Beamline (HEBT-II)*, TRIUMF report TRI-DN-01-xx, December, 2003.
5. G. M. Stinson, *On the use of existing magnets during the initial operation of the ISAC-II experimental area*, TRIUMF report TRI-DNA-03-1, March, 2003.
6. R. E. Laxdal, *Private communication*, TRIUMF, December, 2003.
7. G. M. Stinson, *A preliminary study of beam transport to the ISAC-II experimental area*, TRIUMF report TRI-DNA-01-4, September, 2001.
8. R. E. Laxdal and M. Pasini, *ISAC-II Optics Specifications*, TRIUMF report TRI-DN-01-xx, March, 2002.
9. G. M. Stinson, *ISAC II initial layout as of May 18, 2005*, Memo to J.-M. Poutissou, TRIUMF, May 24, 2005.
10. G. M. Stinson, *On the use of existing magnets during the initial operation of the ISAC-II experimental area*, TRIUMF report TRI-DNA-03-1, TRIUMF, March 28, 2003.
11. K. Reiniger, *Private communication*, TRIUMF, July, 2005.
12. B. Gasparri, *Private communication*, TRIUMF, July, 2005.
13. A. Hurst, *Private communication*, TRIUMF, August, 2005.

Table 1

TRANSPORT input for vault transport line for multi-charge operation from medium- β accelerator
for $A = 30$, $Q = 10$, $E = 7.162 \text{ MeV}/\mu$, $\epsilon_x = \epsilon_y = 3\pi \text{ mm-mr}$, and a 2 mm beam spot at M5

'VAULT LINE - A=30,Q=10,E=7.162 MEV/U - 3PI, 2MM, MULTI'					
0					
13.		12.00000;			
16.00	G/2	5.00000	2.50000;		
16.00	K1	7.00000	0.45000;		
16.00	K2	8.00000	2.80000;		
16.00	X0	16.00000	19.00000;		
16.00	Z0	18.00000	26.10100;		
1.000000	BEAM	0.15480	2.75630	0.24930	2.48050
		0.00000	1.00000	0.34720;	
12.		0.10640	0.00000	0.00000	0.00000
		0.00000	-0.24160	0.00000	0.00000
		0.00000	0.00000	0.00000	0.00000
		0.00000	0.00000	0.00000;	
3.0		0.64500;			
5.00	VQ1	0.32500	-36.92949	100.00000;	
3.0		0.27000;			
5.00	VQ2	0.32500	56.54055	100.00000;	
3.0		0.64500;			
3.0		0.64500;			
5.00	VQ3	0.32500	-47.95309	100.00000;	
3.0		0.27000;			
5.00	VQ4	0.32500	38.09707	100.00000;	
3.0	M1	0.64500;			
-10.0		1.00000	1.00000	0.30100	0.00010;
-10.0		3.00000	3.00000	0.30100	0.00010;
-10.0		12.00000	1.00000	0.60000	0.00010;
-10.0		13.00000	4.00000	-0.60000	0.00010;
3.0		0.64500;			
5.00	VQ5	0.32500	30.02418	100.00000;	
3.0		0.27000;			
5.00	VQ6	0.32500	-30.02418	100.00000;	
3.0		0.64500;			
3.0		0.64500;			
5.00	VQ7	0.32500	30.02418	100.00000;	
3.0		0.27000;			
5.00	VQ8	0.32500	-30.02418	100.00000;	
3.0	M2	0.64500;			
3.0		0.64500;			
5.00	VQ9	0.32500	30.02418	100.00000;	
3.0		0.27000;			
5.00	VQ10	0.32500	-30.02418	100.00000;	
3.0		0.64500;			
3.0		0.64500;			
5.00	VQ11	0.32500	30.02418	100.00000;	
3.0		0.27000;			
5.00	VQ12	0.32500	-30.02418	100.00000;	
3.0	M3	0.64500;			
-10.0		1.00000	1.00000	0.30100	0.00010;
-10.0		3.00000	3.00000	0.30100	0.00010;

Table 1 (Continued)

TRANSPORT input for vault transport line for multi-charge operation from medium- β accelerator
for $A = 30$, $Q = 10$, $E = 7.162 \text{ MeV}/\mu$, $\epsilon_x = \epsilon_y = 3\pi \text{ mm-mr}$, and a 2 mm beam spot at M5

-10.0		12.00000	1.00000	0.60000	0.00010;
-10.0		13.00000	4.00000	-0.60000	0.00010;
3.0		0.67645;			
5.00	VQ13	0.32500	30.30199	100.00000;	
3.0		0.27000;			
5.00	VQ14	0.32500	-30.10832	100.00000;	
3.0		0.67645;			
3.0		0.67645;			
5.00	VQ15	0.32500	30.10265	100.00000;	
3.0		0.27000;			
5.00	VQ16	0.32500	-30.29617	100.00000;	
3.0	M4	0.67645;			
-10.0		1.00000	1.00000	0.30100	0.00010;
-10.0		3.00000	3.00000	0.30100	0.00010;
-10.0		12.00000	1.00000	0.60000	0.00010;
-10.0		13.00000	4.00000	-0.60000	0.00010;
3.0		0.67645;			
5.00	VQ17	0.32500	71.94598	100.00000;	
3.0		0.27000;			
5.00	VQ18	0.32500	-53.33543	100.00000;	
3.0		0.67645;			
3.0		0.67645;			
5.00	VQ19	0.32500	68.57734	100.00000;	
3.0		0.27000;			
5.00	VQ20	0.32500	-73.89696	100.00000;	
3.0	M5	0.67645;			
-10.0		1.00000	1.00000	0.08500	0.00010;
-10.0		3.00000	3.00000	0.08500	0.00010;
-10.0		12.00000	1.00000	0.00000	0.00010;
-10.0		13.00000	4.00000	0.00000	0.00010;
SENTINEL					
SENTINEL					

Table 2

Pole-tip fields (kG) of quadrupoles VQ17/18/19/20 for other emittances and 2 mm beam spot at M5 Medium- β accelerator

Element	$\epsilon = 3\pi$ mm-mr	$\epsilon = 4\pi$ mm-mr	$\epsilon = 5\pi$ mm-mr	$\epsilon = 6\pi$ mm-mr
VQ17	71.94598	76.40671	80.43881	84.12220
VQ18	-53.33543	-53.59195	-53.93199	-54.28407
VQ19	68.57734	68.35328	68.17093	68.02605
VQ20	-73.89696	-74.67322	-75.36286	-75.94165

Table 3

Pole-tip (kG) fields of quadrupoles VQ17/18/19/20 for other emittances and 1 mm beam spot at M5 Medium- β accelerator

Element	$\epsilon = 3\pi$ mm-mr	$\epsilon = 4\pi$ mm-mr	$\epsilon = 5\pi$ mm-mr	$\epsilon = 6\pi$ mm-mr
VQ17	98.63098	107.73805	115.84547	123.23499
VQ18	-55.82188	-56.80668	-57.66470	-58.42345
VQ19	67.61585	67.45081	67.34143	67.26338
VQ20	-77.66731	-78.41302	-78.93111	-79.31376

Table 4

TRANSPORT input for vault transport line for multi-charge operation from high- β accelerator for $A = 30$, $Q = 10$, $E = 7.162 \text{ MeV}/\mu$, $\epsilon_x = \epsilon_y = 3\pi \text{ mm-mr}$, and a 2 mm beam spot at M5

'VAULT LINE - A=30,Q=10,E=7.162 MEV/U - 3PI, 2MM, MULTI, HBETA'					
0					
13.		12.00000;			
16.00	G/2	5.00000	2.50000;		
16.00	K1	7.00000	0.45000;		
16.00	K2	8.00000	2.80000;		
16.00	X0	16.00000	19.00000;		
16.00	Z0	18.00000	26.10100;		
1.000000	BEAM	0.16775	1.78885	0.24304	1.74560
		0.00000	1.00000	0.75403;	
12.		-0.02300	0.00000	0.00000	0.00000
		0.00000	0.00000	0.00000	0.00000
		0.00000	0.00000	0.00000	0.00000
		0.00000	0.00000	0.00000;	
3.0		0.64500;			
5.00	VQ9	0.32500	-118.80799	100.00000;	
3.0		0.27000;			
5.00	VQ10	0.32500	116.38952	100.00000;	
3.0		0.64500;			
3.0		0.64500;			
5.00	VQ11	0.32500	-86.54805	100.00000;	
3.0		0.27000;			
5.00	VQ12	0.32500	26.84534	100.00000;	
3.0	M3	0.64500;			
-10.0		1.00000	1.00000	0.30100	0.00010;
-10.0		3.00000	3.00000	0.30100	0.00010;
-10.0		12.00000	1.00000	0.60000	0.00010;
-10.0		13.00000	4.00000	-0.60000	0.00010;
3.0		0.67645;			
5.00	VQ13	0.32500	65.79405	100.00000;	
3.0		0.27000;			
5.00	VQ14	0.32500	-65.337216	100.00000;	
3.0		0.67645;			
3.0		0.67645;			
5.00	VQ15	0.32500	65.37204	100.00000;	
3.0		0.27000;			
5.00	VQ16	0.32500	-65.79333	100.00000;	
3.0	M4	0.67645;			
-10.0		1.00000	1.00000	0.30100	0.00010;
-10.0		3.00000	3.00000	0.30100	0.00010;
-10.0		12.00000	1.00000	0.60000	0.00010;
-10.0		13.00000	4.00000	-0.60000	0.00010;
3.0		0.67645;			
5.00	VQ17	0.32500	156.27745	100.00000;	
3.0		0.27000;			
5.00	VQ18	0.32500	-115.83800	100.00000;	
3.0		0.67645;			
3.0		0.67645;			
5.00	VQ19	0.32500	148.92927	100.00000;	
3.0		0.27000;			

Table 4 (Continued)

TRANSPORT input for vault transport line for multi-charge operation from high- β accelerator for $A = 30$, $Q = 10$, $E = 7.162 \text{ MeV}/\mu$, $\epsilon_x = \epsilon_y = 3\pi \text{ mm-mr}$, and a 2 mm beam spot at M5

5.00	VQ20	0.32500	-160.48936	100.00000;	
3.0	M5	0.67645;			
-10.0		1.00000	1.00000	0.08500	0.00010;
-10.0		3.00000	3.00000	0.08500	0.00010;
-10.0		12.00000	1.00000	0.00000	0.00010;
-10.0		13.00000	4.00000	0.00000	0.00010;
SENTINEL					
SENTINEL					

Table 5

Pole-tip (kG) fields of quadrupoles VQ17/18/19/20 for other emittances and 2 mm beam spot at M5 High- β accelerator

Element	$\epsilon = 3\pi \text{ mm-mr}$	$\epsilon = 4\pi \text{ mm-mr}$	$\epsilon = 5\pi \text{ mm-mr}$	$\epsilon = 6\pi \text{ mm-mr}$
VQ17	156.27745	165.95161	174.69511	182.74997
VQ18	-115.83800	-116.39324	-117.12472	-117.90188
VQ19	148.92927	148.44694	148.05022	147.73206
VQ20	-160.48936	-162.18527	-163.67278	-164.92843

Table 6

Pole-tip (kG) fields of quadrupoles VQ17/18/19/20 for other emittances and 1 mm beam spot at M5 High- β accelerator

Element	$\epsilon = 3\pi \text{ mm-mr}$	$\epsilon = 4\pi \text{ mm-mr}$	$\epsilon = 5\pi \text{ mm-mr}$	$\epsilon = 6\pi \text{ mm-mr}$
VQ17	214.25240	234.00250	251.59302	267.73937
VQ18	-121.23998	-123.37059	-125.23162	-126.89588
VQ19	148.84239	146.48651	146.24857	146.07720
VQ20	-168.67196	-170.29936	-171.42027	-172.24773

Table 7

Quadrupole settings (kG) for single-charge transport of a 2 mm beam spot to M5—Case 1[†]

Element	Emittance (mm-mr)			
	3π	4π	5π	6π
VQ1	-90.25147	-100.47294	-106.80960	-116.91201
VQ2	62.68981	63.81173	64.32810	65.46385
VQ3	-66.07297	-66.48727	-66.75558	-66.80241
VQ4	66.91876	68.54282	70.08385	70.54973
VQ5	59.39654			
VQ6	-59.39654			
VQ7	59.39654			
VQ8	-59.39654			
VQ9	59.39654			
VQ10	-59.39654			
VQ11	59.39654			
VQ12	-59.39654			
VQ13	58.17276			
VQ14	-58.17276			
VQ15	58.17276			
VQ16	-58.17276			
VQ17	58.17276			
VQ18	-58.17276			
VQ19	58.17276			
VQ20	-58.17276			

[†] Where a setting is listed for only one emittance, that setting is valid for all other emittances.

Table 8

Quadrupole settings (kG) for single-charge transport of a 1 mm beam spot to M5—Case 1[†]

Element	Emittance (mm-mr)			
	3π	4π	5π	6π
VQ1	-146.49512	-165.03484	-181.79310	-197.30225
VQ2	68.08359	69.54789	70.77243	71.82870
VQ3	-66.99456	-67.03101	-67.04091	-67.04029
VQ4	72.79465	73.60081	74.07572	74.37396

[†] The remaining quadrupole settings are as listed in table 7.

Table 9

Quadrupole settings (kG) for single-charge transport of a 2 mm beam spot to M5—Case 2[†]
Unit sections, medium- β accelerator

Element	Emittance (mm-mr)			
	3π	4π	5π	6π
VQ1	-58.25634	-60.80095	-69.53706	-75.66578
VQ2	60.78669	58.78483	60.05908	60.90275
VQ3	-63.35092	-62.56007	-63.96304	-64.82313
VQ4	72.61963	62.68898	63.16142	64.20241
VQ17	21.14397	20.79849	20.94325	21.02702
VQ18	-48.78869	-45.81818	-45.39986	-45.22960
VQ19	63.73423	62.77755	62.68186	62.65368
VQ20	-85.48634	-79.12817	-78.00661	-77.51454

[†] The remaining quadrupole settings are as listed in table 7.

Table 10

Quadrupole settings (kG) for single-charge transport of a 1 mm beam spot to M5—Case 2[†]
Unit sections, medium- β accelerator

Element	Emittance (mm-mr)			
	3π	4π	5π	6π
VQ1	-27.44889	-80.22658	-86.72444	-99.45683
VQ2	46.93623	59.39100	60.00834	61.90491
VQ3	-62.90946	-66.71927	-67.28378	-67.56331
VQ4	80.69950	74.35353	75.52024	75.38266
VQ17	17.90271	17.92672	18.10465	19.85156
VQ18	-38.98895	-38.94868	-38.93673	-41.07594
VQ19	62.97492	62.97320	62.96996	62.93669
VQ20	-81.75733	-81.64436	-81.61528	-80.49741

[†] The remaining quadrupole settings are as listed in table 7.

Table 11

Quadrupole settings (kG) for single-charge transport of a 2 mm beam spot to M5[†]
Unit sections, high- β accelerator

Element	Emittance (mm-mr)			
	3π	4π	5π	6π
VQ9	-166.74751	-181.10687	-193.88266	-205.50401
VQ10	129.95011	130.88432	131.84708	132.78284
VQ11	-147.86404	-148.04641	-148.06915	-148.04163
VQ12	158.52707	161.00811	162.93581	164.45043
VQ13	126.33643			
VQ14	-126.33643			
VQ15	126.33643			
VQ16	-126.33643			
VQ17	126.33643			
VQ18	-126.33643			
VQ19	126.33643			
VQ20	-126.33643			

[†] Where a setting is listed for only one emittance, that setting is valid for all other emittances.

Table 12

Quadrupole settings (kG) for single-charge transport of a 1 mm beam spot to M5[†]
Unit sections, high- β accelerator

Element	Emittance (mm-mr)			
	3π	4π	5π	6π
VQ17	30.25912	30.06798	29.99523	29.95571
VQ18	-90.73400	-90.47264	-90.37166	-90.32265
VQ19	136.53105	136.51894	136.51791	136.51939
VQ20	-170.60491	-170.25527	-170.11783	-170.05547

[†] The remaining quadrupole settings are as listed in table 11.

Table 13(a)

TRANSPORT input beam parameters for beam extracted from the medium- β accelerator
 $A/q = 3$, $A = 30$, $q = 10$, $E = 7.162 \text{ MeV}/\mu$, $\alpha_x = -0.107$, $\beta_x = 0.799 \text{ mm/mr}$, $\alpha_y = 0.249$, and
 $\beta_y = 1.036 \text{ mm/mr}$

Parameter	Emittance (mm-mr)			
	3π	4π	5π	6π
$\pm x$ (cm)	0.1548	0.1788	0.1999	0.2190
$\pm\theta$ (mr)	1.9488	2.2502	2.5158	2.7560
r_{21}	0.1064	0.1064	0.1064	0.1064
$\pm y$ (cm)	0.1763	0.2036	0.2276	0.2493
$\pm\phi$ (mr)	1.7537	2.0249	2.2640	2.4800
r_{43}	-0.2416	-0.2416	-0.2416	-0.2416

Table 13(b)

TRANSPORT input beam parameters for beam extracted from the high- β accelerator
 $A/q = 6$, $A = 30$, $q = 5$, $E = 7.88 \text{ MeV}/\mu$, $\alpha_x = 0.023$, $\beta_x = 0.938 \text{ mm/mr}$, $\alpha_y = 0.0$, and
 $\beta_y = 1.969 \text{ mm/mr}$

Element	Emittance (mm-mr)			
	3π	4π	5π	6π
$\pm x$ (cm)	0.1678	0.1937	0.2166	0.2372
$\pm\theta$ (mr)	1.7889	2.0656	2.3094	2.5298
r_{21}	-0.0230	-0.0230	-0.0230	-0.0230
$\pm y$ (cm)	0.2430	0.2806	0.3138	0.3437
$\pm\phi$ (mr)	1.2344	1.4253	1.5935	1.7456
r_{43}	0.0	0.0	0.0	0.0

Table 14

TRANSPORT input for beam delivery from M5 to the TGT4 and TGT4A locations

'LINE TO TGT4 - A=30, Q=10, E=7.162 MEV/U - 3PI, 2MM, UNITS SECTIONS'					
3.0	'M5 '	0.00001;			
3.0		1.50000;			
3.0		0.10180;			
5.00	'CQ1 '	0.40640	-37.10502	100.00000;	
3.0		0.10180;			
3.0		0.20000;			
3.0		0.10180;			
5.00	'CQ2 '	0.40640	34.04445	100.00000;	
3.0		0.10180;			
3.0	'WALI'	0.32000;			
3.0	'WALX'	0.78740;			
3.0		0.32000;			
5.00	'CQ3 '	0.32500	-8.63807	100.00000;	
3.0		0.30000;			
3.0	'B1IN'	0.37500;			
-20.		180.00000;			
2.0		0.00000;			
4.000	'B1 '	1.04720	5.79059	0.00000;	
2.0		0.00000;			
-20.		-180.00000;			
3.0	'B1EX'	0.00001;			
3.0		0.37500;			
3.0		0.30000;			
5.00	'T4Q1'	0.32500	-8.63807	100.00000;	
3.0		0.32000;			
3.0		0.78740;			
3.0		0.32000;			
3.0		0.10180;			
5.00	'T4Q2'	0.40640	34.04445	100.00000;	
3.0		0.10180;			
3.0		0.20000;			
3.0		0.10180;			
5.00	'T4Q3'	0.40640	-37.10502	100.00000;	
3.0		0.10180;			
3.0	'TGT4'	1.50000;			
-10.		1.00000	1.00000	0.08500	0.00010;
-10.		3.00000	3.00000	0.08500	0.00010;
-10.		2.00000	1.00000	0.00000	0.00010;
-10.		4.00000	3.00000	0.00000	0.00010;

Table 14 (Continued)

TRANSPORT input for beam delivery from M5 to the TGT4 and TGT4A locations

3.0		2.25000;			
5.00	'T4Q4'	0.32500	38.10529	100.00000;	
3.0		0.30000;			
5.00	'T4Q5'	0.32500	-61.42525	100.00000;	
3.0		0.30000;			
5.00	'T4Q6'	0.32500	38.10529	100.00000;	
3.0	'TG4A' [†]	2.25000;			
-10.0		2.00000	1.00000	0.00000	0.00010;
-10.0		4.00000	3.00000	0.00000	0.00010;
SENTINEL					
SENTINEL					

[†] Because the program TRANSPORT allows a maximum of four characters in a label, the TGT4A label is truncated here to TG4A.

Table 15(a)

Dipole and quadrupole settings (kG) for beam delivery to TGT4 as a function of emittance
Extraction from medium- β accelerator[†]

Element	Emittance (mm-mr)			
	3π	4π	5π	6π
CQ1	-37.10502	-81.97658	-82.80257	-83.28972
CQ2	34.04445	73.91533	73.92992	73.96533
CQ3	-8.63807	-16.01692	-14.66597	-14.12042
B1	5.79059	5.79059	5.79059	5.79059
T4Q1	-8.63807	-16.01692	-14.66597	-14.12042
T4Q2	34.04445	73.91533	73.92992	73.96533
T4Q3	-37.10502	-81.97658	-82.80257	-83.28972
T4Q4	38.10529	82.81043	82.81043	38.10051
T4Q5	-61.42525	-61.43965	-61.46557	-61.48098
T4Q6	38.10529	82.81043	82.81043	38.10051

[†] All settings for $A = 30$, $Q = 10$, $E = 7.162 \text{ MeV}/\mu$, and 2 mm beam spots at TGT4 and TGT4A.

Table 15(b)

Beam sizes and overall transfer matrix elements at the TGT4 location

Parameter	Emittance (mm-mr)			
	3π	4π	5π	6π
$\pm x$ (cm)	0.085	0.085	0.085	0.085
$\pm\theta$ (mr)	5.491	6.132	6.991	7.916
$\pm y$ (cm)	0.085	0.085	0.085	0.085
$\pm\phi$ (mr)	3.530	4.707	5.883	7.060
R_{11} (cm/cm)	-0.4877	-0.4166	-0.3709	-0.3351
R_{12} (cm/mr)	0.0235	0.0217	0.0198	0.0186
R_{16} (cm/% $\delta p/p$)	0.0089	0.0057	0.0038	0.0026
R_{21} (mr/cm)	-12.9759	-14.1542	-15.3981	-17.0429
R_{22} (mr/mr)	-1.4247	-1.6620	-1.8743	-2.0376
R_{26} (mr/% $\delta p/p$)	-4.1489	-3.8985	-3.7549	-3.5693
R_{33} (cm/cm)	-0.4916	-0.4100	-0.3751	-0.3371
R_{34} (cm/mr)	-0.0049	-0.0028	-0.0007	0.0015
R_{43} (cm/cm)	-3.0012	-7.2198	-5.9706	-8.2247
R_{44} (cm/mr)	-2.0642	-2.3904	-2.6772	-2.9304

Table 15(c)

Beam sizes and overall transfer matrix elements at the TGT4A location

Parameter	Emittance (mm-mr)			
	3π	4π	5π	6π
$\pm x$ (cm)	0.085	0.085	0.085	0.085
$\pm\theta$ (mr)	5.491	6.132	6.991	7.916
$\pm y$ (cm)	0.085	0.085	0.085	0.085
$\pm\phi$ (mr)	3.530	4.707	5.883	7.060
R_{11} (cm/cm)	0.4713	0.4025	0.3592	0.3251
R_{12} (cm/mr)	-0.0251	-0.0232	-0.0211	-0.0197
R_{16} (cm/% $\delta p/p$)	-0.0137	-0.0093	-0.0065	-0.0046
R_{21} (mr/cm)	15.3222	16.1572	17.1831	18.6568
R_{22} (mr/mr)	1.3058	1.5521	1.7732	1.9438
R_{26} (mr/% $\delta p/p$)	4.0937	3.8620	3.7299	3.5519
R_{33} (cm/cm)	0.4718	0.3897	0.3641	0.3273
R_{34} (cm/mr)	-0.0037	-0.0083	-0.0033	-0.0045
R_{43} (cm/cm)	6.4723	10.1012	8.6340	10.6188
R_{44} (cm/mr)	2.0683	2.3505	2.6677	2.9088

Table 16(a)

Dipole and quadrupole settings (kG) for beam delivery to TGT4 as a function of emittance
Extraction from high- β accelerator[†]

Element	Emittance (mm-mr)			
	3π	4π	5π	6π
CQ1	-80.49850	-81.97658	-82.80257	-83.28972
CQ2	73.89170	73.91533	73.92992	73.96533
CQ3	-18.53886	-16.01692	-14.66597	-14.12042
B1	12.57569	12.57569	12.57569	12.57569
T4Q1	-18.53886	-16.01692	-14.66597	-14.12042
T4Q2	73.89170	73.91533	73.92992	73.96533
T4Q3	-80.49850	-81.97658	-82.80257	-83.28972
T4Q4	82.81043	82.81043	82.81043	82.81043
T4Q5	-133.61062	-133.61062	-133.61062	-133.61062
T4Q6	82.81043	82.81043	82.81043	82.81043

[†] All settings for $A = 30$, $Q = 5$, $E = 7.88 \text{ MeV}/\mu$, and 2 mm beam spots at TGT4 and TGT4A.

Table 16(b)

Beam sizes and overall transfer matrix elements at the TGT4 location
Extraction from the high- β accelerator

Parameter	Emittance (mm-mr)			
	3π	4π	5π	6π
$\pm x$ (cm)	0.085	0.085	0.085	0.085
$\pm \theta$ (mr)	5.486	6.219	7.111	8.093
$\pm y$ (cm)	0.085	0.085	0.085	0.085
$\pm \phi$ (mr)	3.529	4.705	5.883	7.058
R_{11} (cm/cm)	-0.4557	-0.3838	-0.3366	-0.3027
R_{12} (cm/mr)	0.0186	0.0187	0.0180	0.0173
R_{16} (cm/ $\% \delta p/p$)	0.0089	0.0059	0.0041	0.0030
R_{21} (mr/cm)	-11.2322	-12.9343	-14.6867	-16.4057
R_{22} (mr/mr)	-1.7365	-1.9747	-2.1837	-2.3680
R_{26} (mr/ $\% \delta p/p$)	-4.1429	-4.0286	-3.9686	-3.9417
R_{33} (cm/cm)	-0.3493	-0.2909	-0.2325	-0.1830
R_{34} (cm/mr)	-0.0033	-0.0166	-0.0274	-0.0328
R_{43} (cm/cm)	-0.6866	4.6749	9.6247	13.8125
R_{44} (cm/mr)	-2.8561	-3.1703	-3.1681	-2.9923

Table 17(a)

TRANSPORT input for beam delivery from M5 to the TGT1 location—2 mm beam spot

'LINE TO TGT1 - A=30, Q=10, E=7.162 MEV/U - 3PI, 2MM, UNITS SECTIONS'

3.0	'M5 '	0.00001;		
3.0		1.50000;		
3.0		0.10180;		
5.00	'CQ1 '	0.40640	38.33557	100.00000;
3.0		0.10180;		
3.0		0.20000;		
3.0		0.10180;		
5.00	'CQ2 '	0.40640	-36.47297	100.00000;
3.0		0.10180;		
3.0	'WALI'	0.32000;		
3.0	'WALX'	0.78740;		
3.0		0.32000;		
5.00	'CQ3 '	0.32500	48.14621	100.00000;
3.0	'B1IN'	0.67500;		
20.		180.00000;		
2.0		0.00000;		
4.000	'B1 '	1.04720	5.79059	0.00000;
2.0		0.00000;		
20.		-180.00000;		
3.0	'B1EX'	0.00001;		
3.0		1.52211;		
5.00	'T1Q1'	0.32500	48.30157	100.00000;
3.0		0.30000;		
5.00	'T1Q2'	0.32500	-53.79922	100.00000;
3.0	'MID '	1.63400;		
3.0		1.63400;		
5.00	'T1Q3'	0.32500	-53.79922	100.00000;
3.0		0.30000;		
5.00	'T1Q4'	0.32500	48.30157	100.00000;
3.0	'B2IN'	1.52211;		
20.		180.00000;		
2.0		0.00000;		
4.000	'B2 '	1.04720	5.79059	0.00000;
2.0		0.00000;		
20.		-180.00000;		
3.0	'B2EX'	0.00001;		
3.0		0.67500;		
5.00	'T1Q5'	0.32500	48.14621	100.00000;
3.0		0.32000;		
3.0		0.78740;		
3.0		0.32000;		
3.0		0.10180;		

Table 17(a) (Continued)

TRANSPORT input for beam delivery from M5 to the TGT1 locations—2 mm beam spot

5.00	'T1Q6'	0.40640	-36.47297	100.00000;	
3.0		0.10180;			
3.0		0.20000;			
3.0		0.10180;			
5.00	'T1Q7'	0.40640	38.33557	100.00000;	
3.0		0.10180;			
3.0	'TGT1'	1.50000;			
-10.		-1.00000	6.00000	0.00000	0.00010;
-10.		-2.00000	6.00000	0.00000	0.00010;
-10.		-1.00000	2.00000	0.00000	0.00010;
-10.		-2.00000	1.00000	0.00000	0.00010;
-10.		-3.00000	4.00000	0.00000	0.00010;
-10.		-4.00000	3.00000	0.00000	0.00010;
-10.		1.00000	1.00000	0.08500	0.00010;
-10.		3.00000	3.00000	0.08500	0.00010;
-10.		2.00000	1.00000	0.00000	0.00010;
-10.		4.00000	3.00000	0.00000	0.00010;
SENTINEL					
SENTINEL					

Table 17(b)

Version 1 dipole and quadrupole settings (kG) for beam delivery to TGT1—1 mm and 2 mm beam spots
Extraction from medium- β and high- β accelerators[†]

Element	medium- β accelerator ($p = 0.34720 \text{ GeV}/c$)	high- β accelerator ($p = 0.75403 \text{ GeV}/c$)	maximum momentum ($p = 0.93000 \text{ GeV}/c$)
CQ1	38.33557	83.25510	102.68456
CQ2	-36.47297	-79.21001	-97.69546
CQ3	48.14621	104.56131	128.96306
B1	5.79059	12.57569	15.51051
T1Q1	48.30157	104.89871	129.37921
T1Q2	-53.79922	-116.83821	-144.10505
T1Q3	-53.79922	-116.83821	-144.10505
T1Q4	48.30157	104.89871	129.37921
B2	5.79059	12.57569	15.51051
T1Q5	48.14621	104.56131	128.96306
T1Q6	-36.47297	-79.21001	-97.69546
T1Q7	38.33557	83.25510	102.68456

[†] Settings are for $A = 30$, $Q = 10$, $E = 7.162 \text{ MeV}/\mu$ (medium- β extraction), for $A = 30$, $Q = 5$, $E = 7.88 \text{ MeV}/\mu$ (high- β extraction), and $A = 150$, $A/q = 7$, and for $E = 6.5 \text{ MeV}/\mu$ (maximum momentum).

Table 18(a)

Beam parameters along the M5–TGT1 beamline as a function of emittance—Version 1
Extraction from medium- β accelerator with 2 mm beam spots at M5 and TGT1

Location	Parameter	Emittance (mm-mr)			
		3π	4π	5π	6π
M5	$\pm x$ (cm)	0.086	0.085	0.085	0.085
	$\pm\theta$ (mr)	3.495	4.704	5.883	7.058
	$\pm y$ (cm)	0.084	0.085	0.085	0.085
	$\pm\phi$ (mr)	3.577	4.707	5.883	7.060
MID	$\pm x$ (cm)	0.573	0.572	0.572	0.572
	$\pm\theta$ (mr)	1.903	2.561	3.203	3.843
	$\pm y$ (cm)	0.094	0.124	0.155	0.186
	$\pm\phi$ (mr)	3.182	3.224	3.224	3.224
TGT1	$\pm x$ (cm)	0.086	0.085	0.085	0.085
	$\pm\theta$ (mr)	3.495	4.704	5.883	7.058
	$\pm y$ (cm)	0.084	0.085	0.085	0.085
	$\pm\phi$ (mr)	3.577	4.707	5.883	7.060

Table 18(b)

Overall transfer matrix elements at the TGT1 location as a function of emittance—Version 1
Extraction from the medium- β accelerator and 2 mm beam spot at TGT1

Parameter	Emittance (mm-mr)			
	3π	4π	5π	6π
R_{11} (cm/cm)	-0.5574	-0.4494	-0.3962	-0.3604
R_{12} (cm/mr)	0.0032	0.0167	0.0161	0.0149
R_{16} (cm/% $\delta p/p$)	0.0000	0.0000	0.0000	0.0000
R_{21} (mr/cm)	0.7610	-9.0751	-11.1322	-12.4801
R_{22} (mr/mr)	-1.7985	-1.8871	-2.0726	-2.2580
R_{26} (mr/% $\delta p/p$)	0.0000	0.0000	0.0000	0.0000
R_{33} (cm/cm)	0.3675	0.3718	0.2807	0.2171
R_{34} (cm/mr)	0.0406	0.0301	0.0325	0.0322
R_{43} (cm/cm)	-13.8486	-11.9886	-18.2219	-22.9477
R_{44} (cm/mr)	1.1915	1.7175	1.4525	1.2010

Table 19(a)

Beam parameters along the M5–TGT1 beamline as a function of emittance—Version 1
Extraction from medium- β accelerator with 1 mm beam spots at M5 and TGT1

Location	Parameter	Emittance (mm-mr)			
		3π	4π	5π	6π
M5	$\pm x$ (cm)	0.045	0.045	0.045	0.045
	$\pm\theta$ (mr)	6.666	8.886	11.112	13.348
	$\pm y$ (cm)	0.045	0.045	0.045	0.045
	$\pm\phi$ (mr)	6.668	8.892	11.112	13.321
MID	$\pm x$ (cm)	0.557	0.557	0.557	0.557
	$\pm\theta$ (mr)	3.630	4.838	6.050	7.268
	$\pm y$ (cm)	0.176	0.234	0.293	0.351
	$\pm\phi$ (mr)	1.707	1.707	1.707	1.709
TGT1	$\pm x$ (cm)	0.045	0.045	0.045	0.045
	$\pm\theta$ (mr)	6.666	8.886	11.112	13.348
	$\pm y$ (cm)	0.045	0.045	0.045	0.085
	$\pm\phi$ (mr)	6.668	8.892	11.112	13.321

Table 19(b)

Overall transfer matrix elements at the TGT1 location as a function of emittance—Version 1
Extraction from the medium- β accelerator and 1 mm beam spot at TGT1

Parameter	Emittance (mm-mr)			
	3π	4π	5π	6π
R_{11} (cm/cm)	-0.2555	-0.2165	-0.1903	-0.1713
R_{12} (cm/mr)	0.0134	0.0122	0.0113	0.0105
R_{16} (cm/% $\delta p/p$)	0.0000	0.0000	0.0000	0.0000
R_{21} (mr/cm)	-21.0501	-25.9379	-30.2737	-34.2262
R_{22} (mr/mr)	-2.8114	-3.1568	-3.4574	-3.7290
R_{26} (mr/% $\delta p/p$)	0.0000	0.0000	0.0000	0.0000
R_{33} (cm/cm)	-0.0198	-0.0333	-0.0392	-0.0420
R_{34} (cm/mr)	0.0251	0.0212	0.0186	0.0167
R_{43} (cm/cm)	-38.8676	-44.5247	-49.3714	-53.6453
R_{44} (cm/mr)	-1.2294	-1.7222	-2.1432	-2.5145

Table 20(a)

Beam parameters along the M5–TGT1 beamline as a function of emittance—Version 1
Extraction from high- β accelerator with 2 mm beam spots at M5 and TGT1

Location	Parameter	Emittance (mm-mr)			
		3π	4π	5π	6π
M5	$\pm x$ (cm)	0.085	0.085	0.085	0.085
	$\pm\theta$ (mr)	3.529	4.706	5.883	7.058
	$\pm y$ (cm)	0.085	0.085	0.085	0.085
	$\pm\phi$ (mr)	3.529	4.705	5.883	7.058
MID	$\pm x$ (cm)	0.572	0.572	0.572	0.572
	$\pm\theta$ (mr)	1.922	2.562	3.203	3.843
	$\pm y$ (cm)	0.093	0.124	0.155	0.186
	$\pm\phi$ (mr)	3.182	3.224	3.224	3.224
TGT1	$\pm x$ (cm)	0.086	0.085	0.085	0.085
	$\pm\theta$ (mr)	3.529	4.706	5.883	7.058
	$\pm y$ (cm)	0.085	0.085	0.085	0.085
	$\pm\phi$ (mr)	3.529	4.705	5.883	7.058

Table 20(b)

Overall transfer matrix elements at the TGT1 location as a function of emittance—Version 1
Extraction from the high- β accelerator and 2 mm beam spot at TGT1

Parameter	Emittance (mm-mr)			
	3π	4π	5π	6π
R_{11} (cm/cm)	-0.4910	-0.4146	-0.3626	-0.3248
R_{12} (cm/mr)	0.0107	0.0126	0.0133	0.0135
R_{16} (cm/% $\delta p/p$)	0.0000	0.0000	0.0000	0.0000
R_{21} (mr/cm)	-5.2198	-7.9855	-10.4075	-12.5864
R_{22} (mr/mr)	-1.9226	-2.1689	-2.3757	-2.5552
R_{26} (mr/% $\delta p/p$)	0.0000	0.0000	0.0000	0.0000
R_{33} (cm/cm)	0.1241	0.0704	0.0407	0.0226
R_{34} (cm/mr)	0.0644	0.0580	0.0527	0.0485
R_{43} (cm/cm)	-13.5775	-16.3096	-18.5341	-20.4503
R_{44} (cm/mr)	1.0142	0.7668	0.5548	0.3700

Table 21(a)

Beam parameters along the M5–TGT1 beamline as a function of emittance—Version 1
Extraction from high- β accelerator with 1 mm beam spots at M5 and TGT1

Location	Parameter	Emittance (mm-mr)			
		3π	4π	5π	6π
M5	$\pm x$ (cm)	0.045	0.045	0.045	0.045
	$\pm\theta$ (mr)	6.666	8.935	11.173	13.331
	$\pm y$ (cm)	0.045	0.045	0.045	0.045
	$\pm\phi$ (mr)	6.666	9.163	11.451	13.332
MID	$\pm x$ (cm)	0.557	0.557	0.557	0.557
	$\pm\theta$ (mr)	3.629	4.865	6.083	7.259
	$\pm y$ (cm)	0.176	0.242	0.302	0.351
	$\pm\phi$ (mr)	1.707	1.707	1.707	1.709
TGT1	$\pm x$ (cm)	0.045	0.045	0.045	0.045
	$\pm\theta$ (mr)	6.666	8.935	11.173	13.331
	$\pm y$ (cm)	0.045	0.045	0.045	0.045
	$\pm\phi$ (mr)	6.666	9.163	11.451	13.333

Table 21(b)

Overall transfer matrix elements at the TGT1 location as a function of emittance—Version 1
Extraction from the high- β accelerator and 1 mm beam spot at TGT1

Parameter	Emittance (mm-mr)			
	3π	4π	5π	6π
R_{11} (cm/cm)	-0.2474	-0.2243	-0.1982	-0.1656
R_{12} (cm/mr)	0.0092	0.0087	0.0081	0.0083
R_{16} (cm/% $\delta p/p$)	0.0000	0.0000	0.0000	0.0000
R_{21} (mr/cm)	-15.4080	-22.7361	-26.5328	-27.4733
R_{22} (mr/mr)	-3.4681	-3.5776	-3.9575	-4.6568
R_{26} (mr/% $\delta p/p$)	0.0000	0.0000	0.0000	0.0000
R_{33} (cm/cm)	0.0428	-0.0094	-0.0239	0.0037
R_{34} (cm/mr)	0.0355	0.0222	0.0197	0.0258
R_{43} (cm/cm)	-26.6859	-44.9662	-49.9428	-38.7755
R_{44} (cm/mr)	1.2480	-0.1919	-0.6107	0.2162

Table 21(c)

Dipole and quadrupole settings (kG) for beam delivery to TGT1—1 mm and 2 mm beam spots
Extraction from medium- β and high- β accelerators—Version 2[†]

Element	medium- β accelerator ($p = 0.34720$ GeV/c)	high- β accelerator ($p = 0.75403$ GeV/c)	maximum momentum ($p = 0.93000$ GeV/c)
CQ1	-43.38161	-94.21381	-116.19707
CQ2	38.32330	83.22845	102.65332
CQ3	-52.54679	-114.11825	-140.81005
B1	5.79059	12.57569	15.951051
T1Q1	37.36532	81.14796	100.08266
T1Q2	-29.00584	-62.99330	-77.68997
T1Q3	-29.00584	-62.99330	-77.68997
T1Q4	37.36532	81.14796	100.08266
B2	5.79059	12.57569	15.96305
T1Q5	-52.54679	-114.11825	-140.81005
T1Q6	38.32330	83.22845	102.65332
T1Q7	-43.38161	-94.21381	-116.19707

[†] Settings are for $A = 30$, $Q = 10$, $E = 7.162$ MeV/ μ (medium- β extraction), for $A = 30$, $Q = 5$, $E = 7.88$ MeV/ μ (high- β extraction), and $A = 150$, $A/q = 7$, and for $E = 6.5$ MeV/ μ (maximum momentum).

Table 21(d)

Beam parameters along the M6–TGT1 beamline as a function of emittance
Extraction from medium- β accelerator with 2 mm beam spots at M5 and TGT1

Location	Parameter	Emittance (mm-mr)			
		3π	4π	5π	6π
M6	$\pm x$ (cm)	0.086	0.085	0.085	0.085
	$\pm\theta$ (mr)	3.495	4.704	5.883	7.058
	$\pm y$ (cm)	0.084	0.085	0.085	0.085
	$\pm\phi$ (mr)	3.577	4.707	5.883	7.060
MID	$\pm x$ (cm)	0.831	0.891	0.961	1.041
	$\pm\theta$ (mr)	0.839	0.831	0.831	0.831
	$\pm y$ (cm)	1.037	1.051	1.051	1.051
	$\pm\phi$ (mr)	0.289	0.381	0.476	0.571
TGT6	$\pm x$ (cm)	0.086	0.085	0.085	0.085
	$\pm\theta$ (mr)	3.495	4.704	5.883	7.058
	$\pm y$ (cm)	0.084	0.085	0.085	0.085
	$\pm\phi$ (mr)	3.577	4.707	5.883	7.060

Table 21(e)

Elements of the overall transfer matrix at the TGT1 location
Extraction from the medium- β accelerator and 2 mm beam spot

Parameter	Emittance (mm-mr)			
	3π	4π	5π	6π
R_{11} (cm/cm)	0.5574	0.4493	0.3962	0.3604
R_{12} (cm/mr)	-0.0032	-0.0168	-0.0161	-0.0149
R_{16} (cm/% $\delta p/p$)	0.0000	0.0000	0.0000	0.0000
R_{21} (mr/cm)	-0.7610	9.0751	11.1322	12.4802
R_{22} (mr/mr)	1.7985	1.8871	2.0726	2.2580
R_{26} (mr/% $\delta p/p$)	0.0000	0.0000	0.0000	0.0000
R_{33} (cm/cm)	-0.3674	-0.3717	-0.2806	-0.2169
R_{34} (cm/mr)	-0.0406	-0.0302	-0.0325	-0.0322
R_{43} (cm/cm)	13.8484	11.9883	18.2217	22.9476
R_{44} (cm/mr)	-1.1915	-1.7175	-1.4526	-1.2010

Table 21(f)

Beam parameters along the M6–TGT1 beamline as a function of emittance
Extraction from medium- β accelerator with 1 mm beam spots at M5 and TGT1

Location	Parameter	Emittance (mm-mr)			
		3π	4π	5π	6π
M6	$\pm x$ (cm)	0.045	0.045	0.045	0.045
	$\pm\theta$ (mr)	6.666	8.886	11.112	13.331
	$\pm y$ (cm)	0.045	0.045	0.045	0.045
	$\pm\phi$ (mr)	6.668	8.892	11.111	13.335
MID	$\pm x$ (cm)	1.014	1.178	1.362	1.556
	$\pm\theta$ (mr)	0.440	0.440	0.440	0.440
	$\pm y$ (cm)	0.556	0.556	0.556	0.556
	$\pm\phi$ (mr)	0.539	0.719	0.899	1.079
TGT6	$\pm x$ (cm)	0.045	0.045	0.045	0.045
	$\pm\theta$ (mr)	6.667	8.886	11.112	13.331
	$\pm y$ (cm)	0.045	0.045	0.045	0.045
	$\pm\phi$ (mr)	6.668	8.892	11.111	13.335

Table 21(g)

Elements of the overall transfer matrix at the TGT1 location
Extraction from the medium- β accelerator and 1 mm beam spot

Parameter	Emittance (mm-mr)			
	3π	4π	5π	6π
R_{11} (cm/cm)	0.2910	0.2372	0.2095	0.1875
R_{12} (cm/mr)	-0.0002	-0.0090	-0.0086	-0.0085
R_{16} (cm/% $\delta p/p$)	0.0000	0.0000	0.0000	0.0000
R_{21} (mr/cm)	-4.2591	17.4774	21.1273	25.6998
R_{22} (mr/mr)	3.4399	3.5519	3.9108	4.1732
R_{26} (mr/% $\delta p/p$)	0.0000	0.0000	0.0000	0.0000
R_{33} (cm/cm)	-0.2237	-0.1498	-0.1077	-0.0551
R_{34} (cm/mr)	-0.0081	-0.0204	-0.0195	-0.0187
R_{43} (cm/cm)	-20.5391	33.8674	42.6685	52.6139
R_{44} (cm/mr)	-3.7299	-2.0689	-1.5640	-0.3253

Table 22

TRANSPORT input for beam delivery from M5 to the TGT5 location—2 mm beam spot, 3π mm-mr

'LINE TO TGT5 - A=30, Q=10, E=7.162 MEV/U - 3PI, 2MM, UNITS SECTIONS'					
3.0	'M5 '	0.00001;			
3.0		1.50000;			
3.0		0.10180;			
5.00	'CQ1 '	0.40640	-45.65171	100.00000;	
3.0		0.10180;			
3.0		0.20000;			
3.0		0.10180;			
5.00	'CQ2 '	0.40640	37.89289	100.00000;	
3.0		0.10180;			
3.0	'WALI'	0.32000;			
3.0	'WALX'	0.78740;			
3.0		0.32000;			
5.00	'CQ3 '	0.32500	-52.02237	100.00000;	
3.0	'B1IN'	0.67500;			
3.0		0.60000;			
-10.		4.00000	3.00000	0.00000	0.00010;
3.0		0.44720;			
3.0	'B1EX'	0.00001;			
3.0		1.43740;			
5.00	'CQ4 '	0.32500	22.13869	100.00000;	
3.0		0.30000;			
5.00	'CQ5 '	0.32500	-67.34978	100.00000;	
3.0		0.30000;			
5.00	'CQ6 '	0.32500	67.68361	100.00000;	
3.0	'M5 '	0.90000;			
-10.		1.00000	1.00000	0.08000	0.00010;
-10.		3.00000	3.00000	0.08000	0.00010;
-10.		2.00000	1.00000	0.00000	0.00010;
-10.		4.00000	3.00000	0.00000	0.00010;
3.0		1.50000;			
5.00	'CQ7 '	0.20000	-97.52968	100.00000;	
3.0		0.20000;			
3.0		0.10180;			
5.00	'CQ8 '	0.40640	59.73781	100.00000;	
3.0		0.10180;			
3.0		0.20000;			
5.00	'CQ9 '	0.20000	-89.06864	100.00000;	
3.0	'B3IN'	0.67500;			
20.0		180.0 ;			
2.0		0.00000;			
4.0	'B3'	1.04720	5.79059	0.00000;	
2.0		0.00000;			
20.0		-180.0 ;			
3.0	'B3EX'	0.00001;			

Table 22 (Continued)

TRANSPORT input for beam delivery from M5 to the TGT5 locations—2 mm beam spot

3.0		0.90030;			
5.00	'56Q1'	0.32500	-40.13305	100.00000;	
3.0		0.30000;			
5.00	'56Q2'	0.32500	31.91417	100.00000;	
3.0	'MID '	0.80620;			
3.0		0.80620;			
5.00	'56Q3'	0.32500	31.91417	100.00000;	
3.0		0.30000;			
5.00	'56Q4'	0.32500	-40.13305	100.00000;	
3.0	'B4IN'	0.90030;			
20.		180.00000;			
2.0		0.00000;			
4.000	'B4 '	1.04720	5.79059	0.00000;	
2.0		0.00000;			
20.		-180.00000;			
3.0	'B4EX'	0.00001;			
3.0		0.67500;			
5.00	'T5Q1'	0.20000	-89.06864	100.00000;	
3.0		0.20000;			
3.0		0.10180;			
5.00	'T5Q2'	0.40640	59.73781	100.00000;	
3.0		0.10180;			
3.0		0.20000;			
5.00	'T5Q3'	0.20000	-97.52968	100.00000;	
3.0	'TGT5'	1.50000;			
-10.		-1.00000	6.00000	0.00000	0.00010;
-10.		-2.00000	6.00000	0.00000	0.00010;
-10.		-1.00000	2.00000	0.00000	0.00010;
-10.		-2.00000	1.00000	0.00000	0.00010;
-10.		-3.00000	4.00000	0.00000	0.00010;
-10.		-4.00000	3.00000	0.00000	0.00010;
-10.		1.00000	1.00000	0.08500	0.00010;
-10.		3.00000	3.00000	0.08500	0.00010;
-10.		2.00000	1.00000	0.00000	0.00010;
-10.		4.00000	3.00000	0.00000	0.00010;

SENTINEL
SENTINEL

Table 23(a)

Dipole and quadrupole settings (kG) for beam delivery to TGT5—2 mm beam spot
Extraction from medium- β accelerator for $A = 30$, $Q = 10$, $E = 7.162 \text{ MeV}/\mu$.[†]

Element	$\epsilon = 3\pi \text{ mm-mr}$	$\epsilon = 4\pi \text{ mm-mr}$	$\epsilon = 5\pi \text{ mm-mr}$	$\epsilon = 6\pi \text{ mm-mr}$
CQ1	-45.65171	-46.45319	-46.70539	-46.87152
CQ2	37.89289	38.00819	38.03535	38.05905
CQ3	-52.02237	-52.63652	-52.94260	-53.05287
CQ4	22.13869	15.56628	13.94595	12.80956
CQ5	-67.34978	-64.17014	-63.23842	-62.62036
CQ6	67.68361	66.81083	66.00070	65.74943
CQ7	-97.52968			
CQ8	59.73781			
CQ9	-89.06864			
B3	5.79059			
56Q1	-40.13305			
56Q2	31.91417			
56Q2	31.91417			
56Q4	-40.13305			
B4	5.79059			
T5Q1	-89.06864			
T5Q2	59.73781			
T5Q3	-97.52968			

[†] An entry given for one emittance only is valid for all emittances.

Table 23(b)

Beam parameters along the M6–TGT5 beamline as a function of emittance
Extraction from medium- β accelerator with 2 mm beam spots at M6 and TGT5

Location	Parameter	Emittance (mm-mr)			
		3π	4π	5π	6π
M6	$\pm x$ (cm)	0.080	0.080	0.080	0.080
	$\pm \theta$ (mr)	3.750	4.999	6.251	7.499
	$\pm y$ (cm)	0.080	0.080	0.080	0.080
	$\pm \phi$ (mr)	3.750	5.002	6.250	7.501
MID	$\pm x$ (cm)	1.713	1.713	1.713	1.713
	$\pm \theta$ (mr)	1.695	2.259	2.825	3.389
	$\pm y$ (cm)	0.500	0.666	0.833	0.999
	$\pm \phi$ (mr)	0.600	0.600	0.600	0.600
TGT5	$\pm x$ (cm)	0.080	0.080	0.080	0.080
	$\pm \theta$ (mr)	3.750	4.999	6.251	7.499
	$\pm y$ (cm)	0.080	0.080	0.080	0.080
	$\pm \phi$ (mr)	3.751	5.002	6.250	7.501

Table 23(c)

Overall transfer matrix elements at the TGT5 location
Extraction from the medium- β accelerator and 2 mm beam spot

Parameter	Emittance (mm-mr)			
	3π	4π	5π	6π
R_{11} (cm/mr)	0.2886	0.3860	0.3873	0.3647
R_{12} (cm/mr)	0.0317	0.0150	0.0054	0.0005
R_{16} (cm/ $\% \delta p/p$)	0.0000	0.0000	0.0000	0.0000
R_{21} (mr/cm)	-20.2620	-14.4792	-8.5599	-4.2663
R_{22} (mr/mr)	1.2395	2.0266	2.4631	2.7358
R_{26} (mr/ $\% \delta p/p$)	0.0000	0.0000	0.0000	0.0000
R_{33} (cm/cm)	-0.4676	-0.3548	-0.2588	-0.1899
R_{34} (cm/mr)	-0.0116	-0.0277	-0.0310	-0.0310
R_{43} (cm/cm)	0.1179	12.2042	19.7987	25.3853
R_{44} (cm/mr)	-2.1356	-1.8673	-1.4918	-1.1199

Table 24(a)

Quadrupole settings (kG) for beam delivery to TGT5—1 mm beam spot
Extraction from medium- β accelerator for $A = 30$, $Q = 10$, $E = 7.162$ MeV/ μ .[†]

Element	$\epsilon = 3\pi$ mm-mr	$\epsilon = 4\pi$ mm-mr	$\epsilon = 5\pi$ mm-mr	$\epsilon = 6\pi$ mm-mr
CQ1	-49.86842	-51.02789	-51.40299	-51.64844
CQ2	38.02801	38.29166	38.36205	38.40784
CQ3	-49.29299	-48.97786	-48.91083	-48.85149
CQ4	21.48576	15.60657	13.95064	12.79679
CQ5	-66.79205	-64.31675	-63.51989	-62.94495
CQ6	65.00518	66.80616	67.07846	67.25334

[†] A11 other quadrupole settings are as in table 23(a).

Table 24(b)

Beam parameters along the M6-TGT5 beamline as a function of emittance
Extraction from medium- β accelerator with 1 mm beam spots at M6 and TGT5

Location	Parameter	Emittance (mm-mr)			
		3π	4π	5π	6π
M6	$\pm x$ (cm)	0.045	0.045	0.045	0.045
	$\pm\theta$ (mr)	6.668	8.886	11.112	13.332
	$\pm y$ (cm)	0.045	0.045	0.045	0.045
	$\pm\phi$ (mr)	6.668	8.892	11.111	13.335
MID	$\pm x$ (cm)	1.707	1.707	1.707	1.707
	$\pm\theta$ (mr)	3.013	4.016	5.023	6.026
	$\pm y$ (cm)	0.888	1.185	1.480	1.777
	$\pm\phi$ (mr)	0.338	0.338	0.338	0.338
TGT5	$\pm x$ (cm)	0.045	0.045	0.045	0.045
	$\pm\theta$ (mr)	6.667	8.886	11.112	13.332
	$\pm y$ (cm)	0.045	0.045	0.045	0.045
	$\pm\phi$ (mr)	6.668	8.892	11.111	13.335

Table 24(c)

Beam sizes and overall transfer matrix elements at the TGT5 location
Extraction from the medium- β accelerator and 1 mm beam spot

Parameter	Emittance (mm-mr)			
	3π	4π	5π	6π
$\pm x$ (cm)	0.045	0.045	0.045	0.045
$\pm\theta$ (mr)	6.667	8.886	11.112	13.332
$\pm y$ (cm)	0.045	0.045	0.045	0.045
$\pm\phi$ (mr)	6.668	8.892	11.111	13.335
R_{11} (cm/cm)	0.2910	0.2533	0.2252	0.2035
R_{12} (cm/mr)	-0.0002	-0.0021	-0.0037	-0.0046
R_{16} (cm/% $\delta p/p$)	0.0000	0.0000	0.0000	0.0000
R_{21} (mr/cm)	-4.2008	-0.0111	5.7060	10.7324
R_{22} (mr/mr)	3.4399	3.9487	4.3457	4.6713
R_{26} (mr/% $\delta p/p$)	0.0000	0.0000	0.0000	0.0000
R_{33} (cm/cm)	-0.2275	-0.1473	-0.0988	-0.0678
R_{34} (cm/mr)	-0.0184	-0.0205	-0.0198	-0.0185
R_{43} (cm/cm)	19.5753	34.3307	43.9977	51.3396
R_{44} (cm/mr)	-2.8121	-2.0052	-1.3115	-0.7105

Table 25(a)

Quadrupole settings (kG) for beam delivery to TGT5—2 mm beam spot
Extraction from high- β accelerator for $A = 30$, $Q = 5$, $E = 7.88$ MeV/ μ .[†]

Element	$\epsilon = 3\pi$ mm-mr	$\epsilon = 4\pi$ mm-mr	$\epsilon = 5\pi$ mm-mr	$\epsilon = 6\pi$ mm-mr
CQ1	-98.04810	-99.70389	-100.12450	-100.42523
CQ2	82.08778	82.39954	82.44675	83.34626
CQ3	-113.34649	-115.66655	-116.86062	-117.52860
CQ4	52.43290	39.07934	37.10045	53.70668
CQ5	-147.54756	-141.51674	-140.22343	-152.34566
CQ6	144.47950	143.15097	140.63795	165.17382
CQ7	-211.80952			
CQ8	129.73529			
CQ9	-193.43441			
B3	12.57569			
56Q1	-87.15878			
56Q2	69.30946			
56Q2	69.30946			
56Q4	-87.15878			
B4	12.57569			
T5Q1	-193.43441			
T5Q2	129.73529			
T5Q3	-211.80952			

[†] An entry given for one emittance only is valid for all emittances.

Table 25(b)

Beam parameters along the M6–TGT5 beamline as a function of emittance
Extraction from high- β accelerator with 2 mm beam spots at M6 and TGT5

Location	Parameter	Emittance (mm-mr)			
		3π	4π	5π	6π
M6	$\pm x$ (cm)	0.085	0.085	0.085	0.085
	$\pm\theta$ (mr)	3.529	4.706	5.883	7.058
	$\pm y$ (cm)	0.085	0.085	0.085	0.085
	$\pm\phi$ (mr)	3.529	4.705	5.883	7.058
MID	$\pm x$ (cm)	1.715	1.715	1.715	1.715
	$\pm\theta$ (mr)	1.595	2.127	2.659	3.190
	$\pm y$ (cm)	0.470	0.627	0.784	0.940
	$\pm\phi$ (mr)	0.638	0.638	0.940	0.638
TGT5	$\pm x$ (cm)	0.085	0.085	0.085	0.085
	$\pm\theta$ (mr)	3.529	4.706	5.883	7.058
	$\pm y$ (cm)	0.085	0.085	0.085	0.085
	$\pm\phi$ (mr)	3.529	4.705	5.883	7.058

Table 25(c)

Overall transfer matrix elements at the TGT5 location
Extraction from the high- β accelerator and 2 mm beam spot

Parameter	Emittance (mm-mr)			
	3π	4π	5π	6π
R_{11} (cm/cm)	0.2767	0.3727	0.3797	-0.1457
R_{12} (cm/mr)	0.0404	0.0225	0.0101	0.0304
R_{16} (cm/% $\delta p/p$)	0.0000	0.0000	0.0000	0.0000
R_{21} (mr/cm)	-17.6319	-12.8346	-6.8862	-27.1925
R_{22} (mr/mr)	2.4485	1.9069	4.7438	-1.1927
R_{26} (mr/% $\delta p/p$)	0.0000	0.0000	0.0000	0.0000
R_{33} (cm/cm)	-0.3497	-0.2675	-0.1996	-0.1524
R_{34} (cm/mr)	-0.0003	-0.0280	-0.0361	-0.0384
R_{43} (cm/cm)	0.0624	7.8740	12.6762	16.1780
R_{44} (cm/mr)	-2.8593	-2.9146	-2.7199	-2.4907

Table 26(a)

Quadrupole settings (kG) for beam delivery to TGT5—1 mm beam spot
Extraction from high- β accelerator for $A = 30$, $Q = 5$, $E = 7.88$ MeV/ μ .[†]

Element	$\epsilon = 3\pi$ mm-mr	$\epsilon = 4\pi$ mm-mr	$\epsilon = 5\pi$ mm-mr	$\epsilon = 6\pi$ mm-mr
CQ1	-107.75450	-108.32328	-108.65494	-97.36899
CQ2	82.41929	82.47900	82.52897	81.00086
CQ3	-107.34787	-107.78676	-107.95601	-114.25603
CQ4	50.45710	51.40170	51.40170	58.54560
CQ5	-146.40352	-146.64676	-146.61446	-147.24456
CQ6	139.31959	138.27463	138.03783	143.32134

[†] A11 other quadrupole settings are as in table 25(a).

Table 26(b)

Beam parameters along the M6-TGT5 beamline as a function of emittance
Extraction from high- β accelerator with 1 mm beam spots at M6 and TGT5

Location	Parameter	Emittance (mm-mr)			
		3π	4π	5π	6π
M6	$\pm x$ (cm)	0.045	0.045	0.045	0.045
	$\pm\theta$ (mr)	6.667	8.889	11.113	13.331
	$\pm y$ (cm)	0.045	0.045	0.045	0.045
	$\pm\phi$ (mr)	6.667	8.888	11.112	13.333
MID	$\pm x$ (cm)	1.707	1.707	1.707	1.707
	$\pm\theta$ (mr)	3.013	4.018	5.023	6.025
	$\pm y$ (cm)	0.888	1.184	1.481	1.776
	$\pm\phi$ (mr)	0.338	0.338	0.338	0.338
TGT5	$\pm x$ (cm)	0.045	0.045	0.045	0.045
	$\pm\theta$ (mr)	6.667	8.889	11.113	13.331
	$\pm y$ (cm)	0.045	0.045	0.045	0.045
	$\pm\phi$ (mr)	6.667	8.888	11.112	13.333

Table 26(c)

Beam sizes and overall transfer matrix elements at the TGT5 location
Extraction from the high- β accelerator and 1 mm beam spot

Parameter	Emittance (mm-mr)			
	3π	4π	5π	6π
R_{11} (cm/cm)	0.2669	0.2316	0.2039	0.1853
R_{12} (cm/mr)	-0.0032	-0.0013	-0.0033	-0.0034
R_{16} (cm/% $\delta p/p$)	0.0000	0.0000	0.0000	0.0000
R_{21} (mr/cm)	-4.1563	3.7395	9.8524	12.1466
R_{22} (mr/mr)	3.6974	4.2971	4.7438	5.1714
R_{26} (mr/% $\delta p/p$)	0.0000	0.0000	0.0000	0.0000
R_{33} (cm/cm)	-0.1489	-0.0992	-0.0684	-0.0307
R_{34} (cm/mr)	-0.0217	-0.0248	-0.0248	-0.0251
R_{43} (cm/cm)	16.3040	24.8949	31.1310	37.7093
R_{44} (cm/mr)	-4.3433	-3.8551	-3.3233	-1.7912

Table 27

Dipole and quadrupole settings (kG) for beam delivery to TGT6—2 mm beam spot
Extraction from medium- β accelerator for $A = 30$, $Q = 10$, $E = 7.162 \text{ MeV}/\mu$.

Element	$\epsilon = 3\pi \text{ mm-mr}$	$\epsilon = 4\pi \text{ mm-mr}$	$\epsilon = 5\pi \text{ mm-mr}$	$\epsilon = 6\pi \text{ mm-mr}$
CQ1	-45.65171	-46.45319	-46.70539	-46.87152
CQ2	37.89289	38.00819	38.03535	38.05905
CQ3	-52.02237	-52.63652	-52.94260	-53.05287
CQ4	22.13869	15.56628	13.94595	12.80956
CQ5	-67.34978	-64.17014	-63.23842	-62.62036
CQ6	67.68361	66.81083	66.00070	65.74943
CQ7	-79.55619	-141.17450	-85.72907	-85.64988
CQ8	57.99765	130.02159	57.34109	56.87301
CQ9	-87.69526	-253.31397	-78.91345	-76.32767
B3	5.79059			
56Q1	-67.13741	-126.71218	-67.54801	-68.72914
56Q2	81.95087	169.90654	82.04087	82.29735
56Q2	81.95087	169.90654	82.04087	82.29735
56Q4	-67.13741	-126.71218	-67.54801	-68.72914
B4	5.79059			
T6Q1	-87.69526	-253.31397	-78.91345	-76.32767
T6Q2	57.99765	130.02159	57.34109	56.87301
T6Q3	-79.55619	-83.81791	-85.72902	-85.64983

Table 28(a)

Beam parameters along the M6–TGT6 beamline as a function of emittance
Extraction from medium- β accelerator with 2 mm beam spots at M6 and TGT6

Location	Parameter	Emittance (mm-mr)			
		3π	4π	5π	6π
M6	$\pm x$ (cm)	0.080	0.080	0.080	0.080
	$\pm\theta$ (mr)	3.750	4.999	6.251	7.499
	$\pm y$ (cm)	0.080	0.080	0.080	0.080
	$\pm\phi$ (mr)	3.751	5.002	6.250	7.501
MID	$\pm x$ (cm)	0.100	0.141	0.182	0.219
	$\pm\theta$ (mr)	22.629	21.132	22.187	22.385
	$\pm y$ (cm)	0.165	0.180	0.205	0.227
	$\pm\phi$ (mr)	1.813	2.221	2.440	2.639
TGT6	$\pm x$ (cm)	0.080	0.080	0.080	0.080
	$\pm\theta$ (mr)	3.750	4.999	6.251	7.499
	$\pm y$ (cm)	0.080	0.080	0.080	0.080
	$\pm\phi$ (mr)	3.751	5.002	6.250	7.501

Table 28(b)

Beam sizes and overall transfer matrix elements at the TGT6 location
Extraction from the medium- β accelerator and 2 mm beam spot

Parameter	Emittance (mm-mr)			
	3π	4π	5π	6π
R_{11} (cm/cm)	-0.2441	-0.3733	-0.3838	-0.3636
R_{12} (cm/mr)	-0.0342	-0.0167	-0.0063	-0.0011
R_{16} (cm/% $\delta p/p$)	0.0000	0.0000	0.0000	0.0000
R_{21} (mr/cm)	21.5097	15.7228	9.4781	5.0072
R_{22} (mr/mr)	-1.0852	-1.9746	-2.4491	-2.7342
R_{26} (mr/% $\delta p/p$)	0.0000	0.0000	0.0000	0.0000
R_{33} (cm/cm)	-0.0316	0.2186	0.2648	0.2777
R_{34} (cm/mr)	-0.0463	-0.0279	-0.0177	-0.0108
R_{43} (cm/cm)	21.8743	21.3099	19.3061	16.8309
R_{44} (cm/mr)	0.3866	1.8509	2.4876	2.9485

Table 29

Quadrupole settings (kG) for beam delivery to TGT6—2 mm beam spot
 Extraction from high- β accelerator for $A = 30$, $Q = 5$, $E = 7.88 \text{ MeV}/\mu$.

Element	$\epsilon = 3\pi \text{ mm-mr}$	$\epsilon = 4\pi \text{ mm-mr}$	$\epsilon = 5\pi \text{ mm-mr}$	$\epsilon = 6\pi \text{ mm-mr}$
CQ1	-98.03815	-100.73928	-101.12450	-102.07009
CQ2	82.07839	82.81268	83.24727	83.40509
CQ3	-113.34887	-114.50305	-114.74036	-114.90671
CQ4	52.42154	30.23383	28.60170	27.58121
CQ5	-147.49741	-138.86931	-139.69081	-139.69081
CQ6	144.24428	152.91388	161.87279	164.73394
CQ7	-222.52461	-214.48856	-207.96966	-202.87160
CQ8	126.74513	124.29783	123.52505	122.90669
CQ9	-158.97605	-150.94011	-150.94011	-250.94011
B3	12.57569			
56Q1	-121.93427	-126.86431	-131.13522	-135.18660
56Q2	172.36773	173.58904	174.61944	175.57408
56Q3	172.36773	173.58904	174.61944	175.57408
56Q4	-121.93427	-126.86431	-131.13522	-135.18660
B4	12.57569			
T6Q1	-158.97605	-150.94011	-150.94011	-150.94011
T6Q2	126.74513	124.29783	123.52505	122.90669
T6Q3	-222.52461	-214.48856	-207.96966	-202.87160

Table 30(a)

Beam parameters along the M6–TGT6 beamline as a function of emittance
Extraction from high- β accelerator with 2 mm beam spots at M6 and TGT6

Location	Parameter	Emittance (mm-mr)			
		3π	4π	5π	6π
M6	$\pm x$ (cm)	0.085	0.085	0.085	0.085
	$\pm\theta$ (mr)	3.529	4.706	5.883	7.058
	$\pm y$ (cm)	0.085	0.085	0.085	0.085
	$\pm\phi$ (mr)	3.529	4.705	5.883	7.058
MID	$\pm x$ (cm)	0.126	0.166	0.201	0.235
	$\pm\theta$ (mr)	20.242	20.621	20.955	21.273
	$\pm y$ (cm)	0.207	0.234	0.270	0.301
	$\pm\phi$ (mr)	1.452	1.712	1.852	1.994
TGT6	$\pm x$ (cm)	0.085	0.085	0.085	0.085
	$\pm\theta$ (mr)	3.529	4.706	5.883	7.058
	$\pm y$ (cm)	0.085	0.085	0.085	0.085
	$\pm\phi$ (mr)	3.529	4.705	5.883	7.058

Table 30(b)

Beam sizes and overall transfer matrix elements at the TGT6 location
Extraction from the high- β accelerator and 2 mm beam spot

Parameter	Emittance (mm-mr)			
	3π	4π	5π	6π
R_{11} (cm/cm)	-0.2852	-0.2192	0.0056	0.0719
R_{12} (cm/mr)	-0.0399	-0.0361	-0.0368	-0.0328
R_{16} (cm/% $\delta p/p$)	0.0000	0.0000	0.0000	0.0000
R_{21} (mr/cm)	17.3980	21.0532	27.1665	29.1578
R_{22} (mr/mr)	-1.0726	-1.0924	0.0950	0.6223
R_{26} (mr/% $\delta p/p$)	0.0000	0.0000	0.0000	0.0000
R_{33} (cm/cm)	-0.2387	-0.0275	0.0491	0.0892
R_{34} (cm/mr)	-0.0503	-0.0594	-0.0525	-0.0454
R_{43} (cm/cm)	10.6128	16.6988	18.4368	19.1555
R_{44} (cm/mr)	-1.9517	-0.3002	0.6689	1.4577

Table 31(a)

Alternate tunes for dipoles and quadrupoles (kG) for 2 mm beam spot at TGT6
Extraction from medium- β and high- β accelerators

Element	medium- β	high- β
CQ7	-65.00509	-141.17450
CQ8	59.86963	130.02159
CQ9	-116.64073	-253.31397
B3	5.79059	12.57569
56Q1	-58.34578	-126.71218
56Q2	78.23502	169.90654
56Q2	78.23502	169.90654
56Q4	-58.34578	-126.71218
B4	5.79059	12.57569
T6Q1	-116.64073	-253.31397
T6Q2	59.86963	130.02159
T6Q3	-65.00509	-141.17450

Table 31(b)

Beam parameters along the M6-TGT6 beamline as a function of emittance
Alternate extraction from medium- β accelerator, 2 mm beam spots at M6 and TGT6

Location	Parameter	Emittance (mm-mr)			
		3π	4π	5π	6π
M6	$\pm x$ (cm)	0.080	0.080	0.080	0.080
	$\pm\theta$ (mr)	3.750	4.999	6.251	7.499
	$\pm y$ (cm)	0.080	0.080	0.080	0.080
	$\pm\phi$ (mr)	3.750	5.002	6.250	7.501
MID	$\pm x$ (cm)	0.115	0.139	0.166	0.193
	$\pm\theta$ (mr)	20.013	20.013	20.013	20.013
	$\pm y$ (cm)	0.692	0.923	1.154	1.385
	$\pm\phi$ (mr)	0.433	0.433	0.433	0.433
TGT6	$\pm x$ (cm)	0.080	0.080	0.080	0.080
	$\pm\theta$ (mr)	7.136	7.864	8.714	9.649
	$\pm y$ (cm)	0.080	0.080	0.080	0.080
	$\pm\phi$ (mr)	3.751	5.002	6.250	7.501

Table 31(c)

Elements of the overall transfer matrix at the TGT6 location
 Alternate extraction from the medium- β accelerator with 2 mm beam spot

Parameter	Emittance (mm-mr)			
	3π	4π	5π	6π
R_{11} (cm/cm)	-0.2886	-0.3860	-0.3873	-0.3647
R_{12} (cm/mr)	-0.0317	-0.0150	-0.0054	-0.0005
R_{16} (cm/% $\delta p/p$)	0.0000	0.0000	0.0000	0.0000
R_{21} (mr/cm)	20.2620	14.4792	8.5599	4.2663
R_{22} (mr/mr)	-1.2395	-2.0266	-2.4631	2.7358
R_{26} (mr/% $\delta p/p$)	-6.0713	-6.0713	-6.0713	-6.0713
R_{33} (cm/cm)	-0.4676	-0.3548	-0.2588	-0.1899
R_{34} (cm/mr)	-0.0116	-0.0277	-0.0310	-0.0310
R_{43} (cm/cm)	0.1179	12.2042	19.7987	25.3854
R_{44} (cm/mr)	-2.1356	-1.8673	-1.4918	-1.1199

Table 32 – Proposed placement of elements of the vault beamline

Element	Label	Quad type	S/N	Nominal L_{eff} (m)	Measured L_{eff} (m)
Drift				0.645	
Quadrupole	SEBT:Q1	L2	87136	0.325	0.33162
Drift				0.270	
Quadrupole	SEBT:Q2	L2	87137	0.325	0.33160
Drift				0.645	
Drift				0.645	
Quadrupole	SEBT:Q3	L2	87139	0.325	0.33165
Drift				0.270	
Quadrupole	SEBT:Q4	L2	87140	0.325	0.33160
Drift	M1			0.645	
Drift				0.7175	
Quadrupole	SEBT:Q5	L1	87102	0.180	0.18181
Drift				0.415	
Quadrupole	SEBT:Q6	L1	02146	0.180	0.18184
Drift				0.7175	
Drift				0.7175	
Quadrupole	SEBT:Q7	L1	87116	0.180	0.18174
Drift				0.415	
Quadrupole	SEBT:Q8	L1	02140	0.180	0.18179
Drift	M2			0.7175	
Drift				0.645	
Quadrupole	SEBT:Q9	L2	87141	0.325	0.33167
Drift				0.270	
Quadrupole	SEBT:Q10	L2	87142	0.325	0.33170
Drift				0.645	
Drift				0.645	
Quadrupole	SEBT:Q11	L2	87143	0.325	0.33157
Drift				0.270	
Quadrupole	SEBT:Q12	L2	87144	0.325	0.33165
Drift	M3			0.645	
Drift				0.7475	
Quadrupole	SEBT:Q13	L1	82444	0.180	0.18004
Drift				0.415	
Quadrupole	SEBT:Q14	L1	82452	0.180	0.18019
Drift				0.7475	
Drift				0.7475	
Quadrupole	SEBT:Q15	L1	82458	0.180	0.18019
Drift				0.415	
Quadrupole	SEBT:Q16	L1	82459	0.180	0.18021
Drift	M4			0.7475	
Drift				0.675	
Quadrupole	SEBT:Q17	L2	87145	0.325	0.33167
Drift				0.270	
Quadrupole	SEBT:Q18	L2	87149	0.325	0.33183
Drift				0.675	
Drift				0.675	
Quadrupole	SEBT:Q19	L2	87150	0.325	0.33162
Drift				0.270	
Quadrupole	SEBT:Q20	L2	87151	0.325	0.33167
Drift	M5			0.675	
Total length (m)				22.340	

Table 33

Settings for the production of a 1 mm beam spot at the TGT1A location
 Example 1: A VHHV configuration of length 7.795 m[†]

Parameter	Length (m)	Quadrupole pole-tip field (kG) at emittance (mm-mr)			
		3π	4π	5π	6π
TGT1	0.00000				
Drift	1.50000				
Quadrupole	0.32500	-101.59139	-104.18889	-104.72807	-105.16717
Drift	0.25400				
Drift	0.10180				
Quadrupole	0.40640	18.01966	20.04216	20.06161	20.29074
Drift	0.10180				
Drift	0.96463				
Drift	0.96463				
Drift	0.16420				
Quadrupole	0.48440	50.62281	50.36113	50.38708	50.36514
Drift	0.16420				
Drift	0.25400				
Drift	0.10180				
Quadrupole	0.40640	-80.48929	-80.46349	-80.53785	-80.55866
Drift	0.10180				
Drift	1.50000				
TGT1A	0.00000				

[†] A bore radius of 100 cm has been assumed for all quadrupoles; quadrupole lengths are effective lengths.

Table 34

Settings for the production of a 1 mm beam spot at the TGT1A location
 Example 2: A VHVHV configuration of length 6.623 m[†]

Parameter	Length (m)	Quadrupole pole-tip field (kG) at emittance (mm-mr)			
		3π	4π	5π	6π
TGT1	0.00000				
Drift	1.50000				
Quadrupole	0.20000	-41.33749	-41.16505	-41.17141	-41.17483
Drift	0.30000				
Quadrupole	0.20000	4.46327	4.46327	4.46327	4.46327
Drift	0.50000				
Drift	0.10180				
Quadrupole	0.40640	-31.34894	-31.43413	-31.43413	-31.43413
Drift	0.10180				
Drift	0.50000				
Drift	0.16420				
Quadrupole	0.48440	68.44696	68.47280	68.47835	68.48137
Drift	0.16420				
Drift	0.30000				
Quadrupole	0.20000	-158.62016	-158.56619	-158.55860	-158.55449
Drift	1.50000				
TGT1A	0.00000				

[†] A bore radius of 100 cm has been assumed for all quadrupoles; quadrupole lengths are effective lengths.

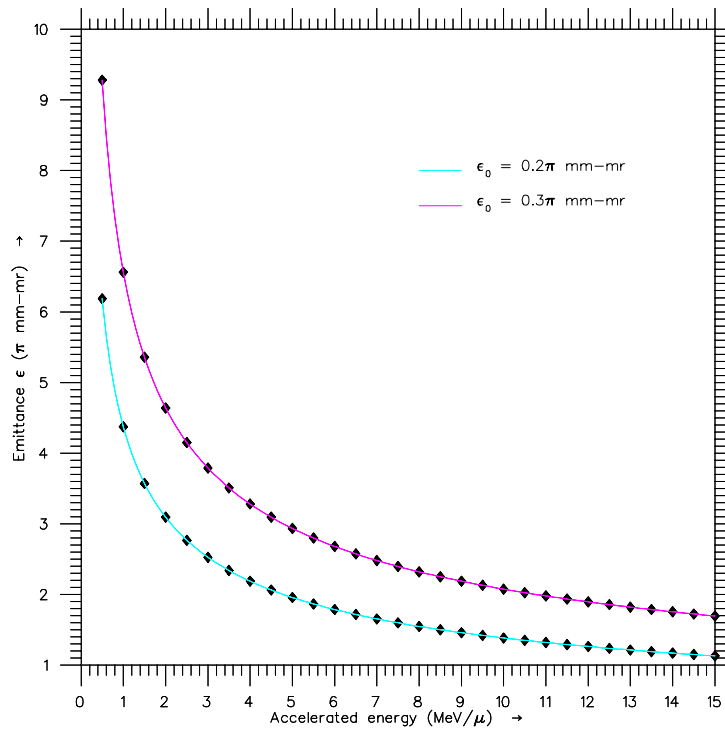


Fig. 1(a). Estimated emittance variation as a function of acceleration energy—large scale.

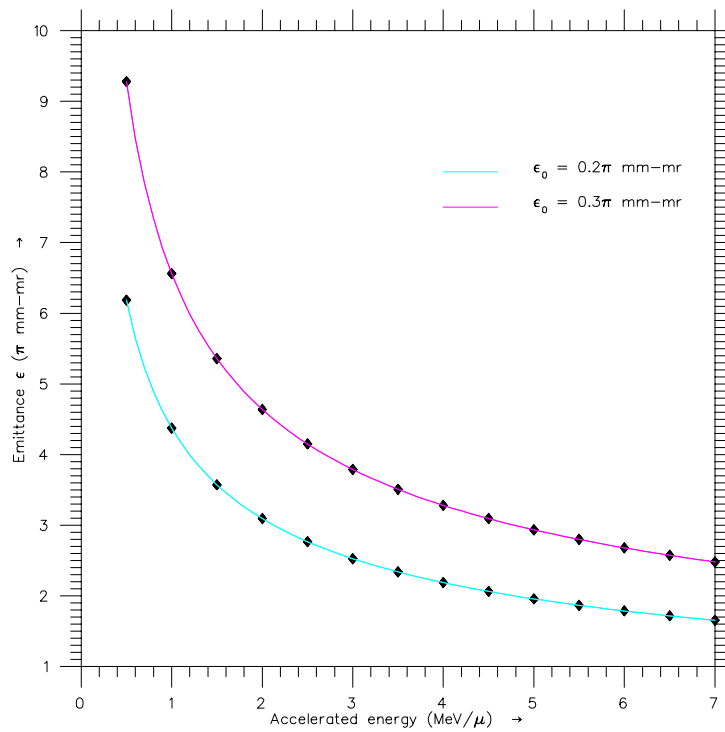


Fig. 1(b). Estimated emittance variation as a function of acceleration energy—small scale.

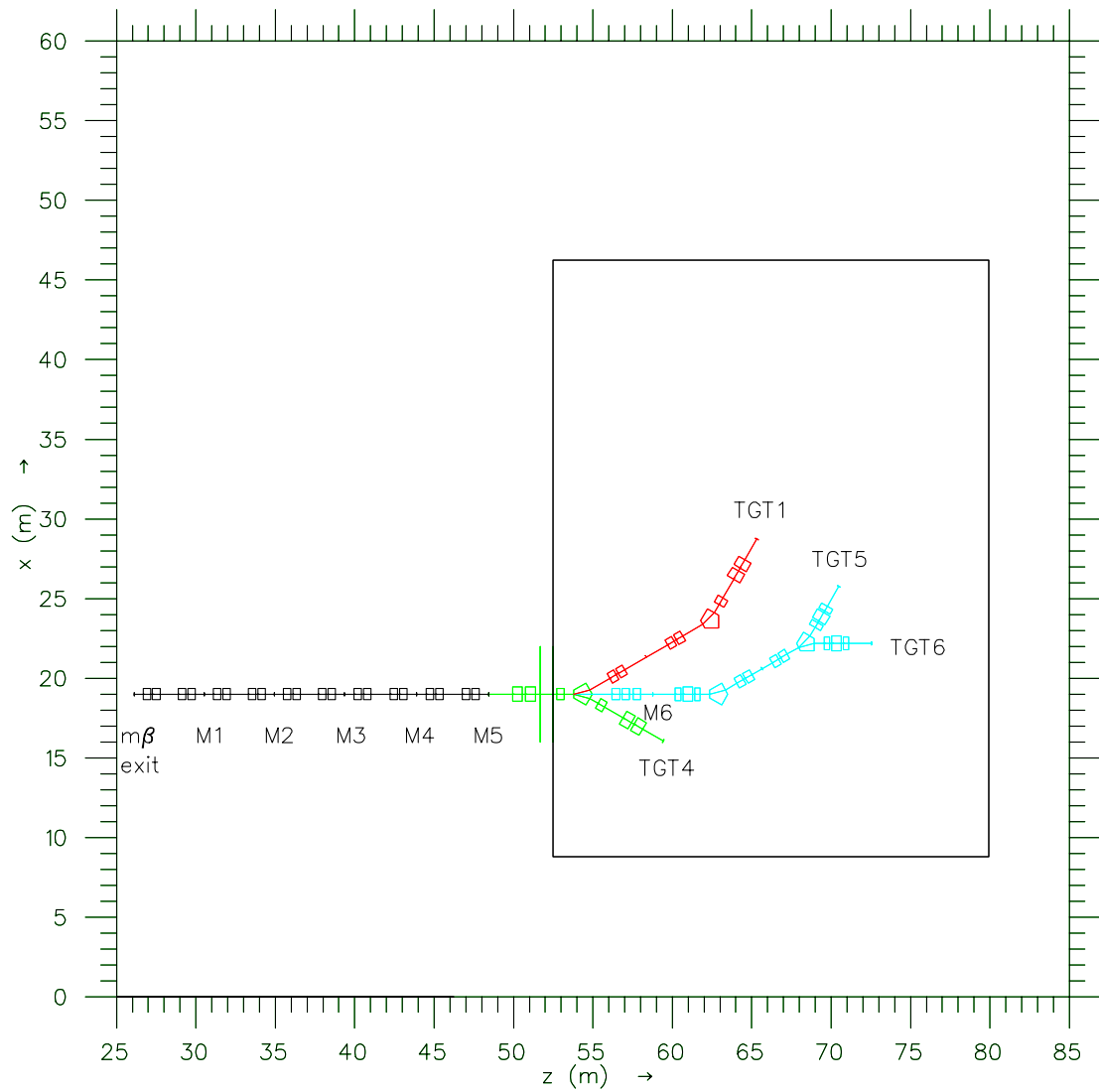


Fig. 2. Proposed final configuration of the ISAC-II experimental hall.

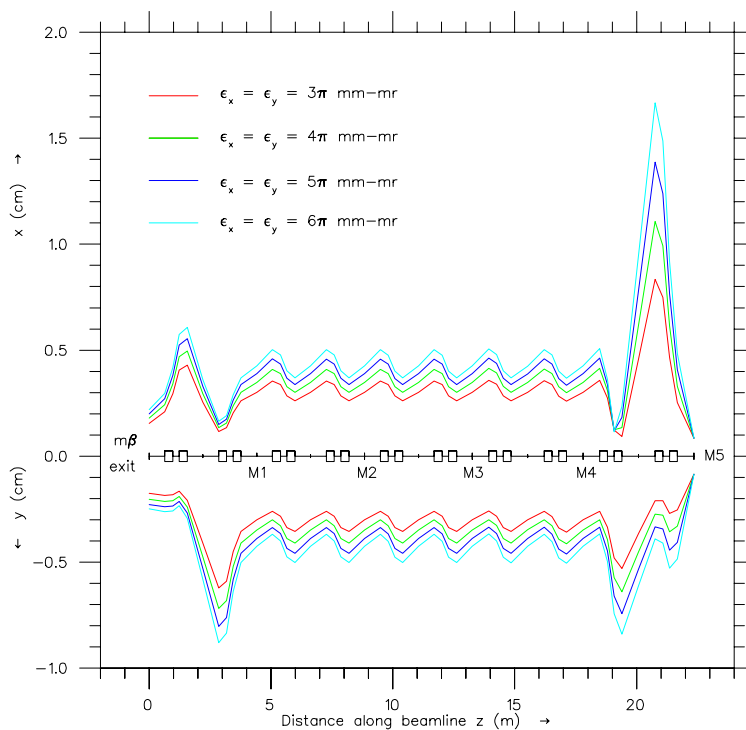


Fig. 3. Beam envelopes in the vault section for the production of a 2 mm beam spot at the M5 location with a multi-charge tune of the beamline. Extraction is from the medium- β accelerator.

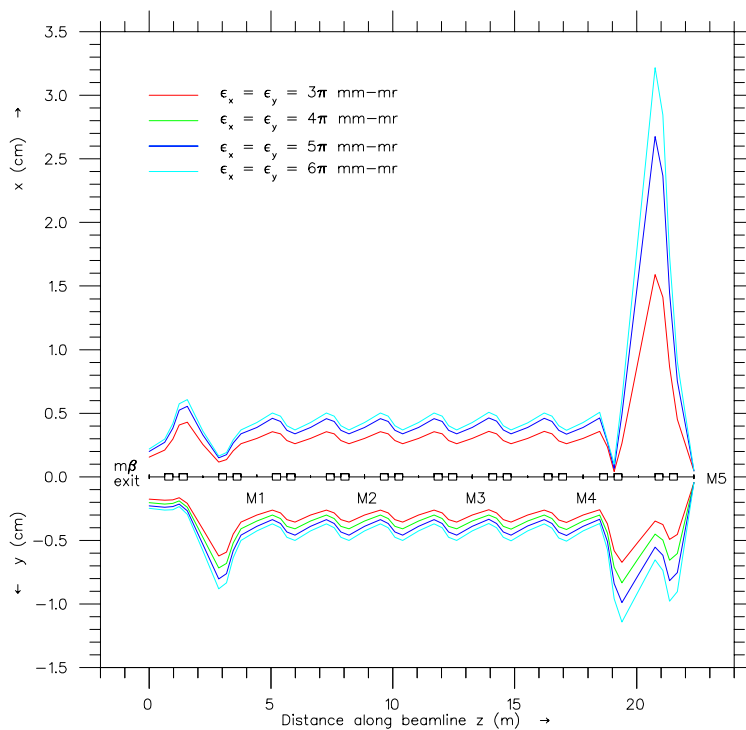


Fig. 4. Beam envelopes in the vault section for the production of a 1 mm beam spot at the M5 location with a multi-charge tune of the beamline. Extraction is from the medium- β accelerator.

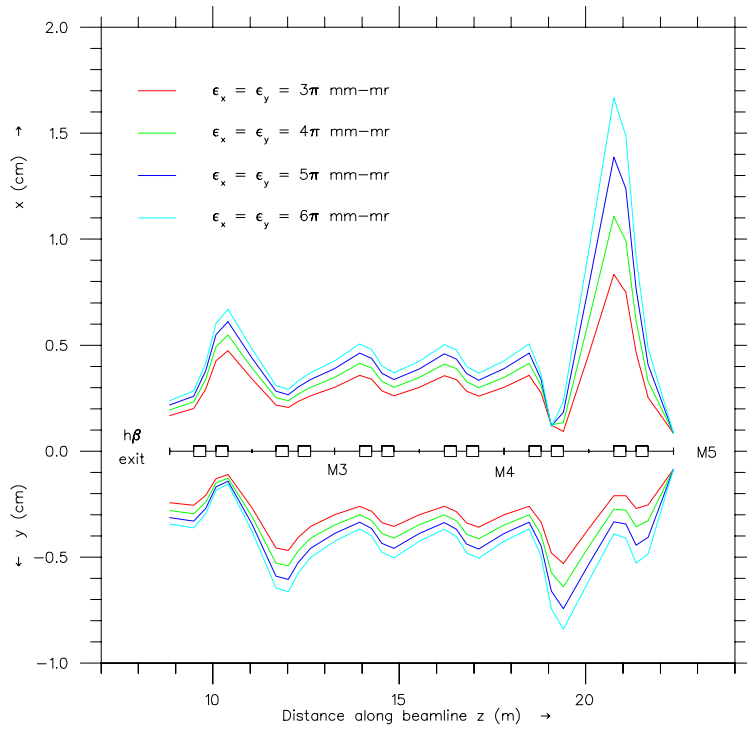


Fig. 5. Beam envelopes in the vault section for the production of a 2 mm beam spot at the M5 location with a multi-charge tune of the beamline. Extraction is from the high- β accelerator.

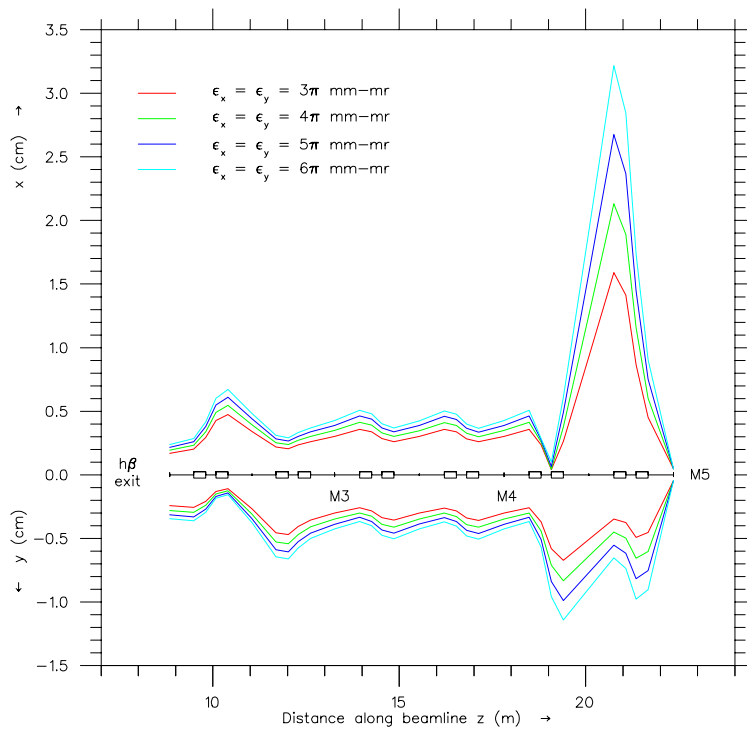


Fig. 6. Beam envelopes in the vault section for the production of a 1 mm beam spot at the M5 location with a multi-charge tune of the beamline. Extraction is from the high- β accelerator.

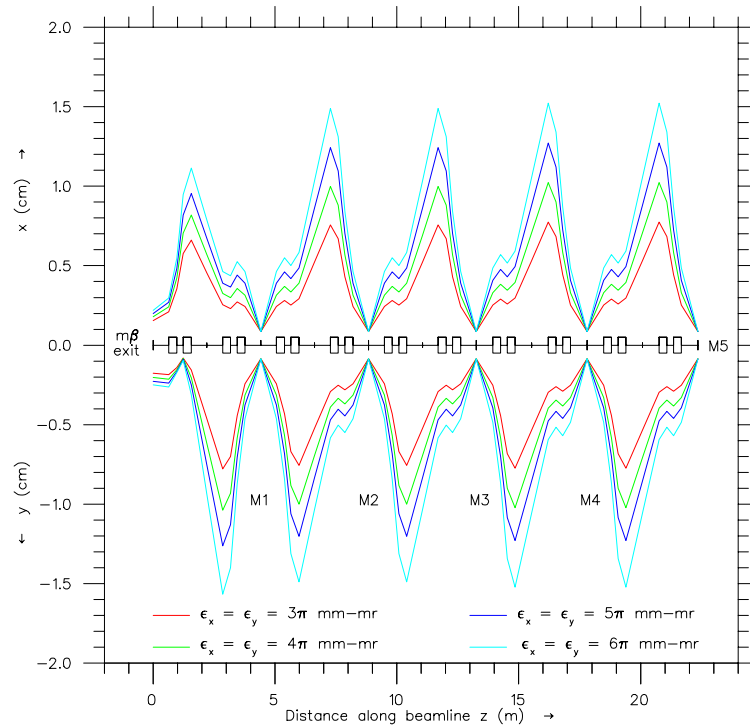


Fig. 7. Case 1. Beam envelopes in the vault section for the production of a 2 mm beam spot at the M5 location with a single-charge tune of the beamline. Extraction is from the medium- β accelerator.

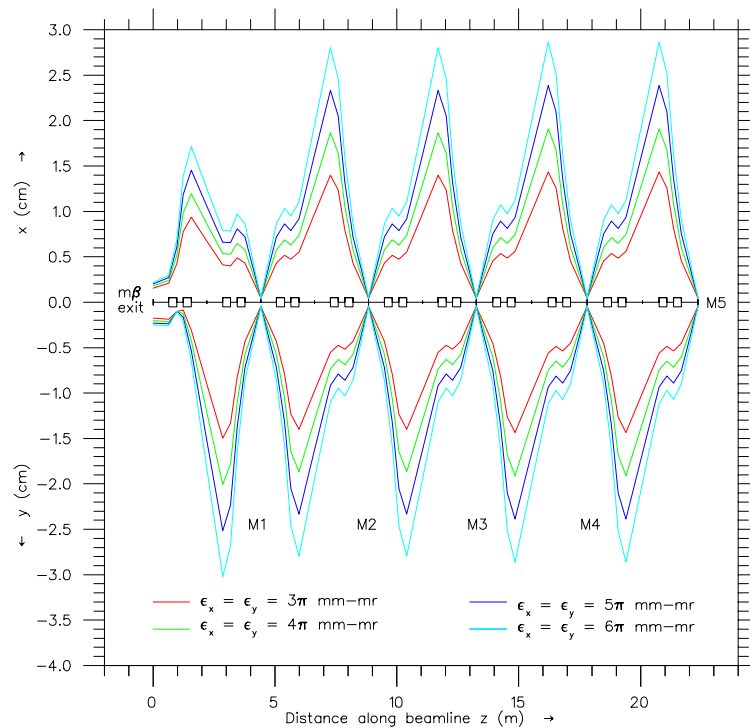


Fig. 8. Case 1. Beam envelopes in the vault section for the production of a 1 mm beam spot at the M5 location with a single-charge tune of the beamline. Extraction is from the medium- β accelerator.

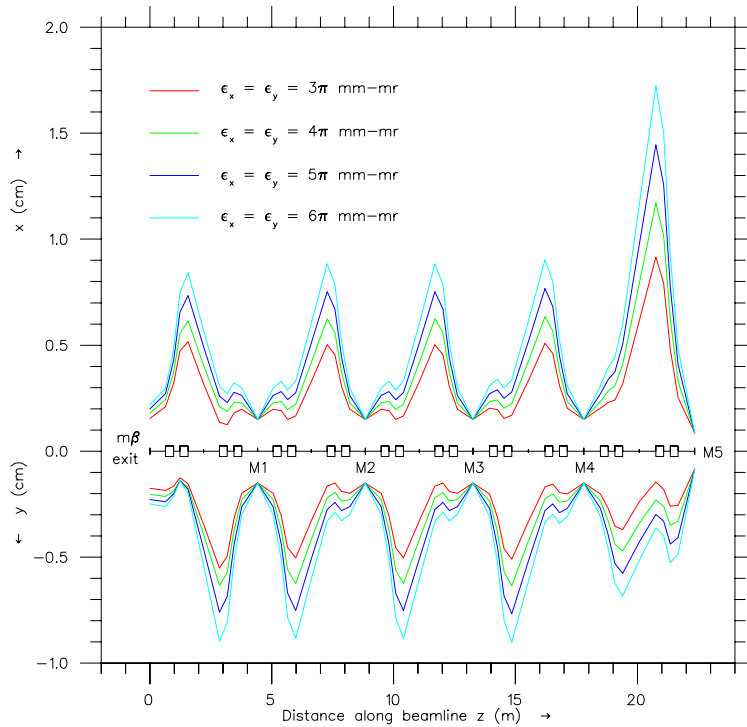


Fig. 9. Case 2. Beam envelopes in the vault section for the production of a 2 mm beam spot at the M5 location with a single-charge tune of the beamline. Extraction is from the medium- β accelerator.

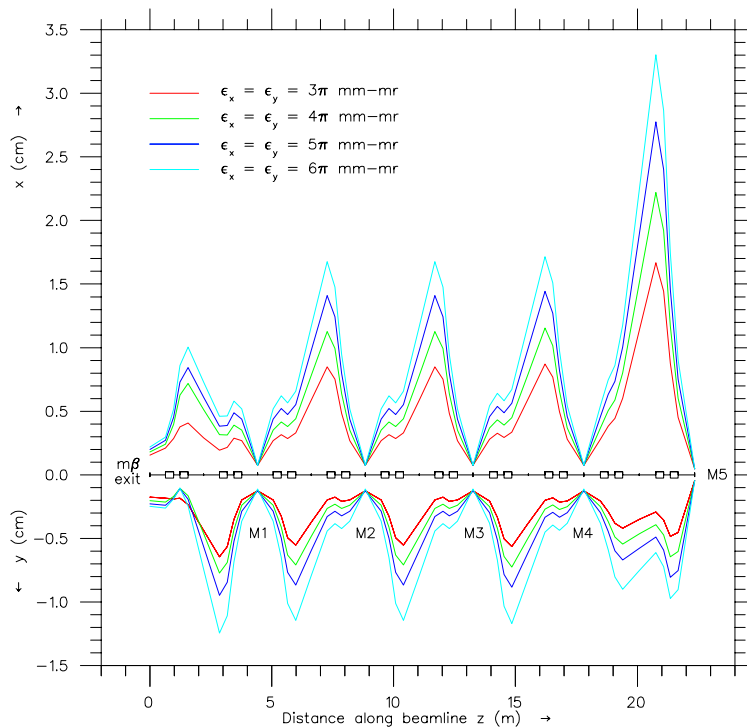


Fig. 10. Case 2. Beam envelopes in the vault section for the production of a 1 mm beam spot at the M5 location with a single-charge tune of the beamline. Extraction is from the medium- β accelerator.

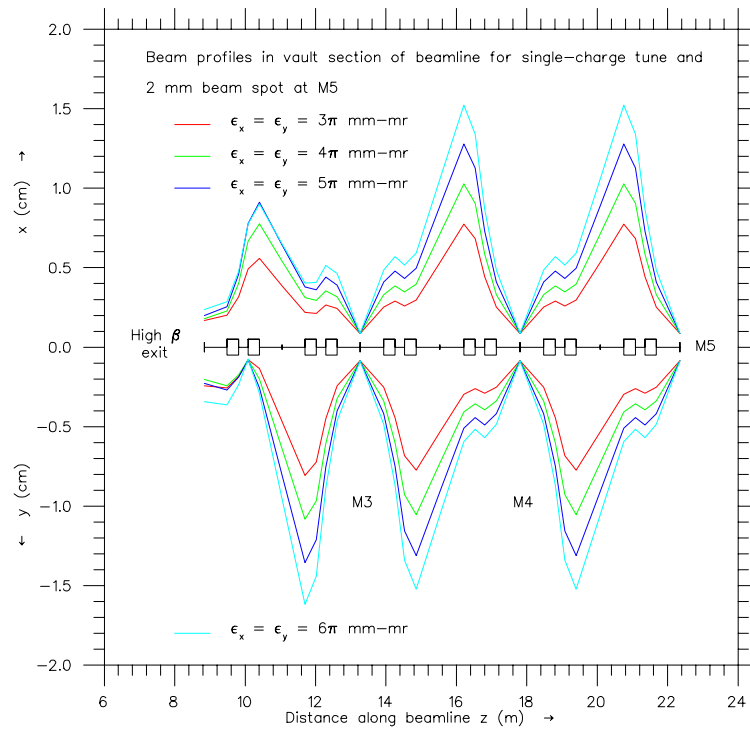


Fig. 11. Beam envelopes in the vault section for the production of a 2 mm beam spot at the M5 location with a single-charge tune of the beamline. Extraction is from the high- β accelerator.

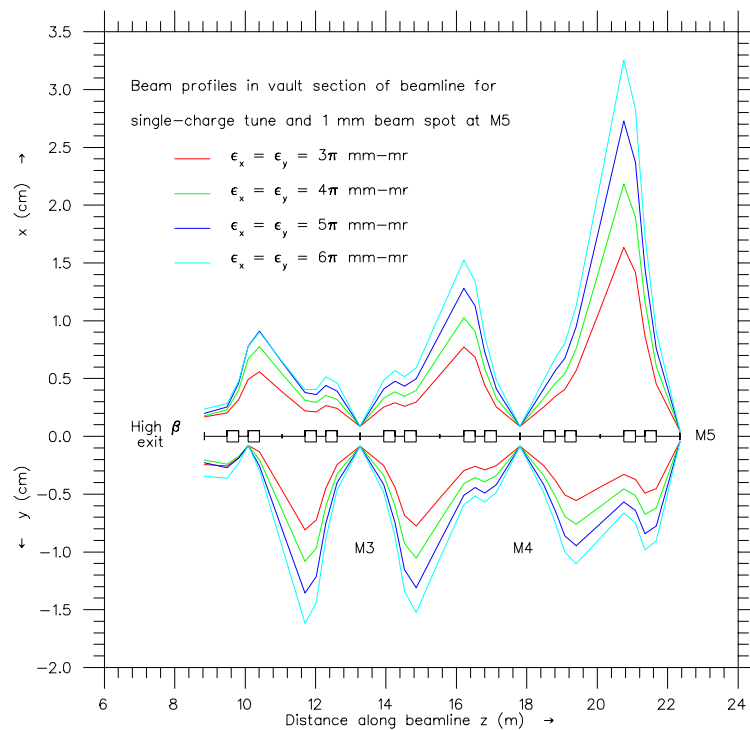


Fig. 12. Beam envelopes in the vault section for the production of a 1 mm beam spot at the M5 location with a single-charge tune of the beamline. Extraction is from the high- β accelerator.

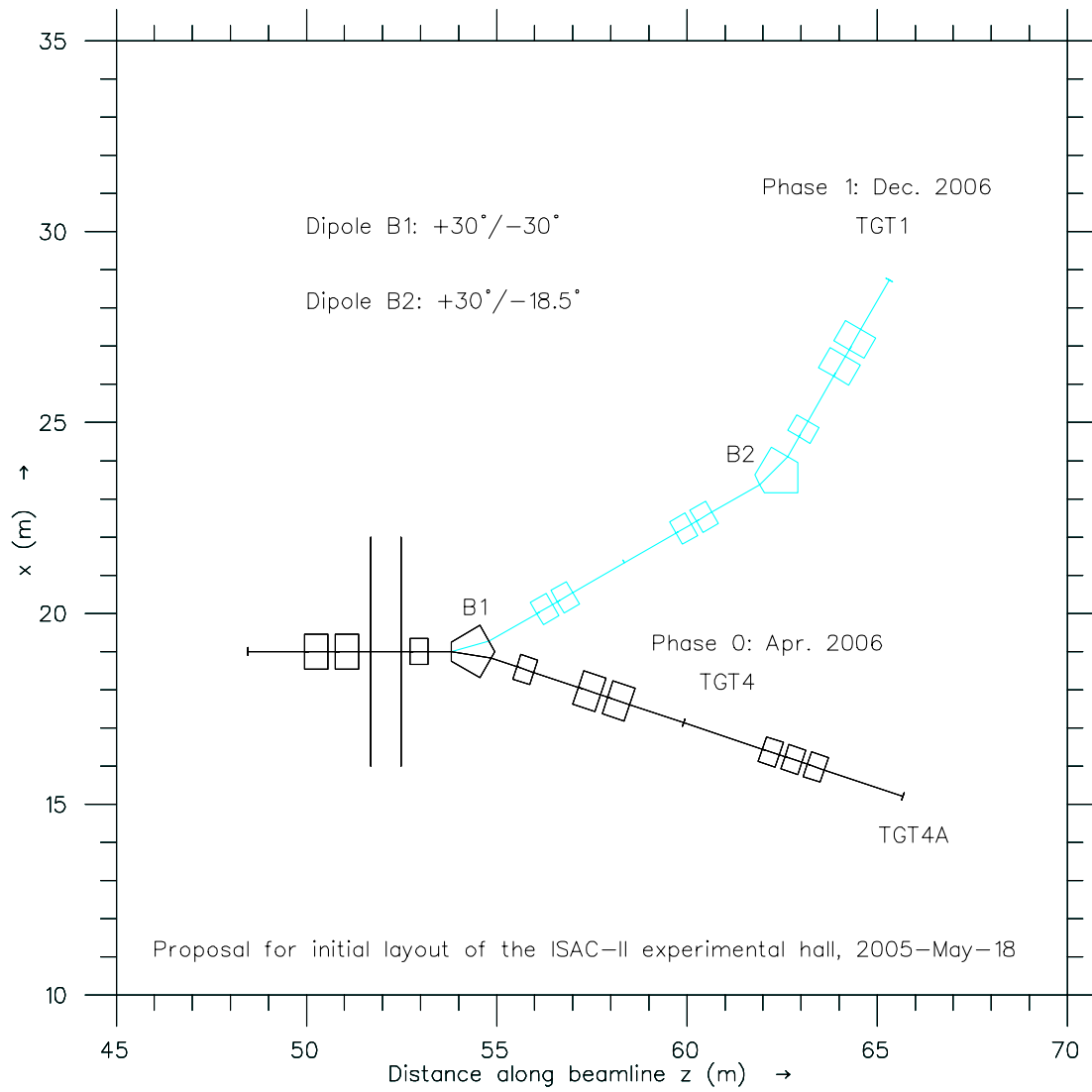


Fig. 13. An alternate beam-transport configuration for initial beam delivery to experimental targets TGT1 and TGT4.

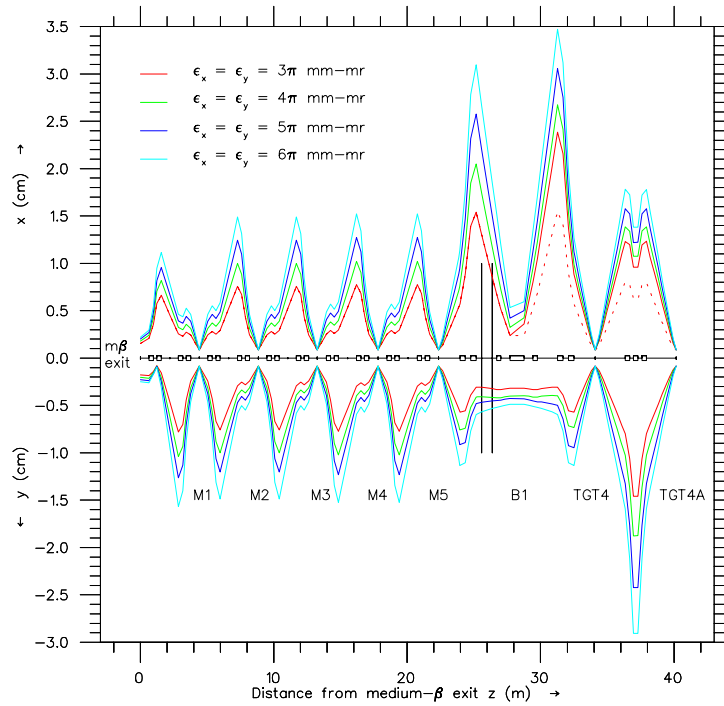


Fig. 14(a). Beam profiles on the beamline from the medium- β exit to the TGT4 and TGT4A locations as a function of emittance for a 2 mm beam spot. See also the caption below.

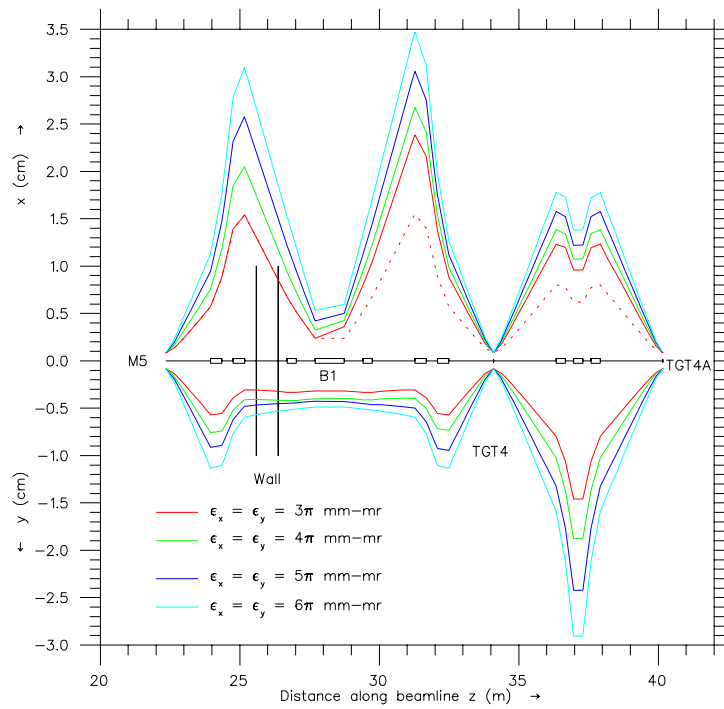


Fig. 14(b). Beam profiles on the beamline from the M5 location to the TGT4 location as a function of emittance. The solid curves are for beams with a momentum spread of $\pm 1\% \delta p/p$; the dotted curve is for an emittance of 3π mm-mrad and a beam with a momentum spread of $\pm 0.1\% \delta p/p$.

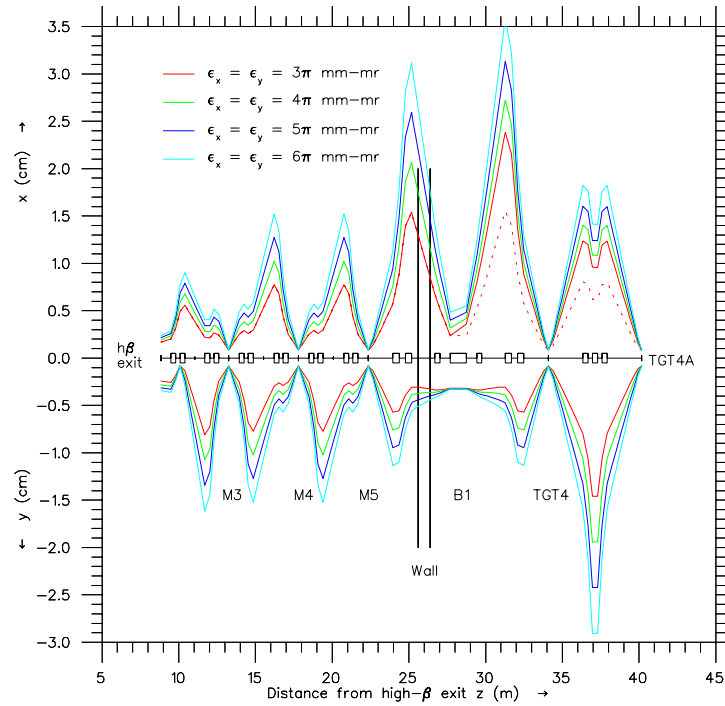


Fig. 15(a). Beam profiles on the beamline from the high-β exit to the TGT4 and TGT4A locations as a function of emittance for a 2 mm beam spot. See also the caption below.

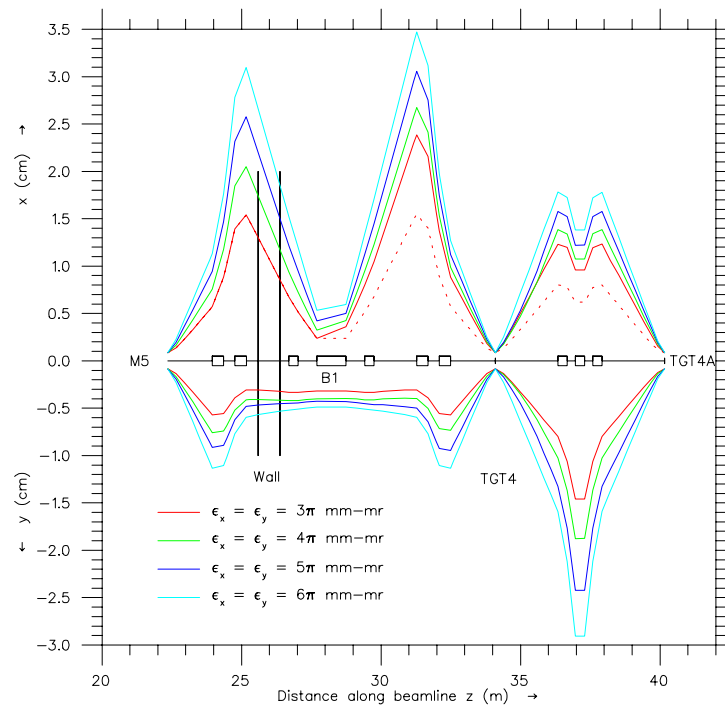


Fig. 15(b). Beam profiles on the beamline from the M5 location to the TGT4 location as a function of emittance. The solid curves are for beams with a momentum spread of $\pm 1\% \delta p/p$; the dotted curve is for an emittance of 3π mm-mrad and a beam with a momentum spread of $\pm 0.1\% \delta p/p$.

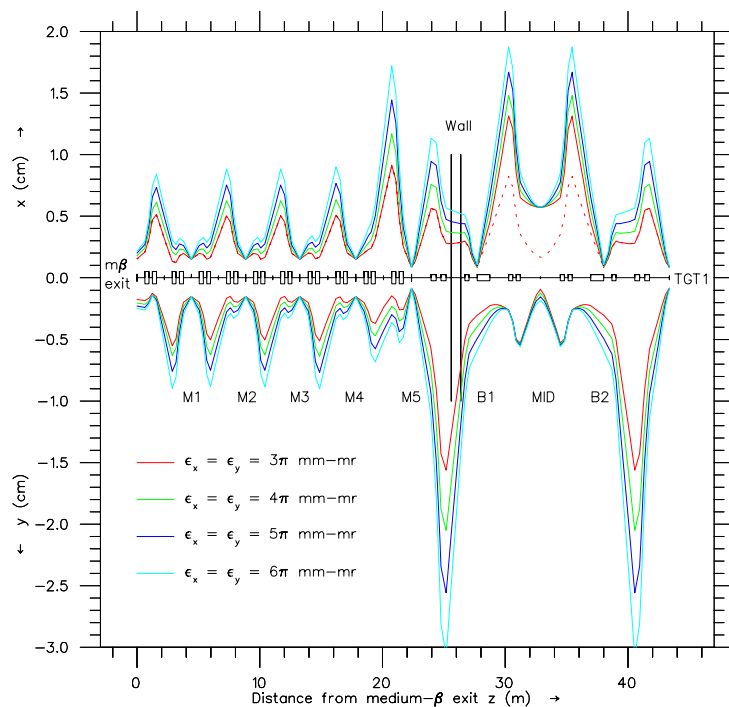


Fig. 16(a). Beam profiles on the beamline from the medium- β exit to the TGT1 location as a function of emittance for a 2 mm beam spot. See also the caption below.

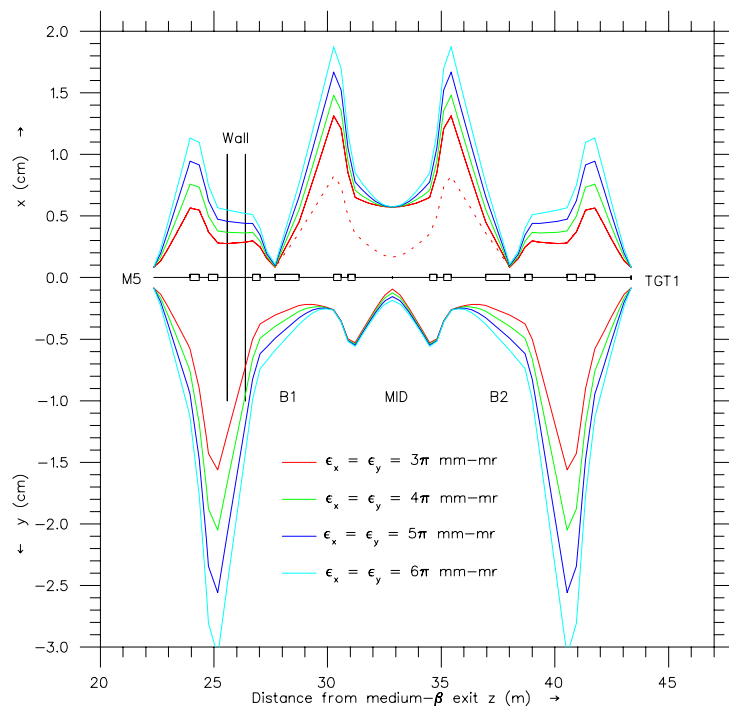


Fig. 16(b). Beam profiles on the beamline from the M5 location to the TGT1 location as a function of emittance. The solid curves are for beams with a momentum spread of $\pm 1\% \delta p/p$; the dotted curve is for an emittance of 3π mm-mrad and a beam with a momentum spread of $\pm 0.1\% \delta p/p$.

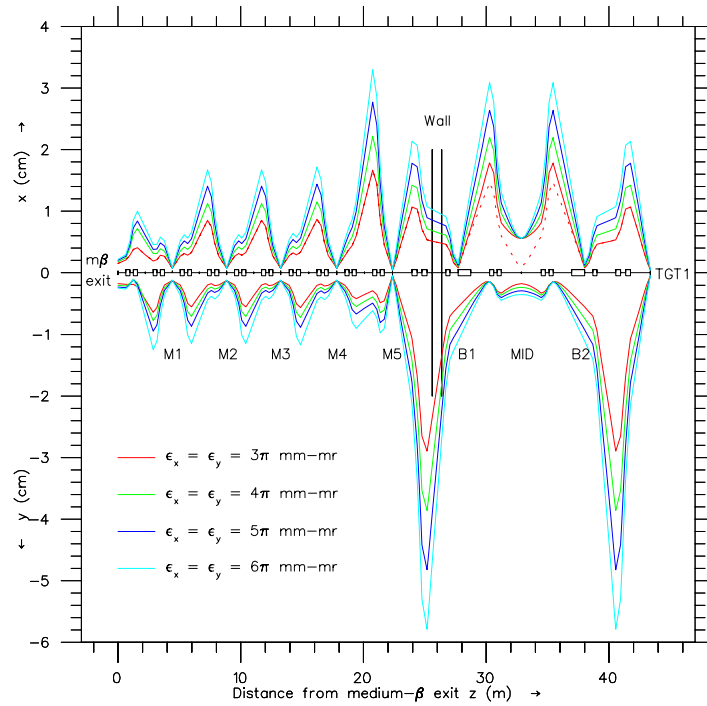


Fig. 17(a). Beam profiles on the beamline from the medium- β exit to the TGT1 location as a function of emittance for a 1 mm beam spot. See also the caption below.

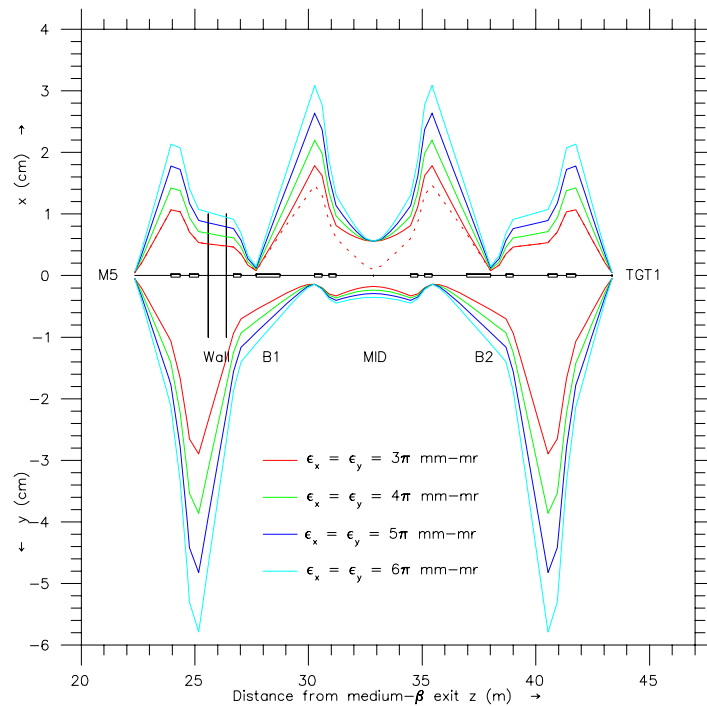


Fig. 17(b). Beam profiles on the beamline from the M5 location to the TGT1 location as a function of emittance. The solid curves are for beams with a momentum spread of $\pm 1\% \delta p/p$; the dotted curve is for an emittance of 3π mm-mrad and a beam with a momentum spread of $\pm 0.1\% \delta p/p$.

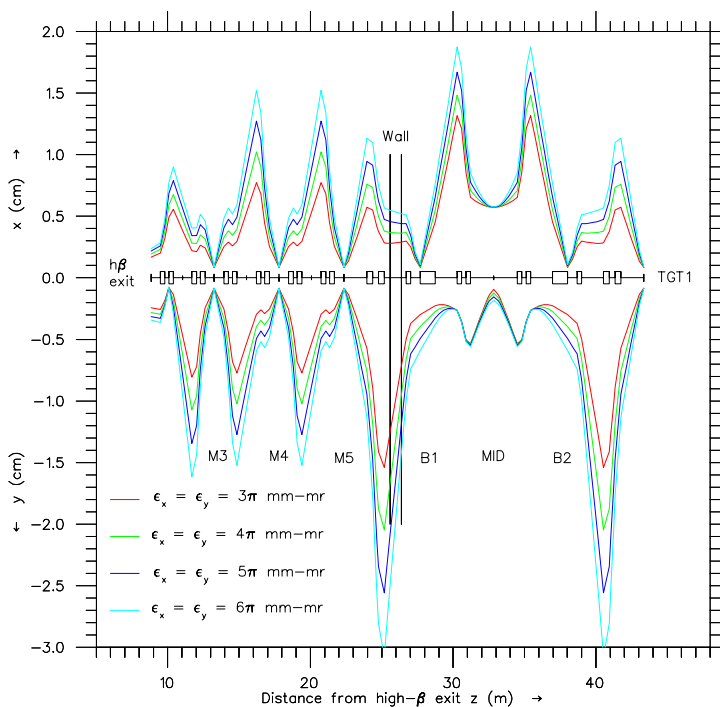


Fig. 18(a). Beam profiles on the beamline from the high- β exit to the TGT1 location as a function of emittance for a 2 mm beam spot. See also the caption below.

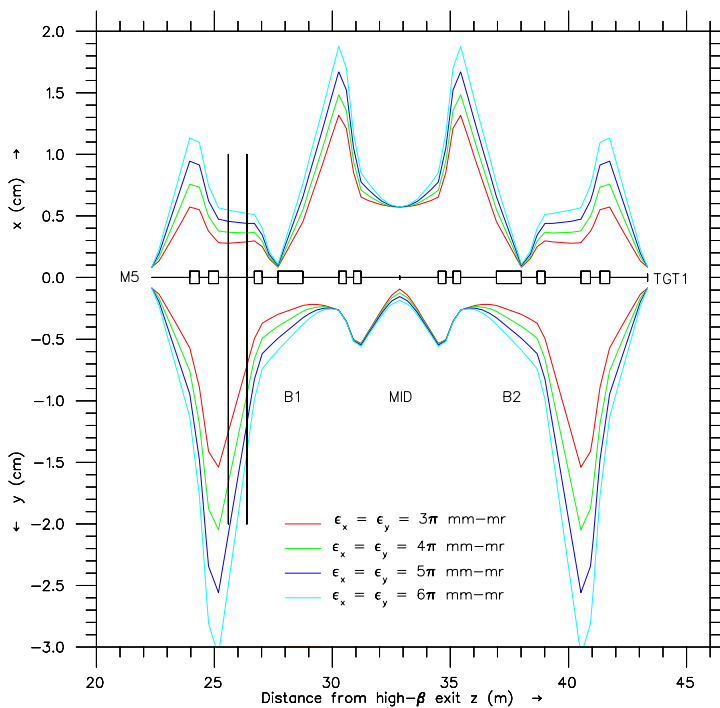


Fig. 18(b). Beam profiles on the beamline from the M5 location to the TGT1 location as a function of emittance. The solid curves are for beams with a momentum spread of $\pm 1\% \delta p/p$.

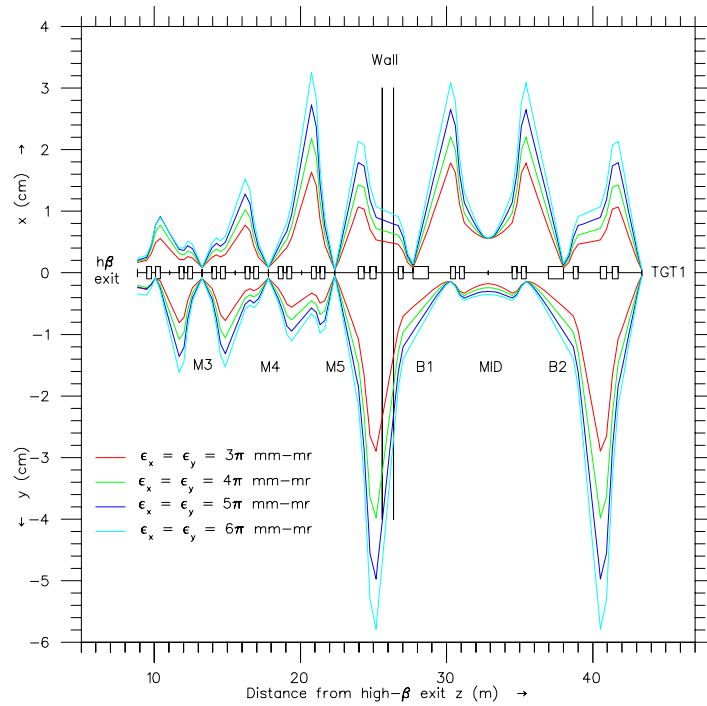


Fig. 19(a). Beam profiles on the beamline from the high- β exit to the TGT1 location as a function of emittance for a 1 mm beam spot. See also the caption below.

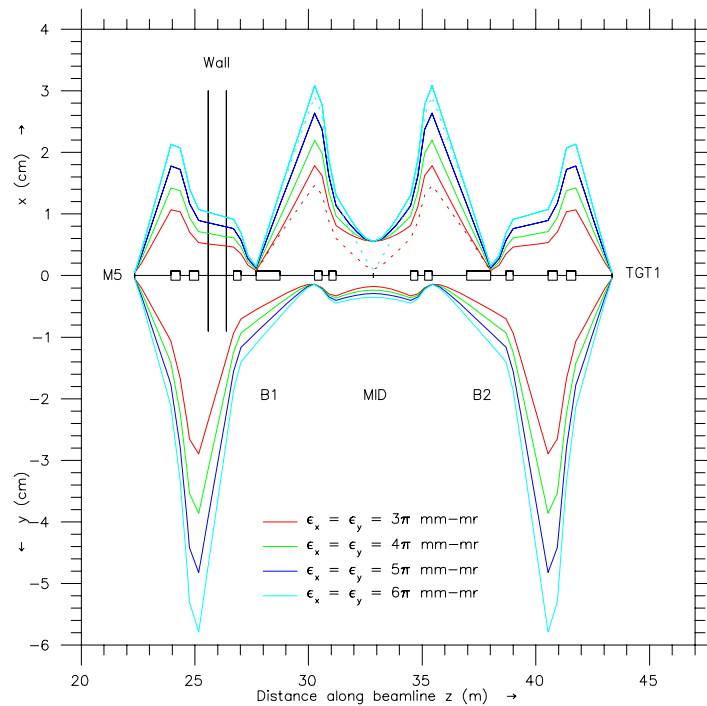


Fig. 19(b). Beam profiles on the beamline from the M5 location to the TGT1 location as a function of emittance. The solid curves are for beams with a momentum spread of $\pm 1\% \delta p/p$; the dotted curves are for an emittance of 3π and 6π mm-mrad and a beam with a momentum spread of $\pm 0.1\% \delta p/p$.

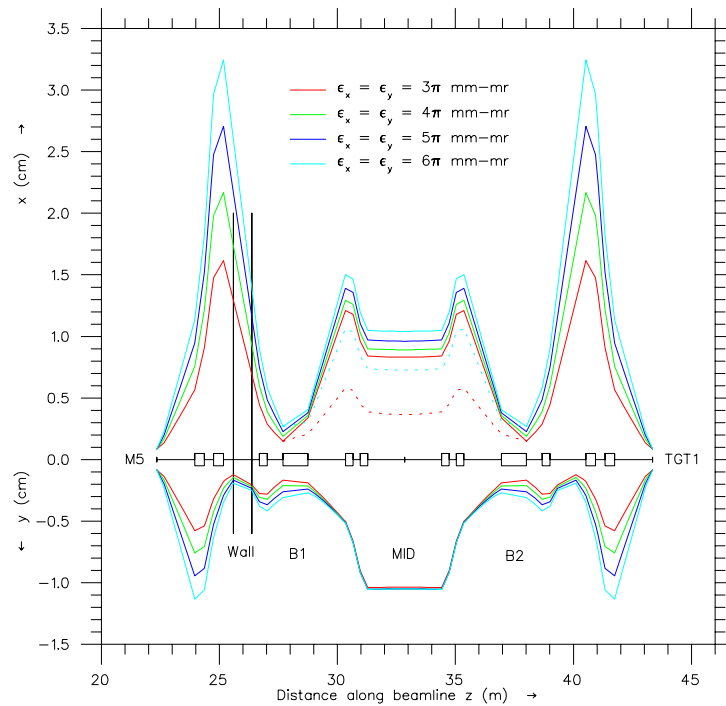


Fig. 19(c). Beam profiles on version 2 of the beamline from the M5 location to the TGT1 location—2 mm beam spot.

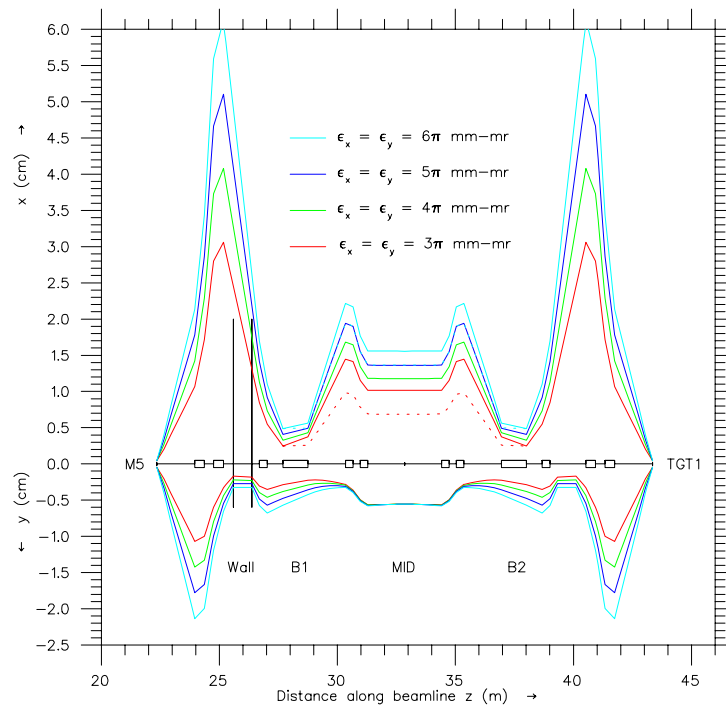


Fig. 19(d). Beam profiles on version 2 of the beamline from the M5 location to the TGT1 location—1 mm beam spot. The solid curves are for beams with a momentum spread of $\pm 1\% \delta p/p$; the dotted curves are for an emittances of 3π and 6π mm-mrad and a beam with a momentum spread of $\pm 0.1\% \delta p/p$.

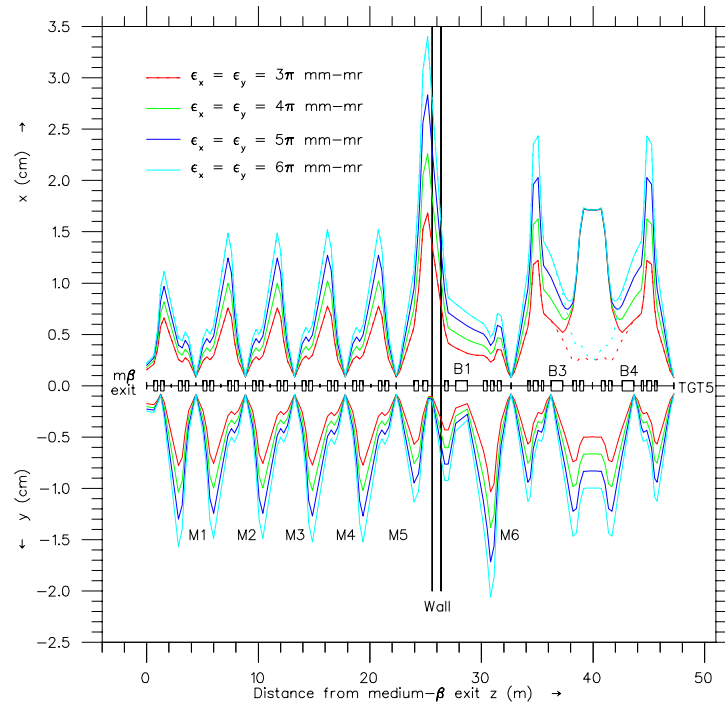


Fig. 20(a). Beam profiles on the beamline from the medium- β exit to the TGT5 location as a function of emittance for a 2 mm beam spot. See also the caption below.

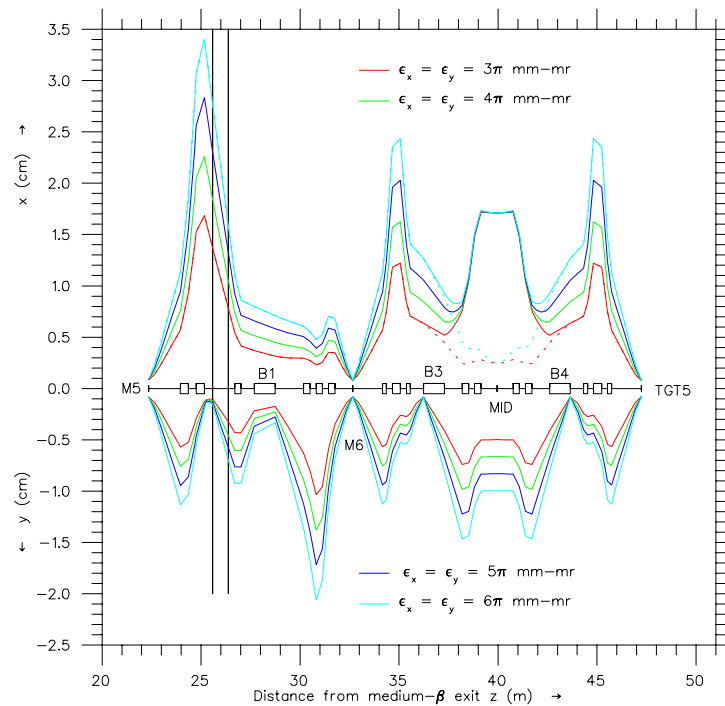


Fig. 20(b). Beam profiles on the beamline from the M5 location to the TGT5 location as a function of emittance. The solid curves are for beams with a momentum spread of $\pm 1\% \delta p/p$; the dotted curves are for an emittances of 3π and 6π mm-mrad and a beam with a momentum spread of $\pm 0.1\% \delta p/p$.

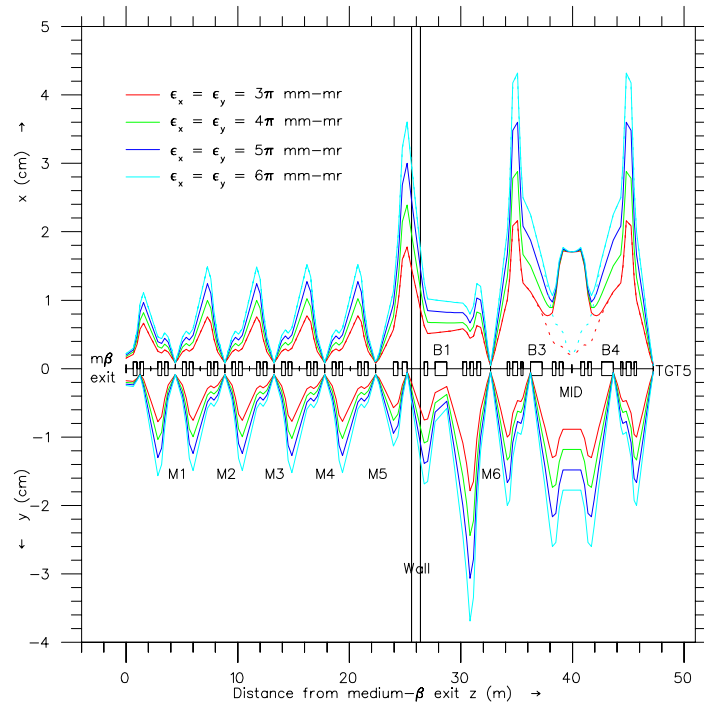


Fig. 21(a). Beam profiles on the beamline from the medium- β exit to the TGT5 location as a function of emittance for a 1 mm beam spot. See also the caption below.

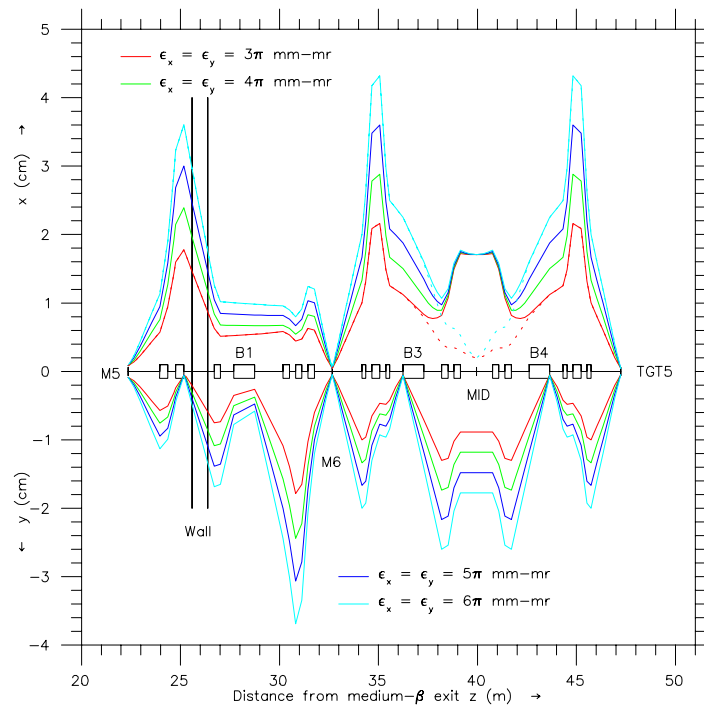


Fig. 21(b). Beam profiles on the beamline from the M5 location to the TGT5 location as a function of emittance. The solid curves are for beams with a momentum spread of $\pm 1\% \delta p/p$; the dotted curves are for an emittances of 3π and 6π mm-mrad and a beam with a momentum spread of $\pm 0.1\% \delta p/p$.

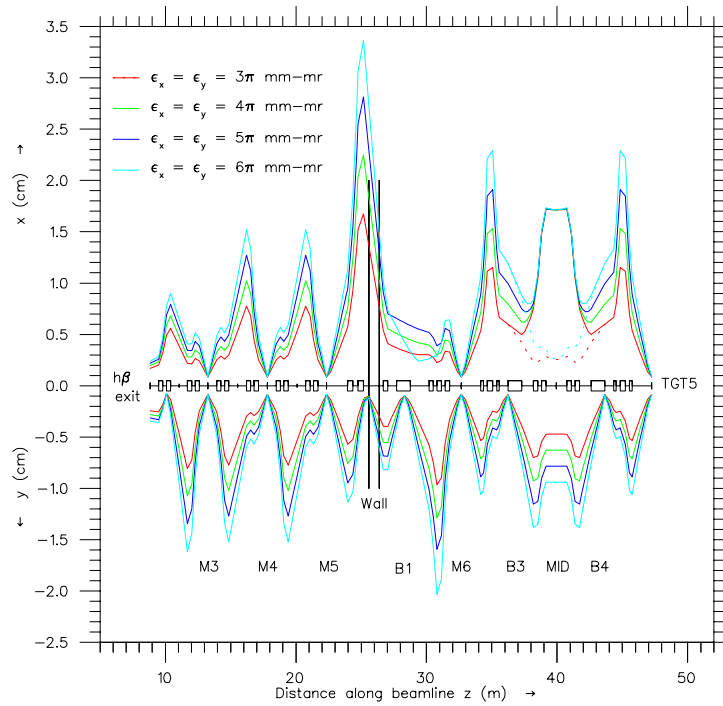


Fig. 22(a). Beam profiles on the beamline from the high- β exit to the TGT5 location as a function of emittance for a 2 mm beam spot. See also the caption below.

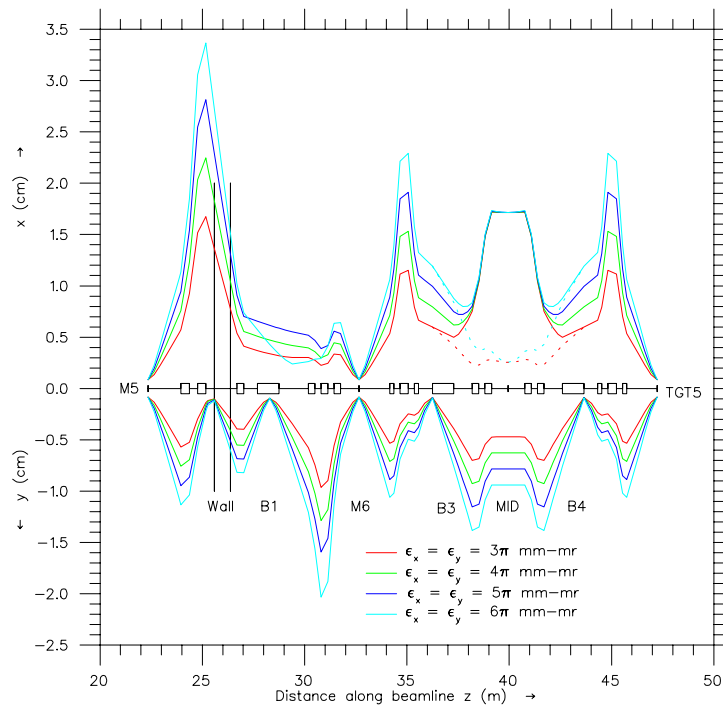


Fig. 22(b). Beam profiles on the beamline from the M5 location to the TGT5 location as a function of emittance. The solid curves are for beams with a momentum spread of $\pm 1\% \delta p/p$; the dotted curves are for an emittances of 3π and 6π mm-mrad and a beam with a momentum spread of $\pm 0.1\% \delta p/p$.

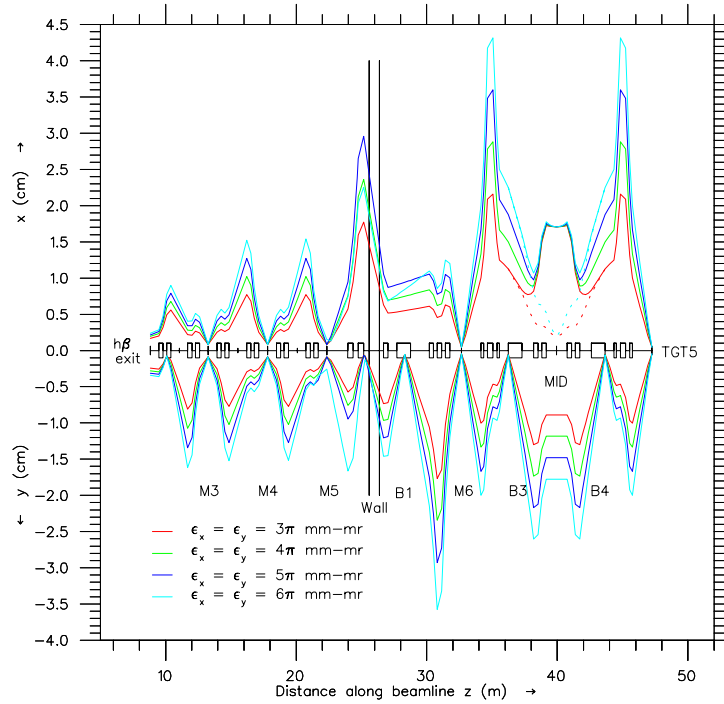


Fig. 23(a). Beam profiles on the beamline from the high- β exit to the TGT5 location as a function of emittance for a 1 mm beam spot. See also the caption below.

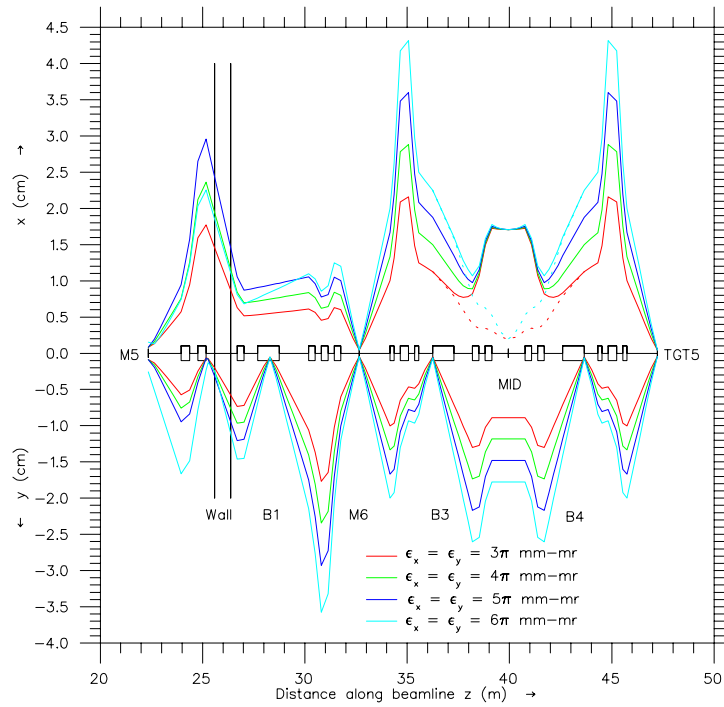


Fig. 23(b). Beam profiles on the beamline from the M5 location to the TGT5 location as a function of emittance. The solid curves are for beams with a momentum spread of $\pm 1\% \delta p/p$; the dotted curves are for an emittances of 3π and 6π mm-mrad and a beam with a momentum spread of $\pm 0.1\% \delta p/p$.

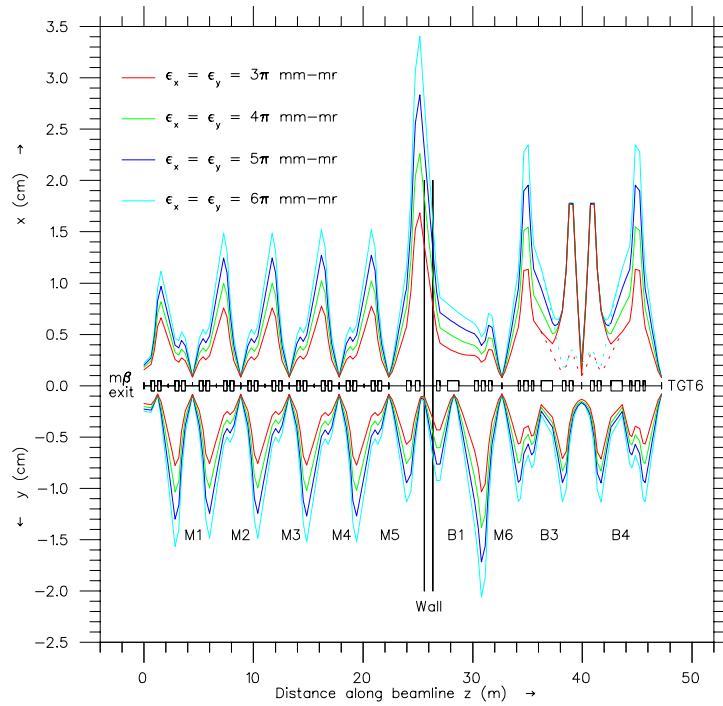


Fig. 24(a). Beam profiles on the beamline from the medium- β exit to the TGT6 location as a function of emittance for a 2 mm beam spot. See also the caption below.

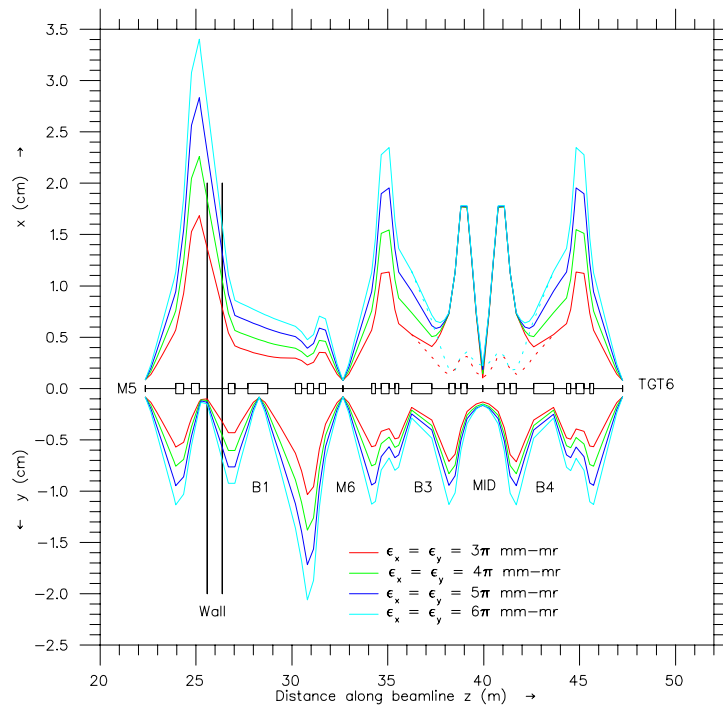


Fig. 24(b). Beam profiles on the beamline from the M5 location to the TGT6 location as a function of emittance. The solid curves are for beams with a momentum spread of $\pm 1\% \delta p/p$; the dotted curves are for an emittances of 3π and 6π mm-mrad and a beam with a momentum spread of $\pm 0.1\% \delta p/p$.

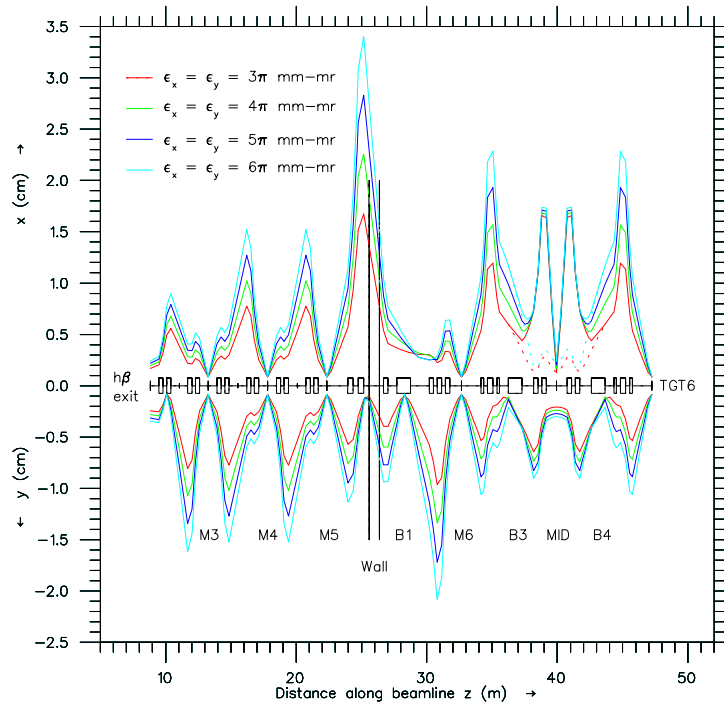


Fig. 25(a). Beam profiles on the beamline from the high- β exit to the TGT6 location as a function of emittance for a 2 mm beam spot. See also the caption below.

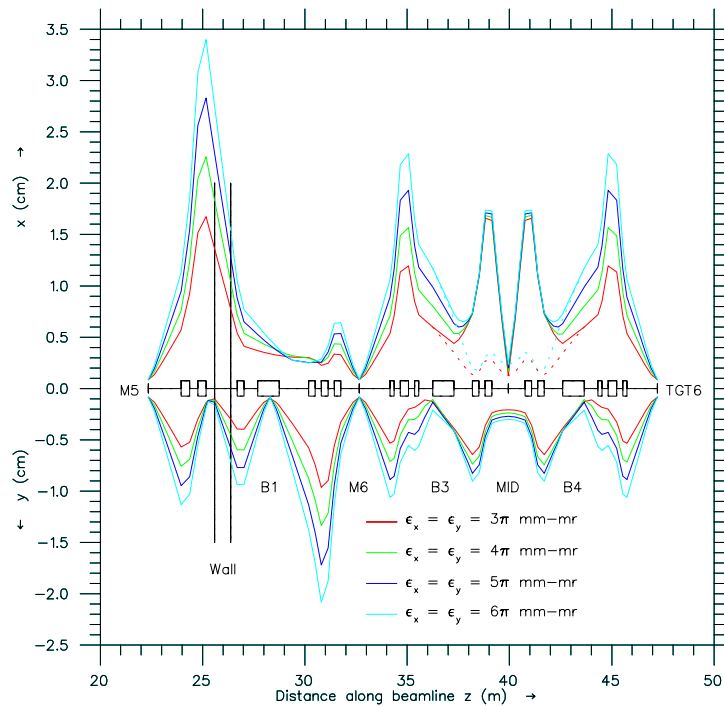


Fig. 25(b). Beam profiles on the beamline from the M5 location to the TGT6 location as a function of emittance. The solid curves are for beams with a momentum spread of $\pm 1\% \delta p/p$; the dotted curves are for an emittances of 3π and 6π mm-mrad and a beam with a momentum spread of $\pm 0.1\% \delta p/p$.

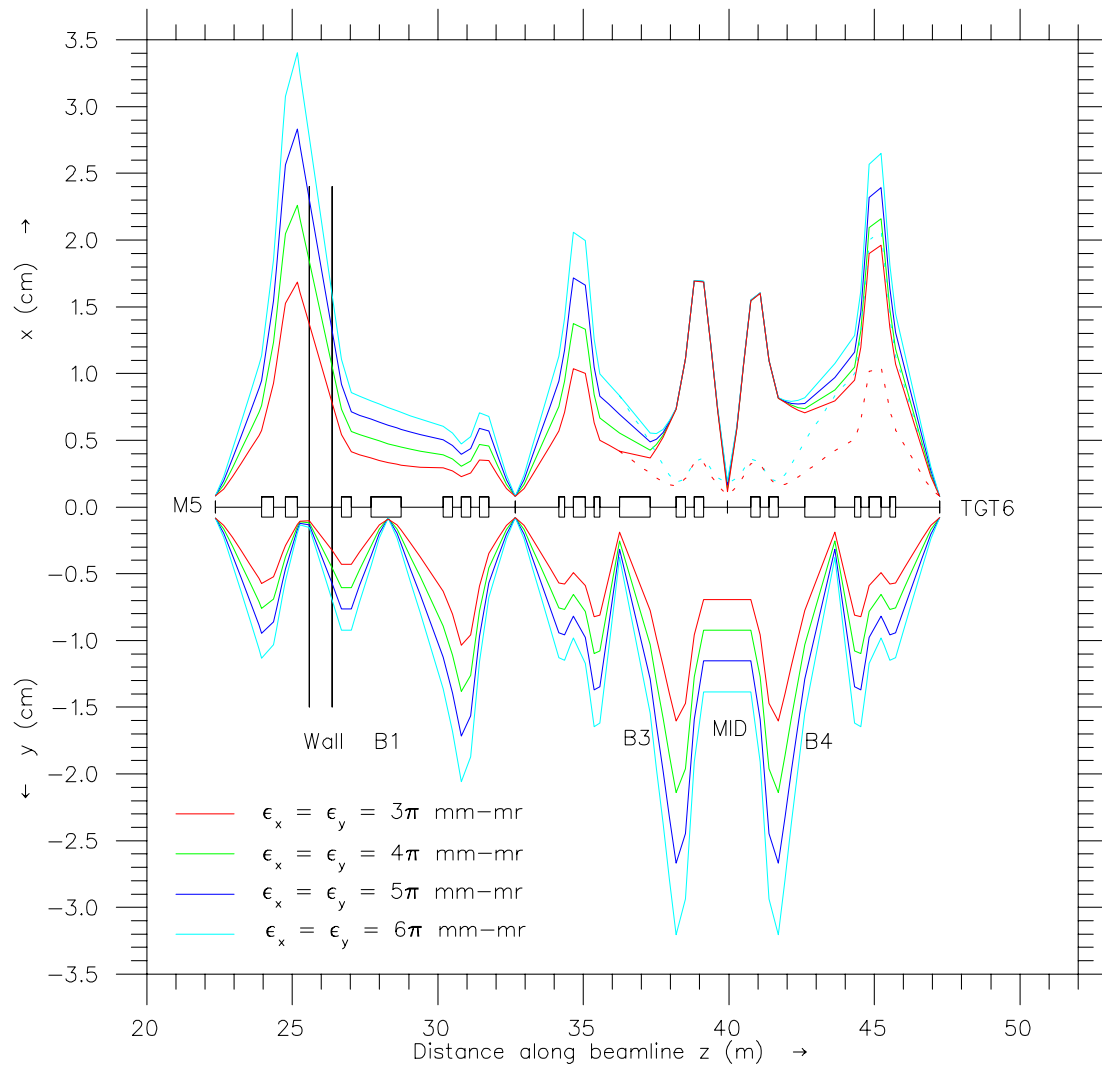


Fig. 26. Beam profiles along an alternate beam-transport configuration for beam delivery to experimental target TGT6.

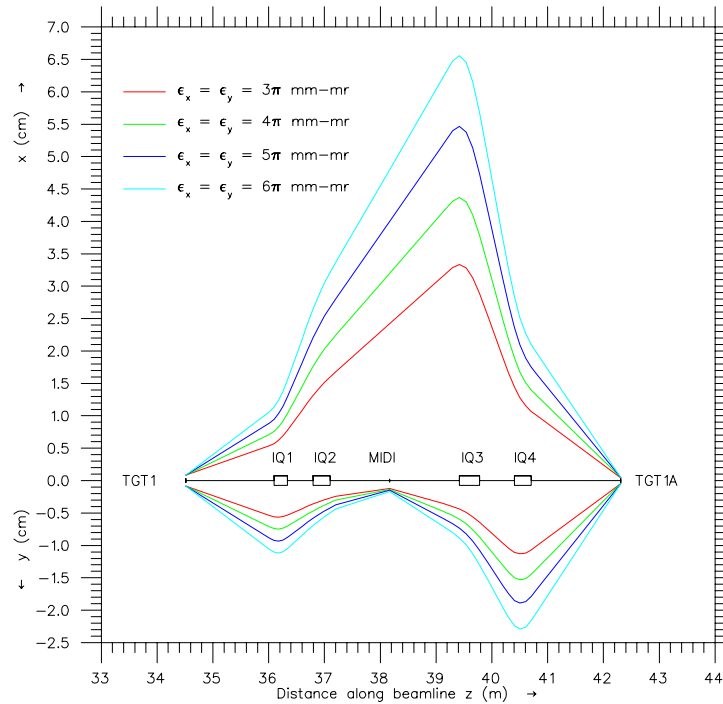


Fig. 27(a). Beam profiles from TGT1 to TGT1A in a VHHV quadrupole configuration designed to produce a 1 mm beam spot at TGT1A from a 2 mm beam spot at TGT1.

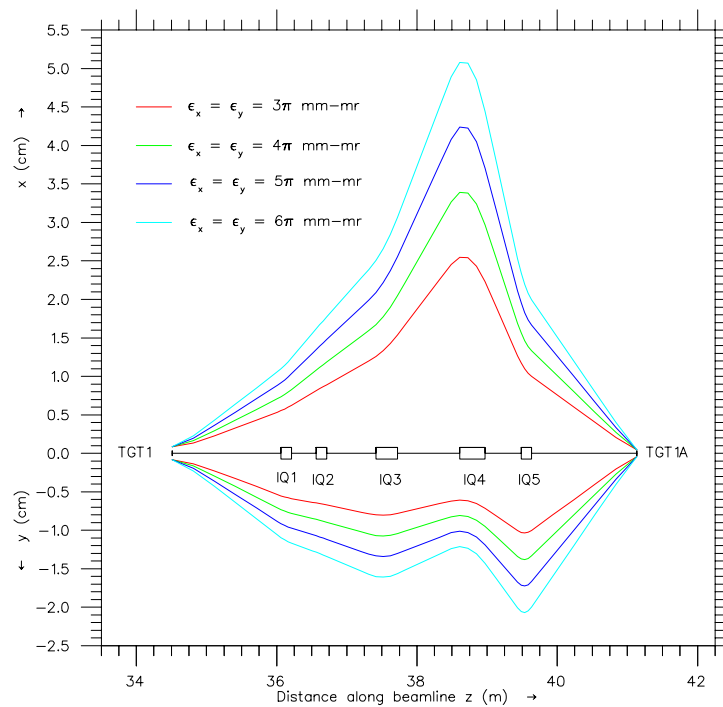


Fig. 27(b). Beam profiles from TGT1 to TGT1A in a VHVHV quadrupole configuration designed to produce a 1 mm beam spot at TGT1A from a 2 mm beam spot at TGT1.